JOURNAL OF
EMERGING
INVESTIGATORS
VOLUME 2, ISSUE 11 | NOVEMBER 2019
emerginginvestigators.org

Nintendo DaVinci

Performing surgeries with the Nintendo Switch

Alzheimer's genetics
Investigating a new mutation that may be behind the disease

Battery innovation
A new composite nanowoven material for improving battery life

Fatty acid biosynthesis
Using yeast to produce petrochemical alternatives

Deception and workout performance
Does deceiving athletes about workout duration help them perform?

Well water contamination
Measuring heavy metal concentrations in HuNan, China

JOURNAL OF EMERGING INVESTIGATORS

The Journal of Emerging Investigators is an open-access journal that publishes original research in the biological and physical sciences that is written by middle and high school students. JEI provides students, under the guidance of a teacher or advisor, the opportunity to submit and gain feedback on original research and to publish their findings in a peer-reviewed scientific journal. Because grade-school students often lack access to formal research institutions, we expect that the work submitted by students may come from classroom-based projects, science fair projects, or other forms of mentor-supervised research.

JEI is a non-profit group run and operated by graduate students, postdoctoral fellows, and professors across the United States.

EXECUTIVE STAFF

Mark Springel EXECUTIVE DIRECTOR
Haneui Bae COO
Qiyu Zhang TREASURER
Michael Mazzola DIRECTOR OF OUTREACH

BOARD OF DIRECTORS

Sarah Fankhauser, PhD
Katie Maher, PhD
Tom Mueller
Lincoln Pasquina, PhD
Seth Staples

EDITORIAL TEAM

Jamilla Akhund-Zade EDITOR-IN-CHIEF
Olivia Ho-Shing EDITOR-IN-CHIEF
Michael Marquis EDITOR-IN-CHIEF
Brandon Sit MANAGING EDITOR
Laura Doherty MANAGING EDITOR
Michelle Frank HEAD COPY EDITOR
Sonia Kim HEAD COPY EDITOR
Naomi Atkin HEAD COPY EDITOR
Alexandra Was, PhD PROOFING MANAGER
Erika J. Davidoff PUBLICATION MANAGER

SENIOR EDITORS

Kiana Mohajeri
Laura Doherty
Chris Schwake
Kathryn Lee

FOUNDING SPONSORS

ALLOY THERAPEUTICS

NEW ENGLAND BioLabs® Inc.
enabling technologies in the life sciences

Contents

VOLUME 2, ISSUE 11 | NOVEMBER 2019

All articles are copyright © 2019 to their respective authors. All JEI articles are distributed under the attribution non-commercial, no derivative license (http://creativecommons.org/licenses/by-nc-nd/3.0/). This means that anyone is free to share, copy and distribute an unaltered article for non-commercial purposes provided the original author and source is credited.

JOURNAL OF
EMERGING INVESTIGATORS

Article

Expression of anti-neurodegeneration genes in mutant *Caenorhabditis elegans* using CRISPR-Cas9 improves behavior associated with Alzheimer's Disease

Roshni Mishra, Leya Joykutty, and Kepa Oyarbide
American Heritage School, Plantation, FL

SUMMARY

Alzheimer's is ranked as the 6th leading cause of death in the United States, and mainly presented as neurodegeneration. In order to begin to understand its physiology, the specific role of proteins in neurodegeneration, LRP1 and AQP4, need to be studied. This study tested the effect of using the CRISPR-Cas9 system to overexpress the LRP1 and AQP4 proteins, associated with transport of materials and waste across the cell membrane, in *Caenorhabditis elegans* to assess effects on neurodegeneration, such as chemosensation, size, and average speed phenotypes. I hypothesized that combinatorial overexpression of AQP4 and LRP1 would have the greatest effect on reducing neurodegeneration. I tested chemosensory behavior using a chemotaxis test, revealing a decrease in neurodegeneration when both LRP1 and AQP4 were overexpressed. The size of the *C. elegans* did not change, but the speed increased in the strain expressing amyloid beta in the muscle, suggesting that a decrease in amyloid beta allowed muscles more room to contract. These results support our hypothesis and show that the overexpression of LRP1 and AQP4 proteins decrease neurodegeneration and allow *C. elegans* to preserve their olfactory retention. This study will help demonstrate the role of LRP1 and AQP4 in Alzheimer's and determine whether they benefit the system once they are overexpressed.

INTRODUCTION

Approximately 5.7 million people worldwide have Alzheimer's Disease, which eventually causes loss of mental function and memory in those affected. There are a few main hypotheses that try to explain Alzheimer's disease, including the amyloid hypothesis and the Tau hypothesis. The amyloid hypothesis proposes that a protein in the cell membranes of neurons called the amyloid precursor protein (APP) helps transmit signals from the inside of the cell to its environment. APP is eventually broken down by alpha, beta, and gamma secretases. Alpha and gamma secretases break down the protein into a soluble state, but beta secretase activity leads to insoluble APP. Buildup of insoluble APP can generate an amyloid beta plaque that inhibits the connections between neurons (1). Alternatively, the Tau hypothesis suggests that, in Alzheimer's Disease, the Tau protein, which normally stabilizes microtubules, instead separates from these microtubules, causing them to fall apart. The strands of Tau cause tangles, which disable the transport system and destroy the cell (2).

The LDL receptor family functions to bind ligands for internalization and degradation, as well as for cholesterol metabolism. Previous research suggested that LRP1-APP interactions favor APP processing through the amyloidogenic pathway due to LRP1 binding with sAPP770, an isoform of APP. Recent studies have shown that areas of the brain that have decreased amounts of low-density lipoprotein receptor-related protein 1 (LRP1) have an increased amount of amyloid beta plaques. When the activation of LRP1 is inhibited, there is lethality due to molting defects during the L3-L4 transitions. LRP1 has been suggested to aid in the uptake of cholesterol from the environment in *Caenorhabditis elegans* (*C. elegans*) (3).

Aquaporin 4 (AQP4) is a water channel in the central nervous system and plays a vital role in the balance of water and ions in the brain. AQP4 deficiency in the brain leads to deficits in memory and ability to learn (4). Scientists agree that expression of AQP4 protects the brain from amyloid beta plaques. An association of AQP4 and GLT1, a glutamate transporter, is present in plasma membranes and may function as a dynamic signaling platform. When this signal is disrupted, it can cause neural impairment (5).

LRP1 plays critical roles in amyloid beta metabolism and clearance in neurons. LRP1 knockdown results in decreased uptake and degradation of amyloid beta. Similarly, the deletion of AQP4 exacerbates cognitive defects and induces an increase in amyloid beta accumulation (6). Furthermore, a deficiency in AQP4 results in the decreased upregulation of LRP1 and consequently the decreased uptake of amyloid beta. This suggests that AQP4 is important in the upregulation of LRP1 and clearance of amyloid beta (7).

C. elegans are often used as a model organism for studying Alzheimer's Disease. These animals reproduce quickly, as the period from fertilization to hatching only lasts 12 hours. They mature into adults over the course of 3 days, and then lay about 300 eggs over the course of the next 3 days. Furthermore, amyloid beta plaques in Alzheimer's Disease are caused by the APP gene in humans, which is homologous to the apl-1 gene in *C. elegans*.

The current treatments of Alzheimer's Disease interfere

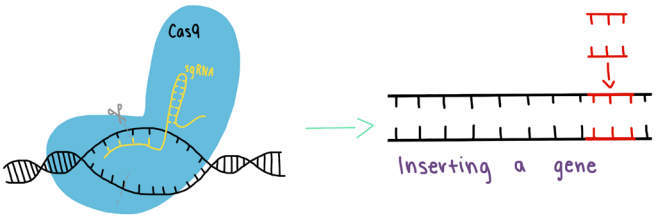

Figure 1: Simplified diagram of CRISPR-Cas9. A double-stranded break is made in the DNA by Cas9, and then the cDNA is inserted.

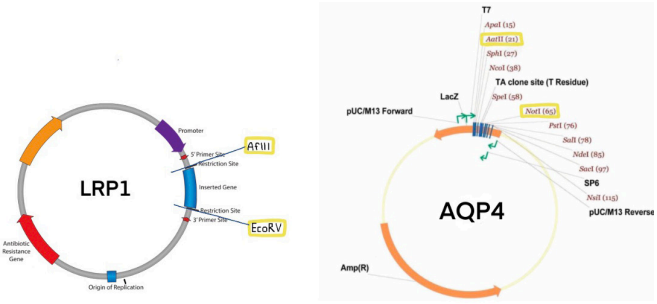

Figure 2: LRP1 and AQP4 plasmid diagrams. Plasmids were commercially obtained. Plasmids were then digested with enzymes depicted to remove the cDNA insert of LRP1(AflII and EcoRV) or AQP4 (NotI and AatI).

with other associated diseases and do not improve cognitive impairment. For example, neprilysin is utilized to break down amyloid beta plaques, but patients with cardiac conditions take a drug called LCZ696 which inhibits neprilysin. Therefore, new therapeutic options are necessary for those that cannot use neprilysin (9).+

A method called CRISPR-Cas9 has been recently implemented to use for gene editing (**Figure 1**). CRISPR-Cas9 requires a single guide RNA (sgRNA) which can be generated from a CRISPR design program. Additionally, a single-stranded oligonucleotide (ssODN) with 5' and 3' homology arms are designed to contain the gene of interest and restriction sites (10). In addition, the Cas9 recombinant protein is used. In this study, the CRISPR Cas9 system was used for gene knock in of LRP1 and/or AQP4.

Plasmids containing genes of interest were microinjected into the *C. elegans* (**Figure 2**).This is the most widely used form of gene editing in *C. elegans* to create transgenic worms. The DNA is inserted into the distal gonad syncytium or directly into the embryos. Transformation markers are inserted with the gene of interest in order to identify the transgenic worms. In order to see which worms show the phenotype, a GFP vector is also inserted which makes the worm or egg glow green to show the presence of the trait (12).

In the study, primers were added to LRP1 and AQP4 genes matching the insertion site in the *C. elegans* genome. Once this construct was developed, the genes were microinjected into the *C. elegans* with Cas9 and a site-specific guide RNA. The effects of the addition of the genes were then tested by running chemosensory, size, and speed assays. The negative control hypothesis was that adding no gene to the *C. elegans* would have no effect on the chemotaxis abilities, brood size, or locomotion. The alternative hypothesis was that given only LRP1 or AQP4 was inserted downstream of the apl-1 promoter, there would be a reduced effect on the chemotaxis abilities, brood size, and locomotion compared to inserting both LRP1 and AQP4 downstream of the apl-1 promoter in conjunction. When both LRP1 and AQP4 are overexpressed, I predict a significant increase in the uptake of beta amyloid, as evidenced by increases in chemotaxis, brood size, and locomotion. This study could be a major step in the research to develop a better method of curing Alzheimer's at the source, which is a DNA mutation. Once the proteins are overexpressed, the primary presentation of Alzheimer's, neurodegeneration, will be limited.

RESULTS

A GFP plasmid was microinjected in conjunction with the LRP1 and AQP4 genes. The fluorescence of the injected *C. elegans* confirmed that the LRP1 and AQP4 genes were being expressed. To assay the predicted changes in the *C. elegans* after the addition of the APQ4 and LRP1 genes, I measured chemotaxis abilities, size, and locomotion. The chemotaxis assay was run using known attractant of *C. elegans* to measure sensory ability. The chemotaxis index shows an increase in chemosensory ability by moving away or towards certain smells. Because neuronal amyloid beta expression is known to induce defects in chemotaxis, I expected that a chemotaxis assay would be an appropriate measure of the effects of various proteins on amyloid beta levels (13). Additionally, apl-1 mutations cause defects in movement and brood size, which correlates with the effects of LRP1 and AQP4 on the apl-1 mutation in Alzheimer's.

To measure the neurological changes after overexpression of the candidate genes, I assayed chemotaxis, brood size, and locomotion. I tested these phenotypes in three different strains of *C. elegans*, including N2 (wildtype), CL2006, a strain that expresses amyloid beta plaques, and VC1246, a strain that expresses mutant apl-1. The chemosensory assay showed that when the *C. elegans* were microinjected with LRP1 or AQP4, there was no significant effect on the chemotaxis index. But, when they were microinjected in conjunction, there was a significant increase in the chemotaxis index in all strains. The VC1246 strain showed an increase in the chemotaxis index by 0.5 when both LRP1 and AQP4 were microinjected (($p= 0.006785$), p-value < 0.05, student's t-test). Whereas, the CL2006 strain showed an increase of 0.12 in the chemotaxis index with both LRP1 and AQP4 overexpressed (**Figure 3**; $p=0.007554$, p-value < 0.05, student's t-test). This was expected and supports the hypothesis that together, LRP1 and AQP4 improve chemotaxis abilities. The simultaneous overexpression of LRP1 and AQP4 improved the neurodegenerative phenotype, but did not completely rescue the phenotype to wildtype levels.

The brood size assay showed that there was no significant increase in brood size for any strains, microinjected with LRP1 or AQP4, or both (**Figure 4**). This was unexpected since the expression of beta amyloid is known to decrease the brood size, and therefore with the addition of LRP1 and AQP4, the brood size should have increased (14). Brood size may have increased growth after a few days and could be tested in the future. In the speed assay, the speed of the *C. elegans* did not increase with the microinjection of LRP1 or AQP4.But when they were microinjected in conjunction, the speed in the VC1246 strain increased significantly by about 20 µm/s overexpressed (**Figure 5**; p=0.0269, p-value < 0.05, student's t-test).This was expected for this strain and suggests that the uptake of the beta amyloid by LRP1 and AQP4 allowed the muscle to contract more efficiently, thereby enabling the animals to move faster. The N2 control did not show a significant increase when microinjected with either of the two genes. Thus, the results support the hypothesis that combined overexpression of LRP1 and AQP4 would increase chemotaxis ability and locomotion more significantly than either protein overexpressed alone.

Overall, the study revealed an increase in the neurological ability of *C. elegans* microinjected with both LRP1 and AQP4 as assessed by an increase in chemosensory ability and speed. These results show that individually, the LRP1 and AQP4 proteins had no significant effect on chemosensation, but when overexpressed in conjunction, they increased the chemosensory capacity of the VC1246, the strain with the apl-1 mutation, and CL2006, the strain with beta amyloid plaques present.

DISCUSSION

Alzheimer's Disease, a disease with an unclear physiology, is a global health issue of increasing importance. Current treatments focus on mitigating side effects, but do not address the underlying mechanism of disease, which is hypothesized to be caused by accumulation of beta amyloid plaques. The results showed that when LRP1 and AQP4 were given in conjunction, this treatment significantly reduces amyloid beta plaques, as seen through the increase in chemotaxis ability and increase in speed in the strain of *C. elegans* that expresses plaques in their muscle. I conclude that LRP1 and AQP4 function in conjunction to reduce the formation of additional amyloid beta plaques and break down the buildup of these plaques that were previously formed. Since the APP mutation in humans results in the depletion of AQP4 and LRP1, replacing these proteins could contribute to a better sense of environment as seen in the VC1246 worms (15). Our analysis suggests that the *C. elegans* overexpressing both LRP1 and AQP4 had the greatest reduction of neurodegeneration, while overexpression of LRP1 or AQP4 alone only improved it to a lesser degree.

Limits on time, budget, and experience restricted the extent of the experiment. The last steps of a gene editing study are to typically sequence the genome and check mRNA and protein expression. These methods were not available due to time and monetary constraints. The expression of the GFP protein, however, suggests a successful edit. Testing of the CRISPR-Cas9 system demonstrated up to an 86% precise genome editing efficiency; while this is high for the current methods of genome editing that exist, it is not perfect (16). Furthermore, genome editing has potential side effects.

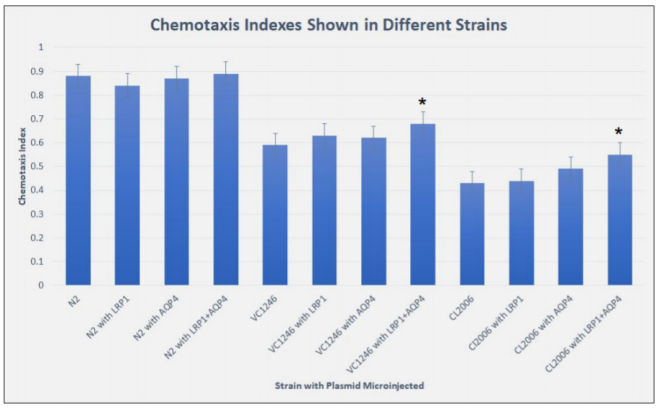

Figure 3: Chemotaxis indexes of different strains after injection. The graph depicts chemotaxis index scores for each strain tested (n=500 for each strain). Error bars represent standard error, and asterisks (*) denote statistical significance (p-value < 0.05, student's t-test).

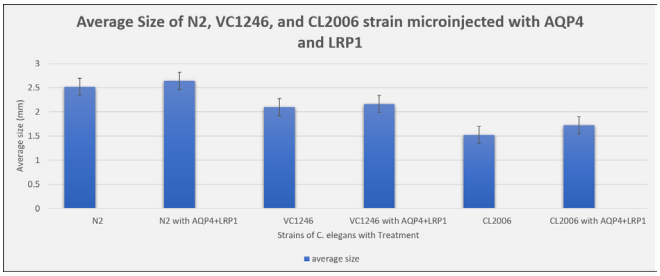

Figure 4: Average size of N2, VC1246, and CL2006 strains microinjected with LRP1 and AQP4. The graph depicts average brood sizes for each strain tests (n=100 for each strain), Error bars represent standard error, and asterisks (*) denote statistical significance (p-value < 0.05, student's t-test).

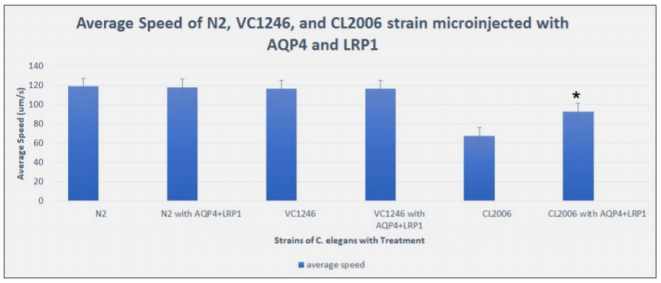

Figure 5: Average speed of N2, VC1246, and CL2006 strains microinjected with LRP1 and AQP4. The graph depicts average speed for each strain tests (n=100 for each strain). Error bars represent standard error, and asterisks (*) denote statistical significance (p-value < 0.05, student's t-test).

The additional copies of LRP1 and AQP4 could potentially interact with other proteins in unknown manners.

Although the data suggests an increase in sensory ability and movement under our experimental manipulations, future research can assess the long-term effects as the worms age, as well as effects on their progeny. The CRISPR-Cas9 system can also be applied to a plethora of other diseases by allowing the correction of many missense mutations. The effect of correcting these mutations can then be studied on a larger scale in other model organisms, such as mice, to assess the potential for reversal of the disease (17). In addition, other genes such as CR1 that control the flow of proteins and waste across cellular membranes can be microinjected to test other possible proteins that could decrease neurodegeneration (18). RNAi feeding strains can also be used to knock out genes to show if the removal of the apl-1 gene influences neurodegeneration. Other strains of *C. elegans* expressing different phenotypes associated with Alzheimer's Disease can be further tested to account for the many different hypotheses currently being debated. Additionally, other properties can be assayed in the future, such as serotonin sensitivity, which can further establish the phenotypic effects of neurodegeneration.

METHODS

C. elegans strains

All strains of *C. elegans* were obtained from the Caenorhabditis Genetics Center at the University of Minnesota. The N2 strain of *C. elegans* is the wildtype strain. The VC1246 strain has the apl-1 gene mutated, which is homologous to an APP gene mutation in humans. The CL2006 strain is categorized with Alzheimer's Disease with the addition of the UNC-54 gene, which codes for amyloid beta in humans. This strain presents amyloid beta in their muscles. The CL2006 strain is temperature-sensitive, meaning that paralysis and egg-laying deficiencies arise when organisms are raised at 20°C.

Transformation of AQP4 and LRP1 plasmids into E. coli with ampicillin selection

Highly Competent DH5alpha E. coli (New England Biolabs, NEB) was thawed on ice and 50 µl were added to LRP1/AQP4 DNA (genomics-online). The reaction was mixed gently by pipetting and flicking the tube 4-5 times. The mixture was placed on ice for 30 min, then heat shocked at 42°C for 30 sec. 950 µl of LB media (NEB) was added, and the tube was placed in a shaking incubator at 37°C for 1 hr. From each culture, 50-100 µl of bacteria were spread onto plates and incubated overnight. The transformed cells were grown on ampicillin plates to select for successfully transformed, ampicillin-resistant bacteria.

DNA extraction

Plasmid DNA was extracted from the transformed bacteria using the Monarch plasmid miniprep kit according to the manufacturer's protocol (NEB).

AQP4 and LRP1 double digests

Using the restriction enzymes around the insertion site, an overnight double digest was run to cut out the cDNA from the cloning vector. For the AQP4 plasmid, the restriction enzymes NotI and AatII (NEB) were used. For the LRP1 plasmid, the restriction enzymes AflII and EcoRV (NEB) were used. Digests were composed of 4µl Multi Core Buffer, 0.2 µl BSA, 10 µL DNA, 1 µl of each enzyme, and 4.8 µl of sterile water and kept in the fridge overnight. To confirm digestion, ethidium bromide (Biolabs) gels were made with 1X TAE Buffer (Biolabs) and then placed into 1X TAE Buffer to run. 1 µl of loading dye and 5 µl of DNA were added per lane. Gels were run at 150 V for an hour. UV light was then used to visualize bands.

PCR and Gibson Assembly to attach primers and DNA fragments

A 25 µl mixture was made with 2.5 µl 10X standard TaqReaction Buffer (NEB), 0.5 µl 10nM dNTPs (NEB), 0.5 µl 10 µM Forward Primers, 0.5 µl 10 µM Reverse Primer, brought up to 25 µl with Template DNA. The reaction was gently mixed and put in the PCR machine. The cycle was 95°C for 30 seconds, 30 cycles of 95°C for 20 seconds, then 60°C for 30 seconds, then 68°C for 1 minute, then 68°C for 5 minutes and finally held at 4°C.

For the Gibson Assembly mix, 1 pmol of DNA fragment, 10 µl of Gibson Assembly Master Mix (NEB), and 10 µl of deionized water were added to a tube and incubated in the thermocycler at 50°C for 60 minutes.

Microinjection

Microinjection was done with the nanoliter (World Precision Instruments) and paraffin oil was used to ensure worms stayed still. A single guide target RNA sequence was created by SYNTHEGO to place the DNA inserts downstream from the apl-1 promoter. The Cas9 protein was obtained from Sigma Aldrich. The final injection mixture was: 5 µmol of single guide RNA, 5 µmol of Cas9 nuclease, 50 ng/µl of DNA insert and GFP plasmid. These components were homogeneously mixed by gentle pipetting. The mixture was loaded into needles and *C. elegans* were injected at the gonad syncytium and then transferred to new NGM plates after recovery.

Chemotaxis Assay

Chemotaxis plates were first labeled with the center in the middle, control on one side, and attractant on the other side. Approximately 100 worms were washed using M9 Buffer three times and then placed in the center, with one drop of sterile water on one end of the plate and a known attractant on the other side of the plate at the marked areas. A disposable plastic pipette was used as the dropper. 2 µl of 0.5M sodium azide (Biolabs) were put on both sides to paralyze the worms. After 1 hour, the plates were chilled at 4ºC for 15 minutes to stop worms from moving and then worms on both sides

of the plate were counted and recorded. The data was then analyzed, and the chemotaxis index was determined. The chemotaxis index is calculated by (number of worms at attractant – number of worms at the control)/ (total number of worms).

Locomotion Assay

Thirty second videos of worms crawling on NGM plates were taken using a microscope. The speed of the worms was quantified by the worm tracker extension in ImageJ.

Measuring Brood Size

Brood size was measured using an application called ImageJ. Images taken of the *C. elegans* were traced using a tool on ImageJ, and the brood size was measured. The sizes were then downscaled based on the amount of zoom in the pictures.

Statistical Testing

T-tests were performed comparing the data to the wildtype and the p values were analyzed in Excel to determine which values were under 5% and therefore statistically significant.

ACKNOWLEDGEMENTS

I would like to thank American Heritage School for funding my research.

REFERENCES

1. Goodsell, D.s. “Amyloid-Beta Precursor Protein.” RCSB Protein Data Bank, 2006, doi:10.2210/rcsb_pdb/mom_2006_7.
2. Alexander, Adanna G., et al. “Use of Caenorhabditis Elegans as a Model to Study Alzheimerâ€™s Disease and Other Neurodegenerative Diseases.” Frontiers in Genetics, vol. 5, 2014, doi:10.3389/fgene.2014.00279.
3. Shinohara, Mitsuru, et al. “Role of LRP1 in the Pathogenesis of Alzheimer’s Disease: Evidence from Clinical and Preclinical Studies.” Journal of Lipid Research, vol. 58, no. 7, 2017, pp. 1267–1281., doi:10.1194/jlr.r075796.
4. Haj-Yasein, N. N., et al. “Glial-Conditional Deletion of Aquaporin-4 (Aqp4) Reduces Blood-Brain Water Uptake and Confers Barrier Function on Perivascular Astrocyte Endfeet.” Proceedings of the National Academy of Sciences, vol. 108, no. 43, 2011, pp. 17815–17820., doi:10.1073/pnas.1110655108.
5. Assefa, Brhane Teklebrhan, et al. “Reactive Astrocytes as Drug Target in Alzheimer’s Disease.” BioMed Research International, vol. 2018, 2018, pp. 1–10., doi:10.1155/2018/4160247.
6. Liu, Chia-Chen, et al. “Astrocytic LRP1 Mediates Brain Aβ Clearance and Impacts Amyloid Deposition.” The Journal of Neuroscience, vol. 37, no. 15, 2017, pp. 4023–4031., doi:10.1523/jneurosci.3442-16.2017.
7. Xu, Zhiqiang, et al. “Deletion of Aquaporin-4 in APP/PS1 Mice Exacerbates Brain Aβ Accumulation and Memory Deficits.” Molecular Neurodegeneration, vol. 10, no. 1, 2015, doi:10.1186/s13024-015-0056-1.
8. Ewald, Collin Y., et al. “APL-1, the Alzheimer’s Amyloid Precursor Protein in Caenorhabditis Elegans, Modulates Multiple Metabolic Pathways Throughout Development.” Genetics, vol. 191, no. 2, 2012, pp. 493–507., doi:10.1534/genetics.112.138768.
9. Bratsos, Sosipatros. “Efficacy of Angiotensin Converting Enzyme Inhibitors and Angiotensin Receptor-Neprilysin Inhibitors in the Treatment of Chronic Heart Failure: A Review of Landmark Trials.” Cureus, 2019, doi:10.7759/cureus.3913.
10. 1Prior, Harriet, et al. “Highly Efficient, Rapid and Co-CRISPR-Independent Genome Editing in Caenorhabditis Elegans.” G3: Genes|Genomes|Genetics, vol. 7, no. 11, 2017, pp. 3693–3698., doi:10.1534/g3.117.300216.
11. Paix, Alexandre, et al. “Precision Genome Editing Using CRISPR-Cas9 and Linear Repair Templates in *C. elegans*.” Methods, vol. 121-122, 2017, pp. 86–93., doi:10.1016/j.ymeth.2017.03.023.
12. Markaki, Maria, and Nektarios Tavernarakis. “Modeling Human Diseases in Caenorhabditis Elegans.” Biotechnology Journal, vol. 5, no. 12, 2010, pp. 1261–1276., doi:10.1002/biot.201000183.
13. Strooper, Bart De. “Loss-of-Function Presenilin Mutations in Alzheimer Disease. Talking Point on the Role of Presenilin Mutations in Alzheimer Disease.” EMBO Reports, vol. 8, no. 2, 2007, pp. 141–146., doi:10.1038/sj.embor.7400897.
14. Hornsten, A., et al. “APL-1, a Caenorhabditis Elegans Protein Related to the Human Beta-Amyloid Precursor Protein, Is Essential for Viability.” Proceedings of the National Academy of Sciences, vol. 104, no. 6, 2007, pp. 1971–1976., doi:10.1073/pnas.0603997104.
15. Liu, Chia-Chen, et al. “Astrocytic LRP1 Mediates Brain Aβ Clearance and Impacts Amyloid Deposition.” The Journal of Neuroscience, vol. 37, no. 15, 2017, pp. 4023–4031., doi:10.1523/jneurosci.3442-16.2017.
16. Hruscha, A., et al. “Efficient CRISPR/Cas9 Genome Editing with Low off-Target Effects in Zebrafish.” Development, vol. 140, no. 24, 2013, pp. 4982–4987., doi:10.1242/dev.099085.
17. Wyvekens, Nicolas, et al. “Genome Editing in Human Cells Using CRISPR/Cas Nucleases.” Current Protocols in Molecular Biology, 2015, doi:10.1002/0471142727.mb3103s112.
18. Fonseca, Maria I., et al. “Analysis of the Putative Role of CR1 in Alzheimer’s Disease: Genetic Association, Expression and Function.” Plos One, vol. 11, no. 2, 2016, doi:10.1371/journal.pone.0149792.

JOURNAL OF
EMERGING INVESTIGATORS

Article

Utilizing a wastewater-based medium for engineered *Saccharomyces cerevisiae* for the biological production of fatty alcohols and carboxylic acids to replace petrochemicals

Rajat Ramesh, Leya M. Joykutty
American Heritage School, Plantation, Florida

SUMMARY

Personal care items, pharmaceutical formulations, food additives, detergents, plasticizers, and industrial solvents manufactured from artificially synthesized acids or petrochemicals can be produced with more sustainable methods. The metabolic engineering of microbial hosts, specifically the heterotrophic yeast *Saccharomyces cerevisiae*, using a cost-effective wastewater-based growth medium could potentially provide a solution. Upregulation of the fatty acid biosynthesis (FAS) pathway present in this species is key to increasing all fatty acid-derived products. Three plasmids containing genes responsible for the production of the enzymes acetyl-CoA carboxylase (ACC1), fatty acid synthase (FAS), and fatty acid reductase (Far1), were transformed into *S. cerevisiae* cells using the PEG-LiOAc method. Transformation was conducted separately and together to optimize efficiency. We hypothesized that transformed cells would display more varied fatty acid and fatty alcohol profiles, and an increased ability to grow in a modified wastewater-based medium while degrading dissolved organics. A spectrophotometric assay predicated on the oxidation of NADPH to $NADP^+$ was performed to determine the activity of the overexpressed enzymes. High performance liquid chromatography (HPLC) analysis underscored the presence of C-16 and C-18 fatty alcohols and fatty acids present in the yeast. Finally, a gas chromatography-mass spectrometry (GC-MS) analysis portrayed a reduction in organic compounds in wastewater media that was metabolized by *S. cerevisiae* while evidence of ethanol production via fermentation was seen. The study adds to research on renewable energy alternatives, but more importantly, demonstrates an effective method in which *S. cerevisiae* can biologically produce valuable specialty and commodity chemicals to mitigate petroleum use while removing organic content from wastewater.

INTRODUCTION

In recent years, biofuels have received growing interest as an alternative fuel source due to concern about the environmental impact of fossil fuels. While extensive research has been done on utilizing microalgae for biofuel production, methods available constrain its prospects as a source for future energy. The commercial production of biofuel is not yet economically viable due to slow rates of production from microalgae and the expensive apparatus needed for algal growth, namely gas exchange equipment. Some yeast species, though in need of carbon sources, can produce lipids at higher efficiencies compared to microalgal species. Therefore, transitioning to yeast, which can be grown anaerobically, provides a promising alternative for fuel production for the future (1).

Currently, there are two practical bio-based options that can replace fossil fuels at least to some degree: bioethanol for gasoline and biodiesel for diesel (2). *Saccharomyces cerevisiae,* or baker's yeast, remains the preferred cell factory for production of bioethanol. While *S. cerevisiae* is responsible for nearly 100% of all bioethanol produced, its promise as a source of fatty alcohols, key in the production of specialty and commodity items, has not been exploited (3). In general, the growth of oleaginous (fatty acid-containing) yeast species is slower compared to that of bioethanol-producing yeast like *S. cerevisiae*, and biolipid production by oleaginous yeasts requires a long period to produce any optimal yield (1).

One of the major advantages of *S. cerevisiae* is the vast knowledge available about its metabolism, which has opened opportunities for metabolic engineering approaches (3). Biolipids, including triacylglycerol produced by oleaginous yeast, are one of the most important feedstocks for biodiesel production. The first step towards increasing the fatty alcohol production potential, and thereby commodity chemical potential of *S. cerevisiae*, is the upregulation of the fatty acid biosynthesis (3). In fatty acid biosynthesis, fatty acids are generated from three hydrocarbon chains esterified with a glycerol backbone (4). Malonyl-CoA is used in this process to elongate acyl-CoA chains and is synthesized by the enzyme acetyl-CoA carboxylase (ACC1) (5). Overexpression of the gene encoding for this rate-limiting enzyme could possibly increase production of malonyl-CoA and fatty acid-derived products. Second in the biosynthesis pathway, C-16 fatty acid (palmitic acid) assembly is initiated with the use of fatty acid synthase (FAS) (6). Finally, the introduction of a synthetic fatty acid reductase (Far1) allows for the reduction of fatty acids to fatty alcohols (7,8). Fatty alcohols provide an ideal class of chemicals that can replace petrochemicals in specialty and commodity chemical production due to their amphipathic nature, and act as non-ionic surfactants.

While using yeast for lipid and ethanol production has

	Time (minutes)						
	0	5	10	15	20	25	30
Control	0.0543	0.34578	0.84203	0.234235	0.10777	0.045443	0.02435
ACC	0	0.17153	0.38653	0.13897	0.04467	0.031241	0.022435
FAS	0	0.15342	0.345924	0.124422	0.05362	0.04257	0.02907
FAR	0	0.124215	0.27688	0.116478	0.05589	0.04864	0.025651
ACC + FAS	0	0.09535	0.19245	0.105852	0.04648	0.039842	0.024385
ACC + FAR	0	0.066346	0.165624	0.07324	0.04467	0.031241	0.018493
ACC + FAS + FAR	0	0.024364	0.121234	0.05866	0.03362	0.02257	0.01947

Table 1: Average absorbance of transformed *S. cerevisiae* cell lysates (ten replicates of separate 30 minute intervals). Values are given in absorbance units.

distinctive advantages in terms of lipid quality, cultivation ease, and overall productivity, the heterotrophic nature of yeast like *S. cerevisiae* reduces its competitiveness as a biodiesel source (10). It is this reason that there have been attempts to utilize wastewater as a free source of water, nutrients, and even carbon sources (11). The practical use of wastewater requires a prior treatment that eliminates contaminants and most significant malevolent bacteria, as well as balances nutrient composition (11).

Here, *S. cerevisiae* was metabolically engineered for enhanced fatty alcohol and free carboxylic acid production while utilizing wastewater as a cost-effective nutrient culture source. We show that if the *ACC1* (encoding a deregulated acetyl-CoA carboxylase), *FAS*, and *Far1* (*Mus musculus*) genes are overexpressed in *S. cerevisiae in vitro* via plasmid-based expression, then fatty acid, fatty alcohol, and ethanol content accumulated. By the same token, it was also predicted that if mixed liquor was utilized as a carbon source, after sterilization and nutrient balance, then yeast cell viability persisted in wastewater media, and organics in the media were degraded (12).

RESULTS

Determination of Activity of ACC1, FAS, and Far1 Enzymatic Products

We used a lithium acetate heat shock method to transform the three plasmids containing the *ACC1, FAS, Far1* genes and confirmed transformation with selection for the URA-3 or LEU-2 nitrogenous base markers. However, to ensure enzymatic activity of acetyl-CoA carboxylase, fatty acid synthase, and fatty alcohol reductase, we monitored the oxidation of NADPH to $NADP^+$ indicative of three steps involving the enzymes in the *S. cerevisiae* fatty acid metabolism. Around 10 minutes after the start of the reaction, the oxidation of NADPH to $NADP^+$ for all *S. cerevisiae* strain lysates was lowest in the wildtype control yeast based on elevated absorbance values (**Figure/Table 1**). Transformed *S. cerevisiae* cell lysates had a consistently lower absorbance than the control, with the lowest observed in the *ACC1* + *FAS* + *Far1* strain (one-tailed t-test, $p<0.05$). This indicated that not only was NADPH being converted to $NADP^+$ in the FAS pathway, but it also suggested greater enzymatic activity in the transformed cells (**Figure/Table 1**).

Quantification of Fatty Acid Metabolites

We used high-performance liquid chromatography (HPLC) to demonstrate the presence of C-16 and C-18 fatty alcohols and fatty acids, which we induced with the overexpression of *ACC1*, *FAS*, and *Far1*. Before running cell pellet extracts containing lipids from engineered strains, we analyzed standards of hydroxy-palmitic acid, palmitic acid, 1-hexadecanol, and stearyl alcohol, and recorded elution times to compare against the samples. We ran a control *S. cerevisiae* strain which outputted minimal detection of palmitic acid (**Figure 2**). However, in the strain transformed with just the *Far1* gene, C-16 fatty alcohol, 1-hexadecanol, and palmitic acid were identified (**Figure 3**). Furthermore, the strain that was transformed with the *ACC1, FAS*, and *Far1* genes demonstrated concentrations of 1-hexadecanol, hydroxy palmitic acid and in fact, even C-18 fatty alcohol, stearyl alcohol was identified (**Figure 4**). This HPLC analysis provided evidence of intracellular fatty-derived components.

Gas Chromatography-Mass Spectrometry (GC-MS)

We used gas chromatography using a silica-based capillary column connected to a spectrometric interface to quantify metabolites present in metabolized mixed liquor. The data suggested, in comparison between the two tables, that

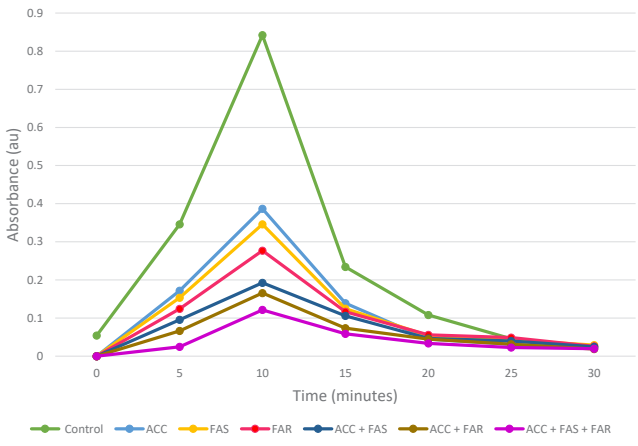

Figure 1. Enzymatic activity of S. cerevisiae. The reduction of NADPH to $NADP^+$ was seen around 10 minutes into the reaction for all *S. cerevisiae strain* lysates. Optimal absorbance was indicated at the peak of the reaction (where NADPH was being reduced). Values are given in absorbance units.

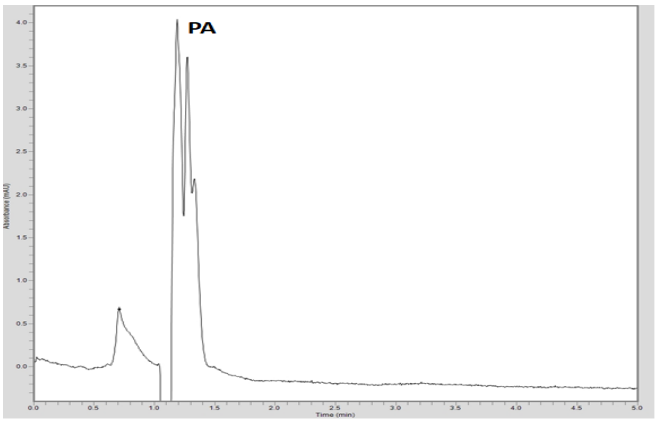

Figure 2. Fatty-derived products of non-transformed cells. A control *S. cerevisiae* strain was run through the silica-based column, which outputted minimal detection of palmitic acid and hydroxy-palmitic acid. PA refers to palmitic acid.

an overall reduction in phenolic, volatile organic compounds (VOCs), and aromatics was seen, while concentrations of succinic acid, malic acid, and oxalic acid (all carboxylic acids) and increased concentrations of acetone and ethanol were identified after "treatment" with yeast (**Table 2 and 3**). This indicates an ability of *S. cerevisiae* to effectively remove organics from wastewater while utilizing the organics to grow. We found acetone, ethanol, methanol, and acetaldehyde in much larger quantities than other metabolites, while phenolic compounds (namely pentachlorophenol and 4-tert-Butylphenol) and aromatics (benzene, bromomethane, and chloroethane) were found in much smaller quantities (**Table 3**).

DISCUSSION

The goal of this study was to successfully transform the *ACC1*, *FAS*, and *Far1* plasmids into *S. cerevisiae* to create a viable microbial strain that could treat wastewater while also producing specialty and commodity chemicals in the form of fatty alcohols. In this project, we examined the role of the fatty acid biosynthesis pathway in the production of lipids and bioethanol, and the potential use of wastewater organic content as a suitable nutrient source for yeast-related industries. To address this, we successfully transform *S. cerevisiae* with plasmids the enzymes acetyl-CoA carboxylase, fatty acid synthase, and fatty acid reductase, as demonstrated by the spectrophotometric enzymatic assay. Transformed *S. cerevisiae* demonstrated increased oxidation of NADPH to $NADP^+$ compared with non-transformed strains. A final lipid extraction and HPLC analysis allowed for the identification of stearyl alcohol, 1-hexadecanol, hydroxy-palmitic acid, and palmitic acid, supporting the notion that the transformation of the plasmids would allow for the overexpression of the three enzymes (first hypothesis). An analysis utilizing GC-MS of a viable *S. cerevisiae* culture in wastewater-based media indicated a reduction VOCs, aromatic hydrocarbons, and phenolics, while carboxylic acids and ethanol concentrations were determined. We demonstrate that the hypotheses, which stated that plasmid overexpression would lead to fatty alcohol production and yeast viability would persist in wastewater-based media while organics were degraded, were effectively supported based on successful transformation and expression of the three recombinant plasmids and reduction of volatile organics in mixed liquor used as growth media.

Thus, we demonstrate the creation of metabolically engineered *S. cerevisiae* strains that successfully grew in a nutrient-balanced, synthetic wastewater-based media. While the study reinforces the ability of *S. cerevisiae* to replace algae in renewable energy developments, the implications are far-reaching. The project effectively underscores the value of microbial hosts, in that they can produce important bio-based chemicals through engineering of cell metabolism. The fatty alcohols, fatty acids, and carboxylic acids identified in the project can be used to produce a variety of important items, including cosmetics, shampoos, toothpastes, concrete additives, pest control formulations, pharmaceutical formulations, food additives, textiles, biopolymers and bioplastics, detergents, industrial solvents, and plasticizers. Furthermore, conventional production of these very same fatty-acid derived chemicals using petroleum or artificial synthesis is environmentally harmful. As such, the prices of these chemicals fluctuate with the price of petroleum and will become more expensive and scarce as the non-renewable petroleum supply dwindles.

Furthermore, the utilization of wastewater as a cost-effective media is key to implementing chemical production from yeast on a commercial scale. Our wastewater method is less expensive in comparison to standard yeast peptone dextrose-based full medium, as expensive nutrients and trace element supplements are not needed. We further reveal that while *S. cerevisiae* utilizes the media to grow, the study reveals that a plethora of organics were degraded in the wastewater. Excreted acids and ethanol can be harvested from the wastewater with industrial processes like liquid-liquid microextraction, and bioethanol factories that already currently use *S. cerevisiae* can be retrofitted to produce these

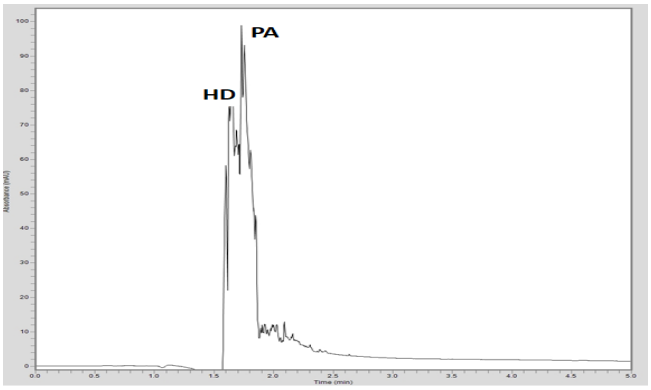

Figure 3. Fatty-derived products of FAR-transformed cells. In the *S. cerevisiae* strain transformed with just the *Far1* gene, concentrations of C-16 fatty alcohol, 1-hexadecanol, and palmitic acid were identified. PA refers to palmitic acid and HD refers to hexadecanol (C-16 fatty alcohol).

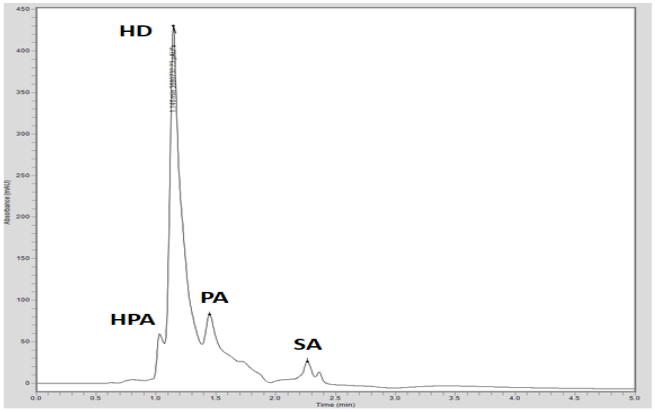

Figure 4. Fatty-derived products of ACC1, FAS, and FAR-transformed cells. The strain that was transformed with the *ACC1*, *FAS*, and *Far1* genes demonstrated a presence of 1-hexadecanol, and in fact, even C-18 fatty alcohol, stearyl alcohol was identified. PA refers to palmitic acid, HPA refers to hydroxy-palmitic acid, HD refers to hexadecanol (C-16 fatty alcohol), and SA refers to stearyl alcohol.

chemicals in metabolically engineered yeast. Expensive wastewater treatment processes to remove organic content could possibly be reduced or eliminated. To address any pathogenic organisms that could be harvested with the yeast, after lipid extraction, dry cell mass can be heated to high temperatures and pressures (350°C and 21,000 kPa).

In the future, analyzing the composition of wastewater through field analysis could improve the means to balance nutrient composition. In this project, overexpressing different genes involved in the production of triacylglycerols, linear saturated, unsaturated, aromatic dicarboxylic acids, and fatty acid methyl esters would allow for the creation of *S. cerevisiae* strains with the potential to replace a great number of artificial and environmentally harmful chemical production methods. Utilizing oleaginous yeast species in addition to *S. cerevisiae* could identify other microbial candidates for specialty and commodity chemical production. To develop commercially viable chemicals, processes such as dispersive liquid–liquid microextraction, cross-current liquid-liquid microextraction, or designing hydrophobic ionic liquids could allow for the isolation of organic acids (carboxylic acids, excreted fatty acids, and ethanol) from fermentation broth while also purifying biochemicals from dry yeast mass.

There were several limitations that impeded the investigation. While carboxylic acids were identified in wastewater GC-MS analysis, a metabolic engineering approach was not developed to increase the concentrations of these biochemicals. It will also be important to test wastewater from numerous sources to expand applicability beyond domestic wastewater treatment. While fatty alcohols and fatty acids were identified, the cost of completely purifying them into a commercially viable form can be calculated to assess economic feasibility. Lastly, GC-MS analysis involved preset parameters, including column thickness and size, mass spectrometer detector, flow rate, and carrier gas used, due its limited accessibility. Method development could have led to cleaner metabolite identification.

Compound	RT (min)	LOQ (ng/L)	Concentration (ng/L)
Acetone	2.02	7500	8400
Ethanol	3.16	7500	14300
Methanol	2.71	7500	7900
Acetaldehyde	1.66	8400	10200
Pentachlorophenol	10.29	1.2	4.5
4-Tert-Butylphenol	5.74	1.5	5.4
Bisphenol A	14.13	0.3	3.8
Triphenyl-phosphate	18.92	0.2	2.3
Chloromethane	9.61	0.6	4.1
Benzene	5.54	0.4	3.9
Bromomethane	5.99	0.8	4.6
Chloroethane	6.78	1.4	5.7
Chlorobenzene	7.61	0.7	3.6
Succinic Acid	ND	ND	ND
Malic Acid	ND	ND	ND
Oxalic Acid	ND	ND	ND

Table 2. Wastewater analysis before treatment. Select organic compounds identified in the initial wastewater obtained. In analysis of wastewater used before inoculation of *S. cerevisiae*, a host of volatile organics, aromatics, and phenols were identified. The table includes retention times (RT) and the limits of quantification (LOQ) for the organic compounds portrayed. ND indicates that the select organic compound was not detected.

METHODS

Saccharomyces cerevisiae (Carolina 173620) was first inoculated into 25 mL of defined medium (YPD) containing yeast extract (0.5 g/L), 20 g/L glucose, 5 g/L $(NH4)_2SO_4$, 14.4 g/L KH_2PO_4, 0.5 g/L $MgSO_4{\cdot}7H_2O$ adjusted to pH 6 (7). After sterilization, 2 mL/L trace element solution and mL/L of vitamin solution were added. The culture was grown for

Compound	RT (min)	LOQ (ng/L)	Concentration (ng/L)
Acetone	1.98	7500	11900
Ethanol	3.2	7500	27500
Methanol	2.77	7500	9500
Acetaldehyde	1.62	8400	20200
Pentachlorophenol	10.21	1.2	4.6
4-Tert-Butylphenol	5.76	1.5	2.7
Bisphenol A	ND	ND	ND
Tri-phenyl-phosphate	ND	ND	ND
Chloromethane	9.57	0.6	3.3
Benzene	5.58	0.4	1.5
Bromomethane	5.94	0.8	4.8
Chloroethane	6.78	1.4	4.6
Chlorobenzene	7.53	0.7	2.3
Succinic Acid	10.81	1.5	2.8
Malic Acid	13.48	1.1	2.3
Oxalic Acid	11.69	0.8	1.9

Table 3. Wastewater analysis after treatment. Select organic compounds identified after S. cerevisiae cells were inoculated in the wastewater-based medium over 4 days at 30°C. Phenolics, volatile organic compounds (VOCs), and aromatics can be seen, while concentrations of succinic acid, malic acid, and oxalic acid (all trace carboxylic acids from metabolic pathways) were also found. The table includes retention times (RT) and the limits of quantification (LOQ) for the organic compounds portrayed. ND indicates that the select organic compound was not detected.

4 days under lights at 25°C with shaking at 150 r.p.m, and spectrophotometry (OD600) was utilized to monitor cell density.

The *ACC1*, *FAS* and *Far1* genes were obtained as recombinant plasmids which all contained a URA-3 or LEU-2 selection marker, and an IPTG inducible marker. *DH5 alpha* cells transformed with plasmids containing *FAS, Far1, or ACC1* were procured from GenScript (*FAS* and *Far1*) and Addgene (*ACC1*). Once the bacteria were propagated using ampicillin as the selection marker for cells containing the respective plasmids, the plasmid DNA was then extracted. An overnight culture was pelleted after growing the LB medium to mid-log phase overnight at 37°C. Using a Monarch® Plasmid DNA Miniprep Kit, the DNA was isolated into 50 µl of elution buffer and quantified at 260 and 280 nm.

A lithium acetate (LiOAc) transformation procedure was used to insert the plasmid DNA into the *S. cerevisiae* cells. Denatured salmon sperm DNA, lithium sorbitol (LiSorb), heat shock (at 30°C and 42°C), and PEG (polyethene glycol) were used to enhance transformation efficiency. Cells were then grown on nitrogen base agar with supplements to take advantage of the URA-3 and LEU-2 selection markers.

We conducted a spectrophotometric assay to assess the activity of the *ACC1*, *FAS*, and *Far1* gene products in cell lysates (the acetyl CoA carboxylase, fatty acid synthase, and fatty acid reductase enzymes) (6). To do this, the reduction of NADPH to $NADP^+$ was analyzed by measuring absorbance at 340 nm. A reaction mix consisting of malonyl CoA, acetyl-CoA, NADPH and PBS was created. This was added to cell extracts containing protein that was extracted with lysis buffer. Over the span of 15 minutes, the absorbance of the solution was taken in 5-minute intervals. Concentrations of enzyme in each cell lysate was calculated using Beer's Law ($A = \varepsilon l c$, with extinction coefficient 6220 $mol^{-1}cm^{-1}$). Therefore, a higher absorbance indicated a smaller activity of the enzyme, as NADPH was reduced less frequently.

To verify the presence of C-16 and C-18 fatty alcohols and fatty acids, a high-performance liquid chromatography (HPLC) was conducted. Lipids were extracted from cell pellets using hexane and petroleum ether. HPLC analyses were performed using a silica-based column with a flow rate of 1 mL/min, a gradient composition, and compound standards of palmitic acid, hydroxy-palmitic acid, 1-hexadecanol, and stearyl alcohol were used.

Finally, mixed liquor (stage 1 wastewater containing solids and dissolved organic material) was collected from a local wastewater facility. Once collected, a modified wastewater-based media was created by adding nutrients, including vitamin B12, D(+) –biotin, nicotinic acid, calcium pantothenate, and thiamine-HCl $2H_2O$. Trace elements were composed of HCl (1 mL/L), $FeCl_2$-$4H_2O$ (15 mg/L), $ZnCl_2$ (7 mg/L), $MnCl_2$-$4H_2O$ (1 mg/L), $CuCl_2$ -$2H_2O$ (0.02 mg/L), NiCl2-$6H_2O$ (2.4 mg/L), and Na_2MoO_4 -$2H_2O$ (0.36 mg/L). Once the wastewater media was prepared, *S. cerevisiae* cells were grown in the media at 30°C over a period of 4 days and monitored for cell viability using spectrophotometry (OD600). Then, the wastewater was analyzed for total phenols, total phosphorus, total nitrogen, chemical oxygen demand, pH, purgable aromatics and purgable organics, C4 carboxylic acids, ethanol, and total hydrocarbons. A gas chromatograph connected to a mass spectrometer interface (GC-MS) was used to analyze for organic and aromatic compounds in association with a trap-and-purge method. We created a standard curve for each identified organic compound using external standards at varying concentrations. Each standard curve was constructed based on outputted peak area of the external standard, and concentrations of the organic compounds identified were subsequently determined. Phenols were identified after extraction from wastewater using methylene chloride and using a 2-propanol solvent.

ACKNOWLEDGEMENTS

I would like to thank Kepa Oyarbide, Diana Sood, and American Heritage School for providing the necessary materials, technical help, and guidance to complete this study at American Heritage School. I would also like to thank Dr. Kallidaikurichi Venkatachalam of Nova Southeastern University for his guidance, assistance in method development, and granting me access to materials.

Received: March 11, 2019
Accepted: June 5, 2019
Published: October 2, 2019

REFERENCES

1. Tanimura, A. "Selection of Oleaginous Yeasts with High Lipid Productivity for Practical Biodiesel Production." *Bioresource Technology*, Vol.153, 2014, pp. 230-235.
2. Chung, J. "Biodiesel Production from Oleaginous Yeasts Using Livestock Wastewater as Nutrient Source after Phosphate Struvite Recovery." *Fuel*, vol. 186, 2016, pp.305-310.
3. Nielsen, J and M. Gossing. "Metabolic Engineering of Saccharomyces Cerevisiae for Overproduction of Triacylglycerols." *Metabolic Engineering and Communications*, vol. 6, 2018, pp. 22-27.
4. Yu, T. *et al*. "Metabolic Engineering of Saccharomyces Cerevisiae for Production of Very Long Chain Fatty Acid-derived Chemicals." *Nature*, Article Number 15587, 2017, www.nature.com/articles/ncomms15587.
5. D'Espaux, L. *et al*. "Engineering High-level Production of Fatty Alcohols by *Saccharomyces cerevisiae* from Lignocellulosic Feedstocks." *Metabolic Engineering*, vol. 42, 2017, pp 115-125.
6. "Determination of NADH or NADPH Concentrations with the FL600™ Fluorescence Microplate Reader Using Fluorescence or Absorbance Modes." BioTek, www.biotek.com/resources/docs/FL600_Determining_NADH_&_NADPH Concentrations.pdf.
7. Runguphan, W. and J.D. Keasling. "Metabolic Engineering

of Saccharomyces Cerevisiae for Production of Fatty Acid-derived Biofuels and Chemicals." *Metabolic Engineering*, vol. 21, 2013, pp. 103-113.
8. Steen, Eric J. *et al.* "Microbial Production of Fatty-acid-derived Fuels and Chemicals from Plant Biomass." *Nature*, vol. 463, 2010, pp. 559-562.
9. Kulkarni, S, and J. Kaware. "Review on Research for Removal of Phenol from Wastewater." *International Journal of Scientific and Research Publications*, vol. 3, no. 4, 2013.
10. Sarris, D. et al. "Conversions of Olive Mill Wastewater-based Media by *Saccharomyces cerevisiae* through Sterile and Non-sterile Bioprocesses." *Journal of Chemical Technology*, Vol. 88, no.5, 2012.
11. Sarris, D. and S. Papanikolaou. "Production of Added-value Metabolites by Yarrowia Lipolytica Growing in Olive Mill Wastewater-based Media under Aseptic and Non-aseptic Conditions." *Engineering in Life Sciences*, vol.17, no. 6, 2017
12. Kawai, Shigeyuki. "Transformation of *Saccharomyces cerevisiae* and Other Fungi." *Bioengineered Bugs*, vol.1, 2010, pp. 395-403,

Copyright: © 2019 Ramesh and Joykutty. All JEI articles are distributed under the attribution non-commercial, no derivative license (http://creativecommons.org/licenses/by-nc-nd/3.0/). This means that anyone is free to share, copy and distribute an unaltered article for non-commercial purposes provided the original author and source is credited.

JOURNAL OF
EMERGING INVESTIGATORS

Article

Comparing Consumer Personality and Brand Personality: Do Fashion Styles Speak of Who You Are?

Brianna Stevenson and Jason Scott
The Neighborhood Academy, Pittsburgh, PA

SUMMARY

Teenagers, especially African American teens, are an important target market for fashion retailers. Identifying what type of customer is interested in which brands is a principal concern. This study investigated how fashion brand personalities are similar to people's personalities and whether people may prefer a particular clothing brand based on their own personal traits. We hypothesized that individuals prefer brands that share similar personality traits to their own. In particular, we expected that there would be significant correlations between people's Big Five Personality Trait scores and how much they desire a specific brand personality. All together, we found that the Big Five Personality Factors are generally not related to participants' preferred brand personalities. Out of the 25 hypothesized relationships, only four were significant. Extraversion was positively related to emotive and sociable brands, and agreeableness was negatively related to sincere or trusted brands. Therefore, if a brand is marketed as outgoing or sociable, then investing in attracting extraverted customers could be useful, and the brand should target people who are high in extraversion. Otherwise, brands should consider different factors besides the Big Five Personality Factors for identifying potential customers.

INTRODUCTION

One important fashion market is teens; teenagers spend an average of 36% of their money on fashion clothing, representing a huge opportunity for businesses. In particular, African American teens spend about $1.2 trillion annually (1). Brands cannot maximize profit if they do not target the right consumers. Furthermore, African Americans' consumer choices create a "halo effect" that can affect the purchases of other social groups, making a study of their brand preferences important (2).

One common way to determine a person's personality is the Big Five personality factors. The Big Five personality group consists of five primary factors of personalities that represent nearly all of the basic personality traits (3). The Big Five is also known by the acronym OCEAN to abbreviate the five personality factors. The Big Five personality factors are: openness to experience, conscientiousness, extraversion, agreeableness, and neuroticism.

Openness to experience is described as an individual's creativity and how they are disposed to open up and try new things. Individuals who are high in openness to experience are more likely to enjoy stepping outside the box and meeting new people. Individuals who are low in openness to experience are more likely to stick to what they already know and their regular routines. Some traits that are commonly related to openness to experience are creativity, curiosity, and having a variety of interests.

The second personality factor is conscientiousness. It is described as an individual's behavior and how they act in sociable ways. People who are high in conscientiousness are more likely to be successful, well-organized, and like to play by the rules. People who are low in conscientiousness are more likely to procrastinate and do things on their own. Traits that describe conscientiousness are hard-working, planner, ambitious, and reliable.

Extraversion is described as how individuals present their energy and how they connect with others. Individuals who are high in extraversion are more likely to interact with others and be very outgoing. Individuals who are low in extraversion are more likely to be shy and keep to him or herself. Traits that are linked to extraversion are socialness, outgoingness, and high energy.

Agreeableness is described as how people get along and interact with others. People who are high in agreeableness are more likely to be caring, be well-liked, and respected. People who are low in agreeableness are more likely to be rude, blunt, and sarcastic. The traits that are connected to agreeableness are trust, loyalty, politeness, and sensitiveness.

Lastly, neuroticism is described as individuals who have negative traits that deal with their lack of emotional stability. Individuals who are high in neuroticism are more likely to have low self-esteem, to be emotional, and be easily angered. Individuals who are low in neuroticism are more likely to be very confident and courageous. The traits that are linked to neuroticism are insecurity, anxiety, moodiness, and lack of confidence.

Brand personality is a group of human characteristics that are attributed to a brand by consumers (4,5). There are five common brand personalities: emotive, trusted, sociable, exciting, and sincere (4). Common traits of these personalities are listed in **Table 1**. Other researchers have proposed other

Brand Personality	Common Traits of Each Brand Personality Type	Brands
Emotive	Emotional, idealistic	Gucci, Pink, Champion
Trusted	truthful, reliable, preserving	North Face, Levi, Old Navy
Sociable	friendly, creative, outgoing	Hollister, Vans, Forever 21
Exciting	active, adventurous, cool	Nike, Jordan, Adidas
Sincere	simple, caring, helpful	Polo, Columbia, H&M

Table 1. Common traits and representative brands for different brand personalities. Previous research suggests these are common personalities traits of the different brand personalities (4).

brand personalities, although these do not relate directly to human personality traits (6). A recent meta-analysis on brand personality found that consumers see their personalities as matching brand personalities they like, and when that happens, positive outcomes occur for businesses (5).

Casidy *et al*. investigated the relationship between consumer personalities and brand personalities among college-aged Australian students (4). They found that there was a significant relationship between some of the Big Five Personality Factors and their corresponding brand personalities. People with more neuroticism and conscientiousness personalities prefer trusted brands. People high in extraversion and openness to experience preferred the sociable brand personality. Exciting, sincere, and emotive brand personalities showed no relationship to any of the Big Five. Their findings suggest that there is a weak relationship between personality and brand personality.

Another study by Ayman and Kaya investigated gender differences in behavior based on branded fashion in a Turkish cohort (6). The authors found that individuals of a certain type of personality tend to like similar brands that shared the same personalities. Also, their study found that individuals associate with brands with which they share personalities. This is important to our study because their study concluded that personality and brand personality have strong relationships, although they did not use the Big Five personality traits or standard named brand personalities. Our study will use different personalities factors and brand personalities, while also using African American teens to see if personality and brand personality also have a stronger relationship.

Personality, mood, and self-concept play a role in individual's clothing choices and clothing preferences. Individuals tend to make their clothing choices based on the way they are feeling. Barquet and Balam researched the effect of clothing preferences on undergraduate students' clothing decisions based on factors such as mood, personal style, desire to feel comfortable, and self-esteem (7). They found that mood, personal style, a desire to feel comfortable, a presentation during class, and weather influenced clothing choices. This is important to our current study because if mood and personality play a role in an individual's clothing preferences, people should prefer brands that reflect their personality.

An additional study found there was a strong relationship between mood and three out of the five Big Five Personality Factors and clothing preferences (8). However, she also found that personality and clothing choice had a very weak relationship. Although personality and clothing choices do not have a strong relationship, the relationship between mood and three out of the five personality factors was strong, which supports our current study.

Burroughs studied the relationship between clothing and social identity (9). In his first study, the kind of person the participant is could be determined based only on clothing, but only for certain personality traits. In his second study, he found that brands by themselves do not seem to reflect a person's personality (9). Dolich, studied the congruent relationship between self-images and product brands. The author found that people preferred brands that were more similar to their ideal self-image rather than their real self-image (10). This study is similar to our current study because we are looking to see if people connect with brands that are similar to their personality. The study shows that people's ideal-self connects with brands that are similar to their personalities.

Another study by Piacentini and Mailer investigated symbolic consumption, the importance of goods and consumables in teenagers' clothing choices (11). They found that clothing choices made by young people are closely bound to their self-concept and used as a means of self-expression, a way of judging people and situations they have faced. They also found that teens use symbolic consumption to maximize their ability to belong to a group. This study is helpful because it discussed how people's self-concept plays a role in clothing choices and how they try to fit in to a group.

We investigated how fashion brand personalities are similar to people's personalities and how people may prefer a particular brand based on their own personal traits. Overall, research suggests that there are some relationships between how people see themselves and their clothing preferences. However, there is limited research on how the Big Five and brand personalities are related, especially with African American consumers. Our experiment consisted of African American students from a private college-preparatory high school called The Neighborhood Academy. We will have a group of the upperclassmen list a variety of brands that they prefer or like and categorize them into brand personalities. Next, we will have the other students take the Big Five Inventory (BFI) and connect their personalities with The Big Five personality factors. Then, we will take the list of the brands and ask students do they or will they prefer or desire that brand. We hypothesized that individuals prefer brands that share similar personality traits to their own and that there would be significant correlations between people's Big Five scores and how much they desire a specific brand personality. This agrees with previous research on personality and self-concept (4, 5, 7, 10, 11), which found significant but not strong relationships between people's personalities and brand personalities. We are not predicting specific relationships between the Big Five and individual brand personalities because many of the brand traits could align with multiple of the Big Five factors. Our intent is to explore all the possible

Subject personality factor (max = 10)	Openness	Conscientiousness	Extraversion	Agreeableness	Neuroticism
Mean	7.0	6.3	5.9	6.1	5.3
SD	0.78	0.14	0.14	1.13	0.71
Preference for brand personality (max = 5)	**Trusted**	**Sincere**	**Sociable**	**Excited**	**Emotive**
Mean	3.8	3.3	3.5	3.3	3.1
SD	0.71	0.99	0.71	0.77	0.64

Table 2. Means and Standard Deviations for Big Five Personality Traits and Brand Personalities.

Personality Factor / Brand Personality	Openness to Experience	Conscientiousness	Extraversion	Agreeableness	Neuroticism
Trusted	0.173	0.022	-0.202	-0.254*	0.109
Sincere	-0.091	-0.145	0.119	-0.347*	0.050
Sociable	0.049	0.065	0.34*	0.033	0.022
Exciting	0.089	-0.101	0.071	-0.015	0.014
Emotive	0.195	0.17	0.27*	-0.166	0.202

Table 3. Pearson correlation coeffecient matrix between personality factors and brand personalities. Significant correlations marked with an asterisk ($p < 0.05$, $n = 55$).

relationships between the two.

RESULTS

We sought to investigate how fashion brand personalities are like people's personalities and how people may prefer a brand based on their own personal traits. A focus group of 14 African American teens generated a list of 15 brands, three for each brand personality. Then, fifty-five African American teenage participants completed the Big Five Inventory as well as a survey to measure their preference towards each of the brands from the focus group. The brand questionnaire consisted of 15 clothing brands, three for each brand personality. The participants were to rate each brand on a scale of one through five with five being very likely to desire or prefer that specific brand. Each person's preference score for each brand personality was found by averaging the preference score for each brand of the three brands (**Table 2**). We calculated correlations between subject's preference for brands of different brand personalities and the Big Five personality factors (**Table 3, Figure 1**).

We observed a significant positive Pearson correlation coefficient between the extraversion personality factor and the sociable brand personality ($r(53) = 0.339$, $p = 0.006$). People who are high in extraversion tend to desire a sociable brand. There was also a significant positive correlation between a person's extraversion and desiring of an emotive brand ($r(53) = 0.270$, $p = 0.02$). People who are high in extraversion tend to prefer an emotive brand. As seen, there was a significant negative correlation between agreeableness and a trusted brand ($r(53) = -0.254$, $p = 0.03$). People who are high in agreeableness tend to like, prefer, or desire a less trusted brand. Lastly, there was a significant negative correlation between agreeableness and a sincere brand ($r(53) = -0.346$, $p = 0.004$). People who are high in agreeableness tend to not like a sincere brand. All other correlations were not significant (**Table 3**).

These correlations are significant ($p < 0.05$) and

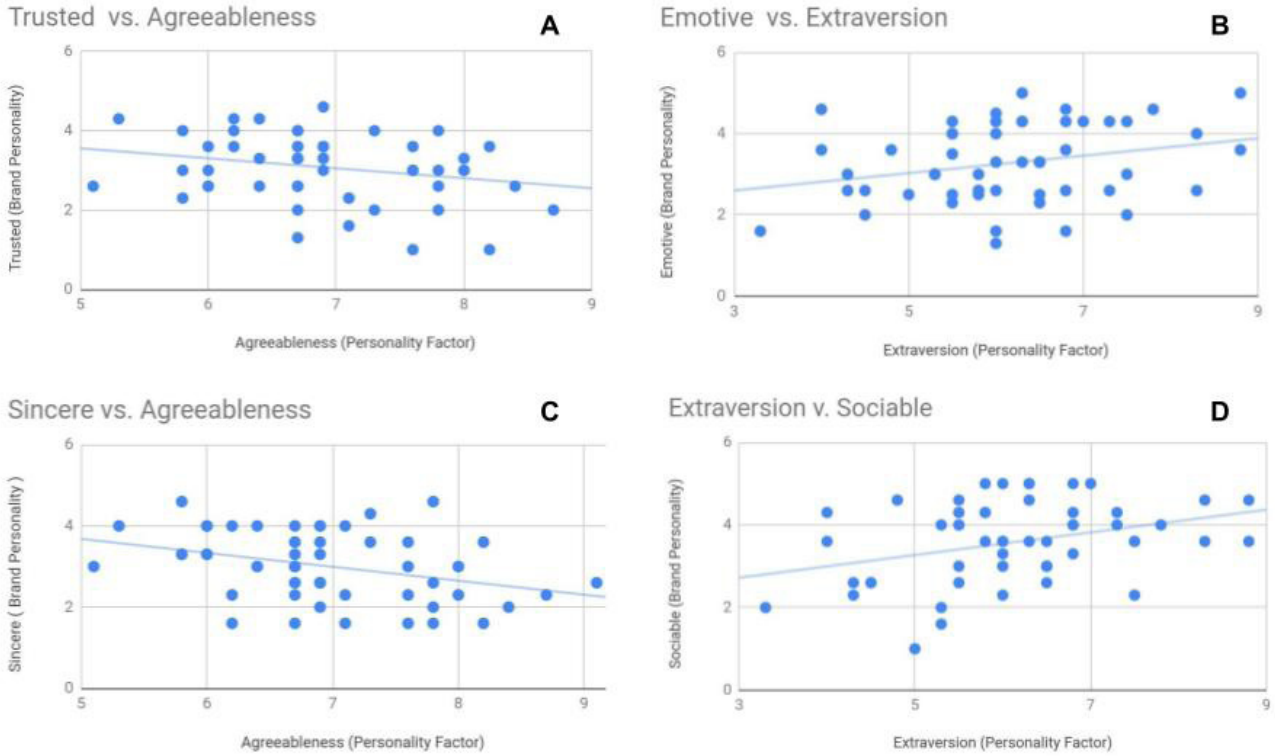

Figure 1. Significant correlations between personality factors and brand personalities. Listed above are the four significant correlations between personality factors and brand personalities ($p<0.05$, $n=55$). Agreeableness was negatively correlated with trusted brands (A) and sincere brands (C). Extraversion was positively correlated with emotive (B) and sociable brands (D).

demonstrate a significant relationship between a participant's personality factors and their preference for brands of a certain brand personality type. This suggests that there is a relationship between how a person views themselves and the types of brands he/she wishes to buy.

DISCUSSION

We found that some of the Big Five Personality Factors (openness, conscientiousness, extraversion, agreeableness, and neuroticism) had a relationship with five common brand personalities (trusted, sincere, sociable, exciting, and emotive). Four out of the 25 correlations had a significant relationship (**Table 3**). People who reported being more agreeable tended to dislike a sincere brand or a trusted brand. A person who was high in extraversion tended to prefer a sociable brand or an emotive brand (**Figure 1**).

Our research was partially consistent with prior research (4). Casidy *et al*. found that there was a significant relationship between some of the Big Five and their corresponding brand personalities. People with higher neuroticism and conscientiousness personality scores preferred trusted brands and the sociable brand personality was preferred by people high in extraversion and openness to experience. Exciting, sincere, and emotive brand personalities showed no relationship to any of the Big Five in their study. We found that there was also a significant relationship between some of the Big Five and brand personalities. One relationship that we found in common was that people who are high in extraversion prefer a sociable brand. Altogether, this was important because the Big Five Personality Factors are not very useful when it comes to brands. Unless a brand is outgoing or sociable, then investing in finding extra customers is useful and they should target people that are high in extraversion. Otherwise, brands should consider other factors besides the Big Five Personality Factors for market segmentation and advertising.

Our study was also partially consistent with prior research on personality and clothing preference (6). Ayman and Kaya found that individuals of a certain type of personality tend to like similar brands that shared the same personalities. We found that there was also a significant relationship between some of the Big Five Personality Factors and brand personalities. Although they did not use the Big Five Personality Factors or standard named brand personalities, their research was similar to our study. They concluded that there was a strong relationship between personality and brand personality, which we did not find.

Prior research by Eisend and Stockburger-Sauer, who did a meta-analysis review on brand personalities, was also partially consistent with our research (5). They found that consumers see their personalities as matching brand personalities. Because of that, positive things may happen, like building trust and strong brand relationships. This is like what we found because if a brand is outgoing or sociable, then investing in finding extraverted customers may be useful, and brands should target people who are high in extraversion

One surprising result of our study was the negative correlation between agreeableness and sincere and trusted brands. Agreeableness is described as when people get along and interact with others well. People who are high in agreeableness are more likely to be someone who cares for others, is well-liked, and respected. The brands that were categorized by the focus group as sincere were Polo, Columbia, and H&M and for trusted North Face, Levi, and Old Navy. We are uncertain why agreeableness had a negative relationship with sincere and trusted brands. We hypothesized that they would have a positive relationship because they shared similar adjectives like trusting, caring, and helpful. However, both relationships were very weak. Therefore, we would not recommend that marketers use this information when reaching customers. It is also possible our results are unique to the brands the focus group picked, and a different list of brands might have a different result.

There were two limitations to our study, which might have affected the results. First, our focus group had difficulty agreeing on some brand personalities. Our focus group consisted of 14 high school seniors. During the focus group, members often could not agree on the designation of a specific brand to a brand personality group. The group had to vote to come to a decision. Therefore, the brands in each category could be different when assigned by a different focus group. Also, some students complained the questionnaire was too long. So, it is possible that some of the students rushed through it, which could have affected our data. We saw no direct evidence of people randomly circling, but the complaints do tell us some rushing may have happened.

We recommend future research have other people take the Big Five Inventory to describe another person instead of having them take it about him or herself. We believe it would be interesting to use ratings of personality by friends instead of self-ratings because they may not be telling the truth, compared to how a friend would view them. It is possible that the personality that other people see might be more related to the brand personalities people prefer, since clothing choices often reflect the social group to which one wishes that he/she belonged (9).

In conclusion, the Big Five Personality Factors may not be useful when describing people's preferences for brand relationships. Our study, as well as others, have found few and weak relationships between the two. We recommend that marketers and brand promoters use other factors to target customers who will buy and promote their brands.

METHODS

The participants were students from 9th through 11th grade from The Neighborhood Academy, a college preparatory, private high school. There were 60 students invited to participate in total, 64% female and 36% male. Five students declined to participate in the study so we had 55 participants in our study. We also had a focus group with the senior class

(14 students), in order to develop a list of brand personalities.

The materials were The Big Five Inventory and a self-created brand survey. The BFI is a personality test that measures the Big Five dimensions to determine a person's personality (3). We modified the test because students did not understand certain words. Words such as quarrels, aloof, and assertive were replaced with similar words that students knew such as argues, not friendly, and demanding.

We also made a brand personality questionnaire, which 14 senior students, acting as a focus group, helped create. The focus group categorized the brands into different brand personalities (**Table 1**).

In the focus group, we had participants each write down ten clothing brands that they like, desire, or prefer. Then they placed them into the brand personalities where they best believe they connect to, and we discussed why they chose to place the brands where they did. After the discussion, the group had to agree on three brands for each of the brand personalities. When the group could not agree, the brand personality was assigned by voting. At the conclusion of the focus group session, a total of 15 clothing brands were divided into brand personality groups with three brands per group.

After the focus group helped created the brand personality questionnaire, both the BFI and the brand personality questionnaire were given to the 55 study participants over a two-week period. On the brand personality questionnaire, the participants were to rate each brand on a scale of one through five with five being very likely to desire or prefer that specific brand. Each person's preference score for each brand personality was found by averaging the preference score for each brand of the three brands. Participants completed the questionnaires during class time in small groups of 5-10 students. Students who participated were given a few pieces of candy in exchange for their participation.

ACKNOWLEDGEMENTS

We would like to thank the 2019 class of seniors at The Neighborhood Academy for participating in our focus group and all of the academic advisors for allowing us to use their advisory time to administer the survey.

REFERENCES

1. Steensland, Pamela. "Piper Jaffray Completes Semi-Annual Generation Z Survey of 8,600 U.S. Teens." *Business Wire*, 2018, www.businesswire.com/news/home/20181022005679/en/Piper-Jaffray-Completes-Semi-Annual-Generation-Survey-8600. Accessed 3 May 2019.
2. "Black Impact: Consumer Categories where African Americans Move Markets." *Nielsen*, February 15, 2018, www.nielsen.com/us/en/insights/news/2018/black-impact-consumer-categories-where-african-americans-move-markets.html. Accessed 3 May 2019.
3. Ackerman, Courtney. "Big Five Personality Traits & The 5-Factor Model Explained." *Positive Psychology Program.* 23 June 2017. https://positivepsychologyprogram.com/big-five-personality-theory/. Accessed 3 May 2019.
4. Casidy, Riza, *et al*. "The Big Five and Brand Personality: Investigating the Impact of Consumer Personality on Preferences Towards Particular Brand Personality." *Journal of Brand Management*, vol. 1, no. 14, 2007, pp. 1-12.
5. Eisend, Martin and Nicola E. Stokburger-Sauer. "Brand Personality: A Meta-Analytic Review of Antecedents and Consequences." *Marketing Letters*, vol. 24, Sept. 2013, pp. 206-16.
6. Kaya, Anil K. and Umut Ayman. "Consumption of Branded Fashion Apparel: Gender Differences in Behavior." *Society for Personality Research*, vol. 42, 2014, pp. 1-8.
7. Barquet, Jasmine and Esenc Balam. "Clothing Preferences of College Students: What Factors Matter?" *The Journal of Undergraduate Ethnic Minority Psychology*, vol. 1, no. 1, March 2015, pp. 4-6.
8. Moody, Wendy. "An Exploratory Study: Relationships Between Trying on Clothing, Mood, Emotion, Personality and Clothing Preference." *Journal of Fashion Marketing and Managment,* vol.14, no.1, pp.161-179.
9. Burroughs, Jeffrey, *et al*. "Clothing and Society." *Clothing and Textiles Research Journal*, vol. 11, no.1, September 1992, pp. 18-23.
10. Dolich, Ira J. "Congruence Relationships Between Self Images and Product Brands." *Journal of Marketing Research*, vol. 6, no.1, Feb. 1969, pp. 80-84.
11. Piacentini, Maria and Greig Mailer. "Symbolic Consumption in Teenager's Clothing Choices." *Journal of Consumer Behavior*, vol. 3 no.3, September 2013, pp. 251-61.

Received: April 09, 2019
Accepted: September 20, 2019
Published: September 24, 2019

Copyright: © 2019 Stevenson and Scott. All JEI articles are distributed under the attribution non-commercial, no derivative license (http://creativecommons.org/licenses/by-nc-nd/3.0/). This means that anyone is free to share, copy and distribute an unaltered article for non-commercial purposes provided the original author and source is credited.

JOURNAL OF
EMERGING INVESTIGATORS

Article

Behavioral Longevity: The impact of smoking, alcohol consumption, and obesity on life expectancy

Jun Ho Han[1] and Yongseung Han[2]
[1]North Oconee High School, Bogart, Georgia
[2]University of North Georgia, Dahlonega, Georgia

SUMMARY

This paper attempts to contribute to our understanding of human longevity by focusing on the impact of our daily life on longevity. In analyzing cross-sectional data from 174 countries in 2015 that are publicly available, e.g., from the World Health Organization, we assumed a simple linear relationship between life expectancy and behavioral factors when other factors, e.g., medical and environmental factors, are held constant. We estimated the parameter values of the behavioral factors in the equation by representing the relationships using ordinary least squares. With the approximately 89% explanatory power in the variation of longevity in the sample of 174 countries, we conclude that an average person's life expectancy in those 174 countries can increase by more than 3 years if smoking and alcohol consumption is reduced by a half and weight is decreased by 10%.

INTRODUCTION

The human life span has extended over the past decades. According to the World Health Organization (WHO), the average life expectancy at birth has increased from 52.5 years in 1960 to 71.7 years in 2015 (1) (**Figure 1**).

As life expectancy has extended, the topic of any influencing factors in longevity has featured prominently in research, both for medical, commercial, and public reasons. Research in academia has focused on individual longevity, e.g., why some individuals live longer than others, and on average life expectancy, e.g., what factors contribute to the mean life expectancy of a population (2-4). For individual longevity, a recent National Institute on Aging study identified a broad range of social, behavioral, genetic, and environmental factors that can affect the risk of mortality among older adults (5). Among those factors, it is notable that approximately 15–25% of the overall variation in human longevity can be explained by genetic differences. It is also worth noting that long-lived individuals have fewer chronic diseases, better mental health, and better physical and cognitive function than short-lived members of their age cohort. For the mean longevity of a population, in addition to the factors identified for longer life spans, social and behavioral factors have been emphasized as crucial to the average level of longevity in a given population.

On genetic factors, studies have produced little consensus on the "maximum" achievable lifespan of an individual. The traditional view held by the scientific community is that the maximum life span has not increased, despite the fact that the average life span has been on the rise for the last several decades. The ideal average life span is approximately 85 years, and the changes in lifestyle that can postpone chronic illness can modify the physiological and psychological markers of aging, causing the morbidity curve to become more rectangular (6). That is, the percentage of the survived in the cohort population decreases slowly for most of the life span, and then drops drastically once it hits a certain point closer to the average life span. On the contrary, other studies have disputed the traditional view, arguing that "maximum" life expectancies can be raised in the future through advances in biomedical research, as well as the reduction of age-related risk factors. It is possible to have a life expectancy of 95 to 100 years with a standard deviation of about 10 years (7). In fact, this view has already been seen in practice in animal research; one study reported that a single mutation in the nematode Caenorhabditis elegans genome doubled life span (8).

Several studies that focused on both medical and environmental factors have discussed how life expectancy has increased over time due to different reasons. Most of the gain in life expectancy before 1950 was due to reductions in infant, child, and early adult mortality as a result of improved standards of living, better public health standards, and the

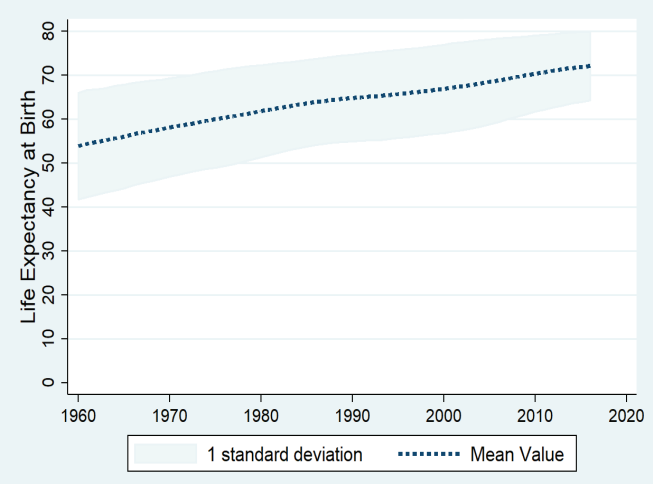

Figure 1: Time trend of life expectancy at birth from 1960 to 2016. The dotted line denotes the mean value of life expectancies of the countries in the world. The shaded area shows one standard deviation of the life expectancies.

advancement of medicine, while the increase in life expectancy since 1950 has largely been due to reductions in mortality at older ages (2, 9). In particular, the role of medical factors in mortality is well documented in comparative studies of several high-income countries (4). In addition to medical factors, average income levels (GDP per capita) and educational environment (e.g., rate of literacy) are closely related to the increase in life expectancy in developing countries (10).

On social and behavioral factors, several studies have identified that individual behavior in smoking, drinking alcohol, and eating also affects longevity. First, the harms of smoking have been near universally acknowledged by many authorities, like the Center for Disease Control and Prevention (11), the Royal College of Physicians (12), and the International Agency for Research on Cancer (13). It was speculated as early as 1938 that smoking was associated with a shortening of duration of life and that the degree of this decease increased as the amount of smoking increased, although tobacco was not supposed to further harm those who had survived to 70 or more (14). A 2014 report from the U.S. Surgeon General concluded that more than 20 million premature deaths can be attributed to smoking (15). Life expectancy among smokers is much shorter than life expectancy among those who never smoke (16). Even among centenarians, smoking is still incompatible with successfully attaining long life (17). And even those who quit smoking in old age, like 65 years of age, can gain 1.4 to 3.7 years in life (18).

Second, unlike smoking cigarettes, alcohol has been recognized as having a U-shaped or J-shaped relation to mortality (19). That is, mortality rate decreases as alcohol consumption increases from zero (i.e., abstinence) to moderate drinking, and then it increases to a higher level as alcohol consumption increases further to heavy drinking. Various health benefits and risks (i.e., cardiovascular or blood pressure, etc.) have been discussed for the relationship between alcohol consumption and longevity (20- 22).

Third, it is now quite well known that obesity causes adverse impacts on health, like diabetes, heart disease, high blood pressure, and some cancers, and thus reduces life expectancy (4). The negative effects of an increase in body mass index (BMI) would overwhelm the positive effects of a decline in smoking, and it is predicted that obesity would shorten life expectancy by 0.71 years between 2005 and 2020 (23) The world-wide phenomenon of an increase in obesity is traced to advancements in technology and an increasingly sedentary lifestyle that have lowered the real price of food as well as the physical expenditure of calories per hour worked, both in market and household production (24).

Variable	Description (Unit)	Mean	Std. Dev	Min	Max
Longevity	Life Expectancy (Years)	71.2	8.4	48.9	83.7
Smoking	No. of cigarettes per person per day	18.2	12.2	1	108.9
Alcohol	Liters of pure alcohol per capita per year	6.2	4.1	0.1	17.4
BMI	Body Mass Index (Kg/m^2)	25.63	2.23	20.50	32.90
Overweight	Prevalence of Overweight and obese (% of adults)	47.12	16.08	17.70	78.30
Disease	Cause of Death by Communicable Disease (% of death)	22.3	19.9	1.4	65.6
Injury	Cause of Death by Injury (% of death)	9.0	4.1	2.7	29.3
HDI	Human Development Index (between 0 and 1)	0.698	0.155	0.352	0.949

Table 1: Summarized Statistics of Data. Data Sources: Longevity, BMI, Overweight, Disease, and Injury are from the World Health Organization, Smoking and Alcohol are from the Our World in Data, and HDI is from the United Nations Development Program.

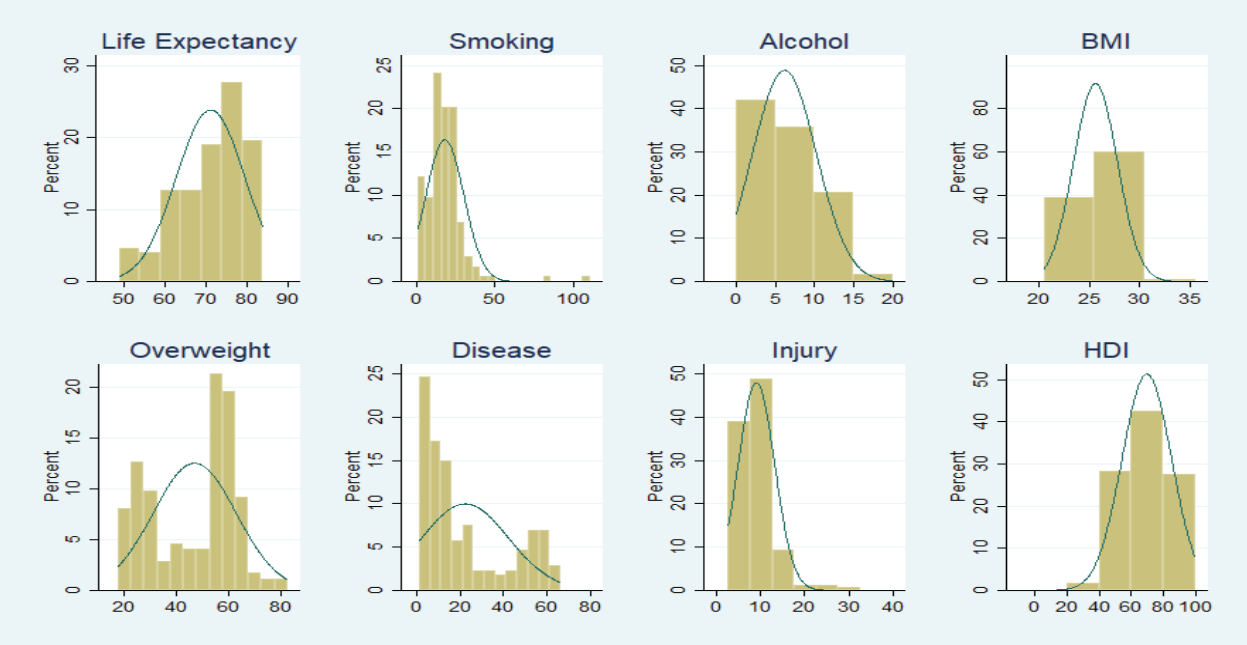

Figure 2: Histograms of data. Histogram shows how a variable is distributed. Bar in each panel indicates what percentage of the countries are clustered in the range of each variable. Line in each panel indicates the normal distribution of each variable.

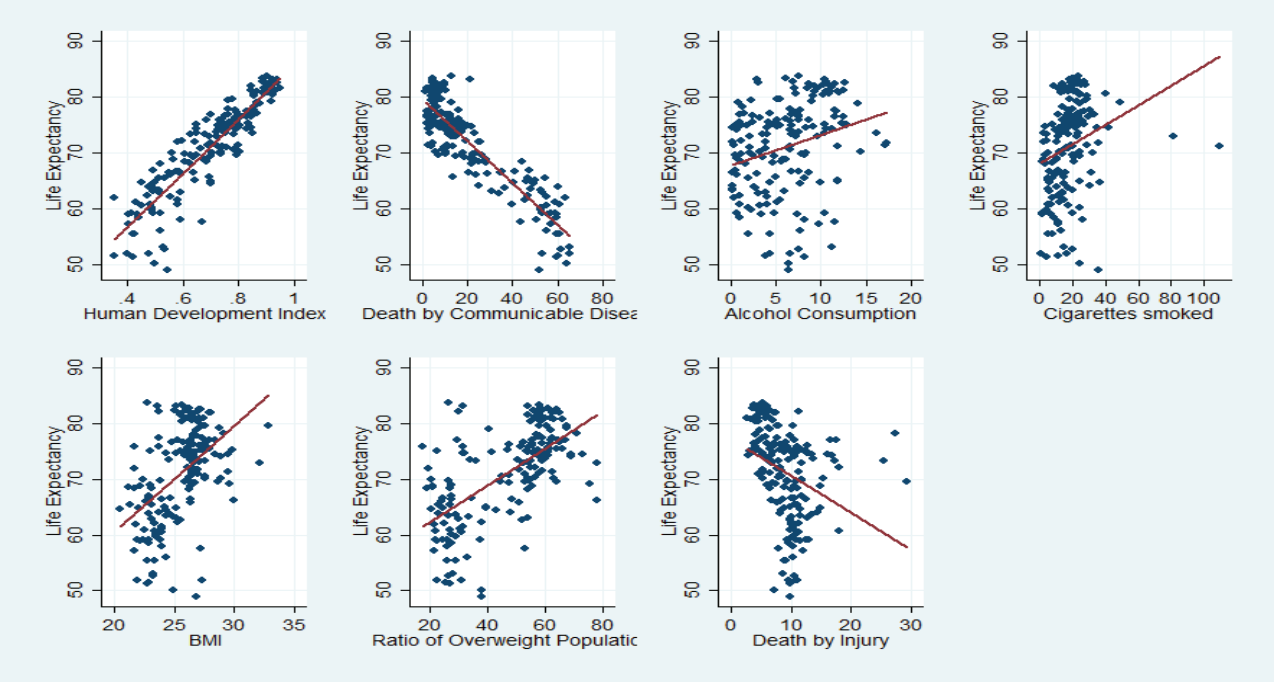

Figure 3: Relationship between life expectancy and contributing factors. Each panel shows how life expectancy and a factor is correlated. The line in each panel shows the linear trend line.

Due to the volume of existing research on longevity, it is important to summarize what is already known about the factors of longevity and determine the importance of behavioral factors on longevity. People eat and drink. Some smoke cigarettes, among other risk factors. However, it is hypothesized that obesity, alcohol consumption, and cigarettes are harmful to longevity. From this hypothesis, this paper will attempt to quantify the consequences of our daily behaviors on longevity. By quantifying any impacts, inferences can be made regarding the relationship between longevity and the behavioral variables of interest, such as alcohol consumption, obesity, and cigarette smoking.

RESULTS

Following the literature review on the behavioral determinants of longevity, we chose 3 behavioral factors, i.e., alcohol consumption, smoking cigarettes, and obesity, and collected data on the factors as well as other variables, i.e., life expectancy, death by disease, death by injury, and the Human Development Index (HDI). The data, collected from 3 different sources (WHO, United Nations Development Program, and Our World in Data), were combined in a way that a country with any missing observations is dropped from our analysis. These data cover 174 countries in 2015 (**Table 1**). As of 2015, the average life expectancy of 174 countries (the mean of Longevity) is 71.2 years, and the world population deviates, on average, 8.4 years from the mean and skewed to the left as more countries clustered on the right side of the mean value (**Figure 2**). The table also shows that an adult smokes 18.2 cigarettes a day (slightly less than one pack of cigarettes a day) and drinks 6.2 liters of alcohol a year (approximately one bottle of beer a day), although there is a huge variation among countries. For obesity, it is somewhat striking that the global average BMI is 25.63 kg/m^2, which is outside normal range (18.5–25.0 kg/m^2), and falls into the category of overweight, and that almost one half of the entire adult population (47.12%) is either overweight or obese. In some countries, most notably Kiribati and Tonga, this ratio even approaches 80% (**Figure 3**).

For the variables whose effects on longevity must be separated, 22.3% and 9.0% of all deaths are caused by communicable diseases and injuries, respectively. The average HDI is 0.698, which means that the world, on average, achieves 69.8% of the arbitrarily defined level of standard living.

We then analyzed how the behavioral factors are correlated to each other. It turns out that the correlation coefficients, measuring the degree of correlation between variables, range 0.135~0.318 that are statistically significant at the level of 0.05 except the correlation between Alcohol and BMI (**Table 2**). The correlation between Alcohol and BMI

	Smoking	*Alcohol*	*BMI*	*Overweight*
Smoking	1.000			
Alcohol	**0.1791** (0.018)	1.000		
BMI	**0.3178** (0.000)	0.135 (0.076)	1.000	
Overweight	**0.3060** (0.000)	**0.2279** (0.003)	**0.8647** (0.000)	1.000

Table 2: Correlation coefficient (ρ) and *p*-values for the test: the null hypothesis (ρ=0) vs. the alternative hypothesis (ρ≠0). Bold numbers represent the correlation coefficients that are statistically significant at 0.05, meaning that zero correlation is as unlikely as less than the probability of 0.05.

	Specification A		Specification B	
	Coefficient	(p-value)	Coefficient	(p-value)
Smoking	**-0.038**	**(0.032)**	**-0.046**	**(0.027)**
Alcohol	**-0.279**	**(0.000)**	**-0.262**	**(0.000)**
Overweight			**-0.059**	**(0.001)**
BMI	**-0.568**	**(0.000)**		
Disease	**-0.206**	**(0.000)**	**-0.201**	**(0.000)**
Injury	0.029	(0.559)	0.014	(0.787)
HDI	**34.645**	**(0.000)**	**37.753**	**(0.000)**
R^2	0.891		0.885	
Adjusted R^2	0.888		0.881	

Table 3: Results of estimating the relation between life expectancy (dependent variable) and contributing factors (independent variables). ( ) denotes *p*-values. The difference of Specifications A and B is what variable is used for obesity. Specification A has BMI for obesity and Specification B has Overweight for obesity.

is statistically significant only at the level of 0.1. The degrees of the correlation are weak, but positive. Thus, we can say that a country in higher consumption in smoking tends to show more consumption in alcohol and to a higher level of obesity.

The estimated results for the relationship between longevity and several other factors are shown in **Table 3**. The results, based upon the ordinary least squares method that estimates the parameters of the variables in a way to minimize the squares of the estimation errors, explain 88.5% (for the model called Specification B where Overweight is included for obesity) or 89.1% (for the model called Specification A where BMI is included for obesity) of the variation in Longevity, as given by the R^2 value. This means that 10.9% or 11.5% of the variation in Longevity is not explained by the factors that are used in the estimation. The unexplained portion in the variation of longevity may be due to genetic factors or something else that is not in the estimation. The adjusted R^2, when the numbers of explanatory variables and observations are considered, merely budged and thus provides the similar explanation.

	Developed Economies 50 countries		Developing Economies 97 countries		Undeveloped Economies 27 countries	
Smoking	0.016	0.012	**-0.041**	**-0.044**	0.078	0.081
	(0.660)	(0.757)	(0.059)	(0.046)	(0.354)	(0.355)
Alcohol	-0.044	-0.022	**-0.318**	**-0.316**	**-0.362**	-0.275
	(0.647)	(0.832)	(0.000)	(0.000)	(0.087)	(0.194)
BMI	**-0.477**		**-0.329**		**-1.178**	
	(0.046)		(0.031)		(0.072)	
Overweight		0.011		**-0.046**		-0.140
		(0.754)		(0.055)		(0.159)
Disease	0.053	0.117	**-0.251**	**-0.253**	**-0.189**	**-0.218**
	(0.527)	(0.240)	(0.000)	(0.000)	(0.070)	(0.048)
Injury	-0.039	-0.084	**0.131**	**0.129**	-0.235	-0.321
	(0.607)	(0.295)	(0.079)	(0.086)	(0.565)	(0.454)
HDI	**53.193**	**57.022**	**29.836**	**30.318**	**45.785**	**40.767**
	(0.000)	(0.000)	(0.000)	(0.000)	(0.011)	(0.023)
R^2	0.716	0.689	0.841	0.839	0.675	0.654
Adjusted R^2	0.676	0.645	0.830	0.828	0.578	0.550

Table 4: Empirical Results by different groups. ( ) denotes *p*-values. Note: the sample of 174 countries is divided into 3 groups (developed, developing, and undeveloped economies) based upon the classification of the World Bank.

For the parameter values, the *p*-values of all variables except Injury, which indicate the probability that the null hypothesis that the parameter is zero, are low. That is, the *p*-values of Alcohol, BMI (or Overweight), Diseases, HDI are less than 0.01 while the *p*-value of Smoking is 0.027~0.032 that is marginally significant. Thus these parameter values can be used to explain the impact on longevity.

For the variables that are controlled to separate the impact of behavioral factors on longevity, a reduction in the deaths by communicable disease (Disease) is sure to increase life expectancy (that is, an 0.2-year increase in life expectancy by lowering the deaths by communicable disease by 1%), while it is unclear that altering the parameter value for death by injury (Injury) would affect longevity. Any improvement in our standard of living (denoted by HDI) also increases life expectancy, as expected.

To see if the above results are robust to social and environmental factors, we divided the whole sample (174 countries) into 3 groups (developed, developing, and undeveloped economies) based upon the country classification of the World Bank (25) among other classifications such as the United Nations Development Program and the International Monetary Fund. The difference in the classification hinges on the definition of development (26). There are 50 countries in the developed economies, 97 countries in developing economies, and 27 countries in undeveloped economies in our data sample. Then, the same estimation method is employed to show the results in the **Table 4**.

Table 4 shows that the significance of behavioral factors to longevity is robust to the developing economies and resembles that in the sample of 174 countries. That is, Smoking, Alcohol, and BMI (and Overweight) all decrease life expectancy in a similar fashion. However, the significance of behavioral factors to longevity weakens in the developed and undeveloped economies. Of these factors, only BMI is significant to longevity in developed economies, while Alcohol and BMI are significant to longevity in the undeveloped economies. A weaker significance of behavioral factors is coupled with a weaker explanatory power of the estimation. The overall explanatory power of the estimation, denoted by R^2, is 65.4% or 84.1%, which is lower than R^2 in the whole sample, when smaller observations are used for estimation. On the contrary, HDI, which gives the standard of living, is significant for all 3 groups, indicating that any improvement in the standard of living is essential to longer life expectancy. Similarly, a decrease in the death by communicable (Disease) is also important to longer life expectancy in both developing and undeveloped economies.

DISCUSSION

Decades of research have shown that human longevity is a complicated result of many different influences, including medical, genetic, environmental, social, and behavioral factors. Here, we focused on behavioral factors such as

smoking cigarettes, alcohol consumption, and obesity to investigate how these factors affect life expectancy and to what extent. By using cross-sectional data from 174 countries in 2015, a simple linear relationship between life expectancy and behavioral factors was assumed when other factors, like medical and environmental factors, were separated.

First, a decrease of one cigarette in daily smoking increases life expectancy by an estimated 0.038 or 0.046 years. Simply speaking, if a person smokes only one half of what he or she currently smokes, the person could live 0.35 or 0.42 years (4.2 or 5.0 months) longer. Second, a reduction of one liter of alcohol in yearly alcohol consumption increases life expectancy by 0.262 or 0.279 years. If a person skips a bottle of beer every other day, the person could live 1.09 or 1.30 years (13 or 15.6 months) longer. Third, a decrease in body weight also leads to longer life spans: a decline in one unit of BMI could extend life spans by 0.568 years. If a person is 175 cm tall, the person could live 6.8 months longer by simply losing 3 kg in weight. If the same person (175 cm tall) loses 10% of his or her weight, that person could live 17.5 months longer. Similarly, the life expectancy of a country could increase by 0.95 years (11.3 months) if a country's ratio of overweight or obese residents declines by its standard deviation (16.1%). In summary, the estimation results predict that life expectancy can increase by more than 3 years if behaviors in smoking cigarettes, drinking alcohol, and eating too much are changed.

Although this study clearly shows the importance of human behavior on longevity, it must be acknowledged that there may be many more factors affecting longevity, such as peace of mind, regular exercise, etc., as human life is very complex and the nature of life is still not completely known. As evidenced in the subsequent estimation by different groups of economies, the significance of behavioral factors diminishes in developed countries and undeveloped countries and the explanatory power of the estimation weakens as a smaller number of countries is analyzed. This empirical evidence humbles our understanding of human life. In this respect, we suggest that the results on the magnitude of behavior's impact be interpreted in a relative sense, not in an absolute sense.

Our study on longevity emphasizes the importance of our daily life in longevity. A change in our daily life in order to smoke fewer cigarettes, drink less alcohol, and prevent obesity does not only extend our life span, but it also reduces a cost of individual and public burden of healthcare. For this reason, any public policies or initiatives discouraging drinking and smoking and preventing obesity should be encouraged. Potential policy interventions might include restricting the marketing of alcohol or tobacco products, mandating simple and informative nutritional labelling on all food products, increasing taxes on tobacco and alcohol products, and launching a public initiative to encourage daily physical exercise.

METHODS

A main goal of this study was to quantify the extent to which behavioral factors, on average, influence longevity. For this purpose, simple linear relations between life expectancy (representing longevity) and each factor is assumed:

$$Longevity = b_0 + b_1 \times Factor_1 + \cdots + b_n \times Factor_2 + e \quad (1)$$

where $b_0 \cdots b_n$ are the parameters (n is the number of the factors), and e represents any errors that cannot be attributed to the factors affecting longevity. By assuming a linear relation, the magnitude of the behavioral factors on longevity can be represented by the values of the parameters in the above equation. While the factors affecting longevity are identified by the real data, the value of the parameters must be estimated. One method to scientifically guess the value is to estimate the parameters in a way that minimizes any errors.

For this purpose, an ordinary least squares method was used to find the value of parameters ($b_0, \cdots b_n$) in a way that minimized the squares of e that represents any errors where

$$e = Longevity - b_0 - b_1 \times Factor_1 - \cdots - b_n \times Factor_n \quad (2)$$

For example, the value of e^2 is calculated by inserting some arbitrary values, e.g., $b_0 = 1, \cdots, b_3 = 1$, given the data on the factors. A scientific guess would be to choose the parameter values to minimize the value of e^2 among many other values of e^2 that are calculated from the different values of parameters.

To use this ordinary least squares method, the factors affecting longevity must be identified. It is known, from the literature review as explained in the Introduction of this paper, that human longevity is affected by factors such as genetic, social and behavioral, medical, and environmental factors. Behavioral factors that are related to our daily life, in particular, are of interest: obesity, tobacco use, and alcohol consumption. Data on smoking cigarettes and tobacco products (a.k.a. Smoking) and drinking alcohol (a.k.a. Alcohol) were obtained from an organization, Our World in Data (https://ourworldindata.org), which compiles various data such as population, health, food, energy, etc. Smoking and Alcohol were retrieved from the menu, research by topic, health, in its website. Smoking shows the number of cigarettes and other tobacco products per person per day, and Alcohol shows the average amount (liters) of pure alcohol per person over a year. For obesity data that were collected from the Global Health Observatory data at WHO (http://apps.who.int/gho/data/node.imr), two different data are used; BMI and Overweight. BMI indicates an average body mass index of a population; body mass index is calculated from a person's weight in kilograms divided by the square of the person's height in meters (kg/m^2). Overweight indicates the percentage of adults who are either overweight or obese. A person with a BMI equal to or more than 25 is considered overweight, and a person with a BMI of 30 or more is considered obese.

The linear equation, shown above in (1), can be better explained when the impact of other factors on longevity, such as medical and environmental, are separated from the impact of behavioral factors on longevity. For this purpose, the following factors are included in the equation: death by communicable disease, death by injury, and standard of living.

The factors of death by communicable disease (or Disease) and death by injury (or Injury) are collected from the Global Health Observatory data at WHO. Disease represents the percentage of all deaths by communicable diseases, while Injury represents the percentage of deaths by injury. The standard of living is represented by the HDI is obtained from the United Nations Development Program (hdr.undp.org/en/data), which includes the Gross National Income per capita (representing income) and years of schooling (representing education), among other factors.

In the equation above, Longevity is the dependent variable. Life expectancy at birth, which was chosen to be a proxy for Longevity, is also collected from the Global Health Observatory data at WHO. It indicates the predicted average number of years a newborn infant would live if prevailing patterns of mortality at the time of its birth were to stay the same throughout its life.

Given this information, the following equation is estimated by the ordinary least squares:

$$Longevity = b_0 + b_1 \times Smoking + b_2 \times Alcohol + b_3 \times BMI\ (or\ Overweight) + b_4 \times Disease + b_5 \times Injury + b_6 \times HDI + e \quad (3)$$

Received: May 19, 2019
Accepted: September 15, 2019
Published: October 3, 2019

REFERENCES

1. Global Health Observatory (GHO) data. *World Health Organization*. 2018, www.who.int/gho/mortality_burden_disease/life_tables/situation_trends/en/. Accessed 26 May 2018.
2. Christensen, Karre, and James W. Vaupel. "Determinants of Longevity: Genetic, Environmental, and Medical Factors." J*ournal of Internal Medicine*, Vol. 240, 1996, pp. 333-341.
3. Caselli, Graziella, and Marc Luy. "Determinants of Unusual and Differential Longevity: an Introduction." *Vienna Yearbook of Population Research*, No. 11, 2013, pp. 1-13.
4. National Research Council. Explaining Divergent Levels of Longevity in High-Income Countries. Edited by Crimmins, Eileen M., et al. Panel on Understanding Divergent Trends in Longevity in High-Income Countries. Committee on Population, Division of Behavioral and Social Sciences and Eduction, *The National Academies Press*, 2011.
5. Mather, Mark, and Paola Scommegna. "Longevity Research: Unraveling the Determinants of Healthy Aging and Longer Life Spans." *Population Reference Bureau Newsletter*, No. 34, 2016, pp. 1-9.
6. Fries, James F. "Aging, Natural Death, and the Compression of Morbidity." *The New England Journal of Medicine*, Vol. 303, No. 3, 1980, pp. 130-135.
7. Manton, Kenneth G., et al. "Limits to Human Life Expectancy: Evidence, Prospects, and Implications." *Population and Development Review*, Vol. 17, No. 4, 1991, pp. 603-637.
8. Kenyon, Cynthia, et al. "A C. elegans Mutant That Lives Twice as Long as Wild Type." *Nature*, Vol. 366, No. 6454, 1993, pp. 461-464.
9. Vaupel, James W. "How Change in Age-Specific Mortality Affects Life Expectancy." *Population Studies*, Vol. 40, 1986, pp. 147-157.
10. Lin, Ro-Ting, et al. "Political and Social Determinants of Life Expectancy in Less Developed Countries: a Longitudinal Study." *BMC Public Health*, Vol. 12, No. 1, 2012, pp. 85-92.
11. "History of the Surgeon General's Report on Smoking and Health." *Centers for Disease Control and Prevention*, 2006, www.cdc.gov/tobacco/data_statistics/sgr/history/index.htm.
12. "What the RCP Thinks about Tobacco." *Royal College of Physicians*. 2018, www.rcplondon.ac.uk/projects/outputs/what-rcp-thinks-about-tobacco.
13. International Agency for Research on Cancer. IARC Monographs on the Evaluation of Carcinogenic Risks to Humans. *World Health Organization*, Vol. 83, 2004.
14. Pearl, Raymond. "Tobacco Smoking and Longevity." *Science*, Vol. 87, No. 2253, 1938, pp. 216-217.
15. National Center for Chronic Disease Prevention and Health Promotion, Office on Smoking and Health. The Health Consequences of Smoking – 50 Years of Progress: A Report of the Surgeon General. U.S. Department of Health and Human Services, 2014.
16. Jha, Prabhat, et al. "21st Century Hazards of Smoking and Benefits of Cessation in the United States" *The New England Journal of Medicine*, Vol. 368, No. 4, 2013, pp. 341-350.
17. Tafaro, L., et al. "Smoking and Longevity: an Incompatible Binomial?" *Archives of Gerontology and Geriatrics*, Vol. 38 Supplement, 2004, pp. 425-439.
18. Taylor, Donald H., et al. "Benefits of Smoking Cessation for Longevity." *American Journal of Public Health*, Vol. 92, No. 6, 2002, pp. 990-996.
19. Pearl, Raymond. Alcohol and Longevity, Alfred A. Knopf Inc. 1926.
20. Marmot, Michael G., et al. "Alcohol and mortality: a u-shaped curve" *The Lancet*, Vol. 317, No. 8220, 1981, pp. 580-583.
21. Gronbæk, Morten, et al. "Influence of Sex, Age, Body Mass Index, and Smoking on Alcohol Intake and Mortality." *British Medical Journal*, Vol. 308, No. 6924, 1994, pp. 302-306.
22. Klatsky, Arthur L. and Gary D. Friedman. "Annotation: Alcohol and Longevity." *American Journal of Public Health*, Vol. 85, No. 1, 1995, pp. 16-18.
23. Stewart, Susan T., et al. "Forecasting the Effects of Obesity and Smoking on U.S. Life Expectancy." *The New England Journal of Medicine,* Vol. 361, No. 23, 2009, pp.

2252-2260.
24. Philipson, Tomas. “The World-Wide Growth in Obesity: an Economic Research Agenda.” *Health Economics*, Vol. 10, 2001, pp. 1-7.
25. World Bank. How does the World Bank classify countries? 2019. datahelpdesk.worldbank.org/knowledgebase/topics/19280-country-classification. Accessed 21 July 2019.
26. Nielsen, Lynge. “Classifications of Countries Based on Their Level of Development: How It Is Done and How It Could Be Done.” IMF Working Paper, No. 11/31, 2011.

Copyright: © 2017 Karuppiah and Ramiah. All JEI articles are distributed under the attribution non-commercial, no derivative license (http://creativecommons.org/licenses/by-nc-nd/3.0/). This means that anyone is free to share, copy and distribute an unaltered article for non-commercial purposes provided the original author and source is credited.

JOURNAL OF
EMERGING INVESTIGATORS

Article

Development of Al_2O_3 Coated PVA (Polyvinyl Alcohol) Composite Nonwoven Separator For Improving Thermal and Electrochemical Properties

Junoh Kim[1] and Ji-Sang Yu[2]

[1] Korea International School, Jeju Campus, Republic of Korea

[2] Advanced Batteries Research Institute, Korea Electronics Technology Institute, Republic of Korea

SUMMARY

In modern world, lithium-ion batteries are widely used in electronic devices, such as smartphones, laptops, and electric cars. However, they are highly unstable during charging and their capacity drops significantly over time, despite them being highly efficient and easy to use. Therefore, it is imperative to develop more efficient batteries. Polyolefin-based lithium-ion battery separators are limited by their weak thermal stability. In order to overcome such limitations, we developed a ceramic-coated and nonwoven materials-based composite separator. We hypothesized that the method used to develop the separator will have improved thermal and electrochemical properties because of superior air permeability and electrolyte uptake. This separator was manufactured by utilizing the Dip-coating method, whereby ceramic layers composed of Al_2O_3 nanoparticles and Polyvinylidene fluoride-hexafluoropropylene (PVDF-HFP) were coated to both sides of a Polyvinyl alcohol (PVA) support which was fabricated by electrospinning. The ventilation map and electrolyte uptake demonstrated that the composite nonwoven separator had superior electrolyte uptake properties when compared to conventional PE separators. This resulted in excellent electrochemical properties - especially a great increase in high-rate discharge characteristics. Finally, thermal shrinkage was improved compared to conventional PE separators indicating greater thermal stability. Overall, our PVA separator displayed superior thermal and electrochemical properties. By gaining knowledge on improving heat and thermochemical properties, we can gain critical insight on future lithium-ion battery designs that have to work in extreme conditions.

INTRODUCTION

The Lithium-ion battery is a type of rechargeable battery that has a graphite cathode and lithium anode. Lithium-ion batteries are currently used as a power source for many modern electronic devices such as drones, electric vehicles, smartphones, and smart watches. The safety of lithium-ion secondary batteries is ultimately determined by their propensity for internal short circuits, which occur when the cathode and anode directly contact with each other. Separators prevent physical contact between the cathode and the anode, and are therefore the most important component of the battery that guarantees safety (1). However, even though the separator plays a vital role in ensuring a battery's safety, it is primarily regarded as a pathway for lithium ions. As a result, most of the studies regarding separators are focused on the battery's performance improvements, which leave studies on safety extremely lacking (2).

The most common separator used in lithium-ion secondary batteries is made with polyolefin materials that provide chemical and electrochemical stability and remarkable mechanical properties (2-4). However, due to the material properties of polyolefin and the manufacturing process for lithium-ion secondary batteries, the components undergo extreme heat contraction at high temperatures, resulting in increased prevalence of internal short circuits (2-4). In order to overcome the limits of polyolefin materials, many recent studies have focused on nonwoven separators that have been produced by electrospinning, due to their great thermal stability (4-7). However, because the manufacturing of most of these nonwoven separators utilizes macromolecules that require organic solvents, they inevitably raise concerns regarding safety, health, and the environment. Moreover, the manufacturing process produces large pore structures that lead to defective charging from internal short circuits (2, 8). It is necessary to control the pore size in nonwoven separators during the manufacturing process, in order to adapt nonwoven separators successfully in lithium-ion secondary batteries. In this vein, many studies are aiming to coat polymer binder or polymer binder plus Al_2O_3 or ZrO_2 ceramics on nonwoven separators (4, 9-14).

In this study, a single composite ceramic nonwoven separator with improved thermal stability and electrochemical properties was developed. We hypothesized that composite PVA and PVA coated with Al_2O_3 nanoparticles and PVDF-HFP (6Al-PVA) separators would produce better electrochemical and thermal stability properties when compared with commercial polyethylene (PE) separators. A Polyvinyl alcohol (PVA) supporter was utilized due to its water-soluble properties, thus precluding the need for organic solvents and rendering the manufacturing process more environmentally friendly. PVA is also extremely chemically stable, has superior physical and chemical properties compares to those of current separator materials, and is widely used in the fabrics and film industry (12). To control the PVA supporter's pore size, layers of Al_2O_3 nanoparticles and

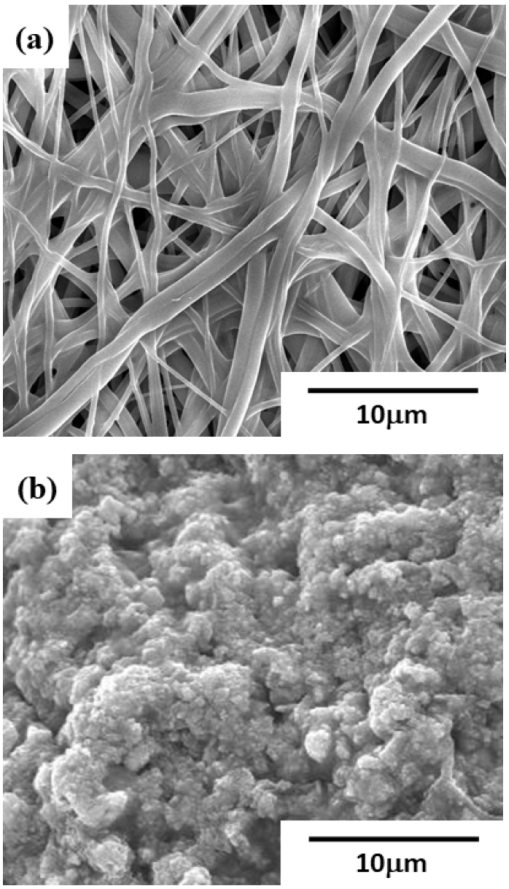

Figure 1. Electron microscopy images of different seperators. **(a)** PVA nonwoven separator and **(b)** 6Al-PVA composite separator. Values mentioned: 1-2 μm, 5-10 μm , less than 1 μm.

Polyvinylidene fluoride-hexafluoropropylene (PVDF-HFP) binders were coated onto both sides of PVA supporter using the Dip-coating method. The electrochemical properties and thermal stability of the resulting separator was then compared against conventional PE separators. Results from this study will evaluate the feasibility of incorporating such separators into lithium-ion secondary batteries. We determined that a battery with PVA separator has improved thermal and electrochemical properties.

RESULTS

We observed the microscopic structure of the PVA nonwoven supporters and PVA coated with Al_2O_3 nanoparticles and PVDF-HFP (6Al-PVA) by electron microscopy (**Figure 1a**). A single strand of the PVA supporter as manufactured by electrospinning had a thickness of roughly 1-2 μm with pore sizes ranging from 5-10 μm (**Figure 1a**). For 6Al-PVA, a ceramic coating layer of Al_2O_3 and PVDF-HFP polymer binder was observed on the surface of the PVA nonwoven supporter (**Figure 1b**). As a result of the additional ceramic coating layers, the pore size of the PVA supporter was reduced to less than 1 μm.

We hypothesized that the addition of a ceramic coating would alter the physical properties of the separator. To test this hypothesis, we measured the air permeability. Higher air permeability, meaning that air experiences more difficulty when penerating an object, is associated with improved battery performance. The uncoated PVA supporter had an air permeability of 2.7 s/sec (**Figure 2**), which is considered extremely poor and can be explained by pore sizes between 5~10 μm. By contrast the 6Al-PVA nonwoven separator's air permeability was much improved at 148.7 s/sec (**Figure 2**).

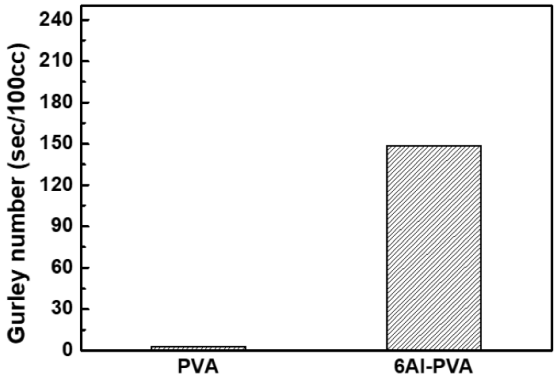

Figure 2. Air permeability test results of PVA nonwoven separator and 6Al-PVA composite separator. Valued mentioned: 2.7 s/sec, 148.7 s/sec.

Given that the introduction of a ceramic coating layer could considerably affect electrolyte uptake, we measured electrolyte uptake. Electrolyte uptake of the 6Al-PVA separator was compared to a conventional PE separator. The 6Al-PVA separator had a greater than 47% increase in electrolyte uptake by comparison to the conventional PE separator (**Figure 3**). The increase in electrolyte uptake means the 6Al-PVA separator has a greater capacity for electrical conductance.

To evaluate the developed separator's electrochemical properties, we built a coin-type full cell. A full cell, just like a typical lithium-ion battery, uses an active material as the anode and materials such as graphite for the cathode. The charge/discharge profiles of coin-type full cells containing PVA nonwoven supporter and 6Al-PVA were measured. The coin-type full cell containing the PVA nonwoven supporter did not reach its final discharge and continued to charge (**Figure 4a**). This phenomenon is explained by minute internal short circuits that are caused by the pores of the PVA nonwoven supporter. This is also commonly observed in other types of nonwoven separators (3.8). In contrast, the 6Al-PVA full cell was able to successfully complete charging (**Figure 4b**). This is because the introduction of the ceramic coating layer allows control of the PVA nonwoven supporter's pore sizes, resulting in decreased pore sizes and the inhibition of internal short circuits. The superior air permeability and electrolyte uptake observed in the 6Al-PVA separator should influence the discharge rate, which was therefore tested directly. The discharge rate of the 6Al-PVA separator was compared against a conventional PE separator. The 6Al-PVA separator,

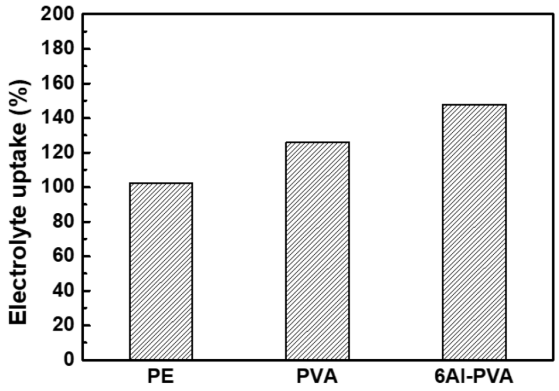

Figure 3. Electrolyte uptake test results of various separators. PVA nonwoven separator, 6AI-PVA composite separator, and conventional PE separator. Value mentioned: 47%.

in 3C discharge had 53.9% of its initial capacity remaining, while the conventional PE separator, in 3C discharge had only 45.7% of its initial capacity remaining (**Figure 4c**). This is likely due to the superior electrolyte uptake of the 6AI-PVA separator.

Lastly, in order to test the thermal stability of the 6AI-PVA separator, we performed a thermal shrinkage test at 150°C. The conventional PE separator had 91% of thermal shrinkage at 150°C, while 6AI-PVA separator had 7.4% of thermal shrinkage at the same temperature (**Figure 4d**). This proves the 6AI-PVA separator's highly increased thermal stability, which can be explained by the PVA nonwoven separator's inherent thermal stability (120°C thermal shrinkage: 19%, 150°C thermal shrinkage: 34%) and the ceramic coating layer functioning as a thermal-resistant material.

DISCUSSION

In this study, we developed a composite ceramic nonwoven separator coated with Al_2O_3 and a polymer binder PVDF-HFP with improved thermal stability and electrochemical properties. We determined that the PVA nonwoven separator's inherent superior air permeability and electrolyte uptake remained consistent even after the coating with a ceramic layer. After the ceramic coating, the PVA nonwoven separator's minuscule pores were reduced to less than 1 μm, which diminished incomplete charging due to internal short circuits. We believe that higher air permeability for PVA nonwoven separator comes from the ceramic coating filling the pores.

As determined by the high-rate discharge experiment, we found that the 6AI-PVA separator exhibited a superior discharge rate in comparison to a conventional PE separator. This may be explained by the 6AI-PVA separator's excellent electrolyte uptake. The improved electrolyte uptake is likely due to the hydrophilic properties of the PVA supporter used in manufacturing the 6AI-PVA. Moreover, micropores on the ceramic coating layer may also retain additional electrolytes.

Lastly, we observed that the 6AI-PVA separator had markedly diminished thermal shrinkage, with only 7.4% of

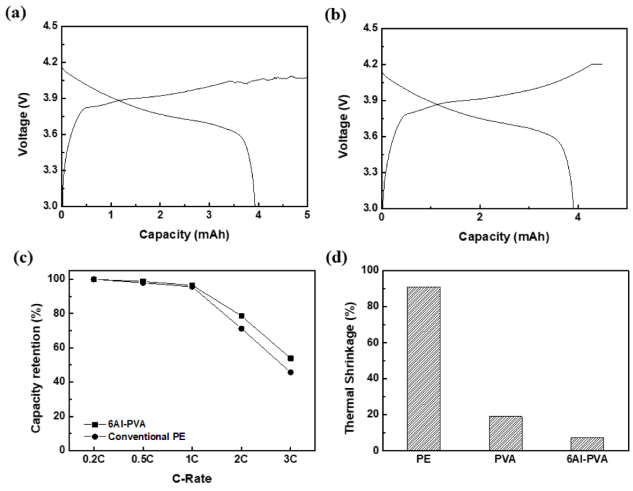

Figure 4. Electrochemical properties of separators. Charge-discharge of PVA nonwoven separator (**a**) and 6AI-PVA composite separator (**b**).The high-rate discharge test results of 6AI-PVA and conventional PE (**c**). Thermal shrinkage test results of conventional PE, PVA, and 6AI-PVA at 150°C (**d**). Values mentioned: 53.9%, 45.7%, 91%, 7.4%.

thermal shrinkage while the conventional PE separator had 91% thermal shrinkage. Thus, the 6AI-PVA separator has superior thermal stability without any loss in electrochemical properties.

Our study has potential limitations regarding reproducibility/batch-to-batch variability in separator construction because only one sample was used. Currently, we found that the moisture content in the experiment can affect the reproducibility of separator morphology strongly. Therefore, sample reproducibility could be improved by producing and testing the supporters in a controlled atmosphere.

In conclusion, the composite ceramic nonwoven separator (6AI-PVA), built by coating a ceramic layer on PVA nonwoven supporter, has superior high-rate discharge properties and thermal stability by comparison to a conventional PE separator. In the near future, we anticipate that such PVA-based, ceramic-coated nonwoven separators may replace conventional PE separators in the lithium-ion batteries of EVs and drones that require a high-rate of discharge.

MATERIALS AND METHODS

The PVA supporter (NTpia, thickness: 20 ± 1 μm) was manufactured by electrospinning, with polymer binder PVDF-12% w/v HFP (Kynar 2801, molecular weight = 470,000, named PVDF-HFP), and 40~50 μm Al_2O_3 nanoceramic particles being used. The coating solution was produced by spraying Al_2O_3 and PVDF-HFP binder in acetone (solids were controlled 5% w/v and Al_2O_3 / PVDF-HFP ratio was controlled 60% w/v Al_2O_3 : 40% w/v PVDF-HFP). The coating solution was coated on PVA nonwoven supporter through Dip-coating. The separator coated with the above solution is referred to as 6AI-PVA.

Structural analysis of the PVA supporter and coated

separator was performed by electron microscopy (FE-SEM, JEOL JSM-7000F), and a Gurley-type densometer (Toyoseiki) was used to analyze air permeability. Gurley-type densometer was used to compress 100 cc of air and measure the time the air takes to go through the separator. The Gurley value represents the time required for a certain air to pass a certain area of separator under certain pressure. A thermal shrinkage test was conducted to test the separator's thermal stability properties. A specimen was prepared at a size of 5 cm x 5 cm and was kept at 120ºC and 150ºC for one hour. Then, the change in area was measured, and shrinkage percentage (%) = (Wf - Wi) / Wi × 100, was calculated (Wi = initial area of the separator, Wf = final area of the separator after putting 1 hour at designated temperatures). To calculate the electrolyte uptake, the separator was immersed in electrolyte solution for one hour, and weighed before and after the immersion was measured. To measure ionic conductivity, a Li metal/separator/Li metal symmetrical cell (2032 coin) was built and Re values were measured via an AC impedance analysis (Solatron 1280C). Ionic conductivity was calculated by using the following equation (σ (ionic conductivity) = d / (A * Re), where d=separator thickness, A=separator area, Re=electrolyte resistance).

To produce a coin-type full cell, $LiCoO_2$ was used to form a cathode, and graphite was used to form an anode. An electrolyte solution was produced by adding 1M $LiPF_6$ and Ethylene Carbonate (EC) / Ethyl Methyl Carbonate (EMC) (30% w/v : 70% w/v) with 3% w/v Vinylene Carbonate (VC). The coin-type full cell was galvanostatically charged and discharged in a voltage range from 3.0 to 4.2 to measure the reversible capacity. And the rate discharge tests were performed in the range of 3.0–4.2 V at currents of 0.2, 0.5, 1.0, 2.0, and 3.0 C. Capacity was calculated by a charge-discharge tester while constructing a coin type full-cell with designated capacities per unit area for anode and cathode. The capacities per unit area for the cathode and anode were 3.4 ± 0.1 mAh/cm^2 and 3.8 ± 0.1 mAh/cm^2, respectively.

Acknowledgements

I wish to express my sincere gratitude to the Korea Electronics Technology Institute for allowing me to use their equipment.

Received: March 18, 2019
Accepted: September 02, 2019
Published: September 00, 2019

REFERENCES

1. Arora, Pankaj, and Zhengming (John) Zhang. "Battery Separators." *Chemical Reviews*, vol. 104, no. 10, 13 Oct. 2004, pp. 4419–4462., doi:10.1021/cr020738u.
2. Lee, Hun, *et al*. "A Review of Recent Developments in Membrane Separators for Rechargeable Lithium-Ion Batteries." *Energy & Environmental Science, The Royal Society of Chemistry*, 18 Aug. 2014, https://pubs.rsc.org/en/content/articlelanding/2014/ee/c4ee01432d#!divAbstract.
3. Zhang, Sheng Shui. "A Review on the Separators of Liquid Electrolyte Li-Ion Batteries." *Journal of Power Sources*, vol. 164, no. 1, 10 Jan. 2007, pp. 351–364., doi:10.1016/j.jpowsour.2006.10.065.
4. Kritzer, Peter. "Nonwoven Support Material for Improved Separators in Li–Polymer Batteries." *Journal of Power Sources*, vol. 161, no. 2, 27 Oct. 2006, pp. 1335–1340., doi:10.1016/j.jpowsour.2006.04.142.
5. Kim, Youngkwon, *et al*. "Shutdown-Functionalized Nonwoven Separator with Improved Thermal and Electrochemical Properties for Lithium-Ion Batteries." *Journal of Power Sources*, vol. 305, 15 Feb. 2016, pp. 225–232., doi:10.1016/j.jpowsour.2015.11.106.
6. Zhang, Xiangwu, *et al*. "Electrospun Nanofiber-Based Anodes, Cathodes, and Separators for Advanced Lithium-Ion Batteries." *Polymer Reviews*, vol. 51, no. 3, 11 Aug. 2011, pp. 239–264., doi:10.1080/15583724.2011.593390.
7. Cho, T. H., *et al*. "Electrochemical Performances of Polyacrylonitrile Nanofiber-Based Nonwoven Separator for Lithium-Ion Battery." *Electrochemical and Solid-State Letters*, vol. 10, no. 7, 17 Apr. 2007, doi:10.1149/1.2730727.
8. Lee, J. -R., *et al*. "SiO2/Styrene Butadiene Rubber-coated Poly(ethylene terephthalate) Nonwoven Composite Separators for Safer Lithium-ion Batteries." *Journal of Electrochemical Science and Technology*, vol. 2, no. 51, 2011., doi:10.5229/2011.2.1.051
9. Cho, Tae-Hyung, *et al*. "Silica-Composite Nonwoven Separators for Lithium-Ion Battery: Development and Characterization." *Journal of The Electrochemical Society*, vol. 155, no. 9, 25 July 2008, doi:10.1149/1.2956965.
10. Choi, Sung-Seen, *et al*. "Electrospun PVDF Nanofiber Web as Polymer Electrolyte or Separator." *Electrochimica Acta*, vol. 50, no. 2-3, 30 Nov. 2004, pp. 339–343., doi:10.1016/j.electacta.2004.03.057.
11. Lee, Yong Min, *et al*. "Novel Porous Separator Based on PVdF and PE Non-Woven Matrix for Rechargeable Lithium Batteries." *Journal of Power Sources*, vol. 139, no. 1-2, 4 Jan. 2005, pp. 235–241., doi:10.1016/j.jpowsour.2004.06.055.
12. Zhang, Chunxue, *et al*. "Study on Morphology of Electrospun Poly(Vinyl Alcohol) Mats." *European Polymer Journal*, vol. 41, no. 3, Mar. 2005, pp. 423–432., doi:10.1016/j.eurpolymj.2004.10.027.
13. Kim, Ki Jae, *et al*. "Enhancement of Electrochemical and Thermal Properties of Polyethylene Separators Coated with Polyvinylidene Fluoride–Hexafluoropropylene Co-Polymer for Li-Ion Batteries." *Journal of Power Sources*, vol. 198, 15 Jan. 2012, pp. 298–302., doi:10.1016/j.jpowsour.2011.09.086.
14. Kim, Ki Jae, *et al*. "Ceramic Composite Separators Coated with Moisturized ZrO2 Nanoparticles for Improving the Electrochemical Performance and Thermal Stability of Lithium Ion Batteries." *Physical Chemistry Chemical Physics*, vol. 16, no. 20, Apr. 2014, pp. 9337–9343.,

doi:10.1039/c4cp00624k.

Copyright: © 2019 Antonides-Jensen and Antonides Campos. All JEI articles are distributed under the attribution non-commercial, no derivative license (http://creativecommons.org/licenses/by-nc-nd/3.0/). This means that anyone is free to share, copy and distribute an unaltered article for non-commercial purposes provided the original author and source is credited.

JOURNAL OF
EMERGING INVESTIGATORS

Article

Longer Exposure to 2% India Ink Increases Average Number of Vacuoles in *Tetrahymena pyriformis*

Alaina Cherry[1], Allison Reilly[1], Michael Edgar[1]
[1] Milton Academy, Milton, Massachusetts

SUMMARY

***Tetrahymena pyriformis* are single-celled phagocytes that feed by forming food vacuoles in a process known as phagocytosis. The goal of this experiment was to examine to what extent exposure of *Tetrahymena* to India ink affects the average number of vacuoles formed. We hypothesized that the increase of feeding time would increase the amount of India ink food vacuoles per *Tetrahymena* in a linear fashion. By observing *Tetrahymena* vacuole formation in response to India ink over a 60-minute period, we found that that vacuole formation in *Tetrahymena* initially increased linearly with increased India ink exposure time. After a certain time, however, vacuole formation ceased due to either a lack of remaining ink or a deficiency in the energy or resources necessary to continue performing phagocytosis. The relationship between India ink exposure time and food vacuole formation also provides insight into correlated changes in metabolic rate in *Tetrahymena* and other organisms for which *Tetrahymena* serves as a model. The way in which *Tetrahymena* budget their energy over time between vacuole formation, metabolism, and the countless other biological processes necessary for survival, particularly when supplied a non-nutritional particle such as India ink, could also be important for further studies on various organisms' reactions to food shortages**

INTRODUCTION

Phagocytes are cells that are capable of ingesting foreign particles via phagocytosis. Phagocytosis takes place when the cilia of a phagocyte sweep food particles into the oral groove of the cell so that the plasma membrane can surround the food particles to form a food vacuole. After the vacuole is formed in the cell, the lysosomes, digestive organelles where food is broken down using hydrolysis, fuse to the food vacuole and break down its contents so the cell can absorb its nutrients (1).

Tetrahymena pyriformis, one type of phagocyte, are ciliated, single-celled, microscopic organisms (2). The goal of this experiment was to determine the effect of *Tetrahymena* exposure to 2% Speedball Superblack India ink on the average number of food vacuoles formed. This experiment is also significant because studies have shown that food vacuole formation rate correlates to respiration rate; specifically, a 1978 experiment conducted by L. Skriver and J. R. Nilsson found that inducing a high rate of vacuole formation in *Tetrahymena pyriformis* caused increased oxygen consumption, indicating increased respiration rate (3). Because of this correlation, the relationship that we find between time exposed to ink and food vacuole formation may also have implications on metabolic rate. This information can give us insight on how organisms budget their energy when exposed to varying amounts of ingestible particles.

While conducting our background research, we found a report for a very similar experiment. In 2016, Carpenter-Boesch et al. analyzed food vacuole formation over time in *Tetrahymena* exposed to various concentrations of Congo Red. The results of their research revealed a positive, linear relationship between time and mean number of Congo Red vacuoles (4). In our lab, we fed the *Tetrahymena* India ink rather than Congo Red or Carmine Red, primarily due to practical reasons; the red colored particles were more difficult to distinguish under the microscope because the *Tetrahymena* had been stained orange by the Iodine used to fix them, and Carmine Red is a larger molecule that would likely take longer to ingest. Nonetheless, we suspected that the linear increasing relationship observed in the Carpenter-Boesch experiment would apply to our findings as well. Additional background research revealed that the process of phagocytosis merely involves intaking food particles nearby and forming food vacuoles. This process neither accelerates nor decelerates unless affected by another factor (1). Thus, based on the Carpenter-Boesch experimental results and our own background research on the limiting aspects of the process of phagocytosis, we hypothesized that as the time that we exposed *Tetrahymena* to India ink increased, the average number of food vacuoles would increase in a linear fashion.

RESULTS

In order to test ingestion of India ink, food vacuoles were counted over a period of 60 minutes following initial exposure to the ink. We observed a linear increase in average number of vacuoles per *Tetrahymena* during the first 20 minutes **(Figure 1)**. We measured a rate of 0.5 food vacuoles per minute with a high R2 value of 0.987, indicating that this linear model closely fit our data. After 20 minutes, the number of food vacuoles remained relatively constant, as supported by the near-zero rate (0.005) food vacuoles per minute) of the linear best fit line for the final three data points. At 20

minutes of exposure to India ink, there were 10.00 ± 1.627 vacuoles per *Tetrahymena*; at 45 minutes, there were 10.024 ± 0.334 vacuoles per *Tetrahymena*; and at 60 minutes, there were 10.208 ± 0.514 vacuoles per *Tetrahymena* (average ± absolute deviation). The first four time points were significantly different (all *p*-values < 0.05, two-tailed t-test with Bonferroni correction), while the final three time points were not significantly different (all *p*-values > 0.05, two-tailed t-test with Bonferroni correction), as labelled in **Figure 1**.

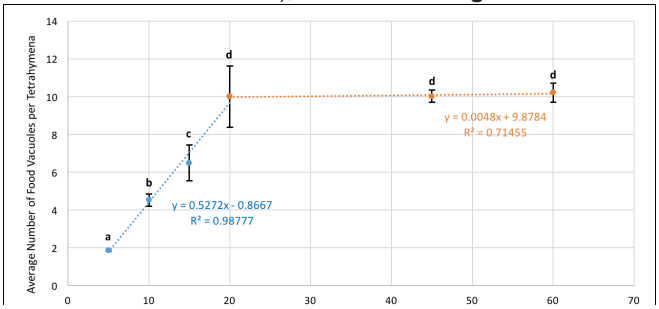

Figure 1: Effect of time exposed to 2% India ink on the average number of food vacuoles per *Tetrahymena*. The blue best fit line represents the increasing linear portion of the graph. The orange best fit line represents the linear horizontal portion of the graph. The equations of the two best fit lines were included to show the difference in slopes; the near-zero slope of the second best fit line shows that a maximum number of food vacuoles was reached after about 20 minutes. The letters represent the statistical relationship between each run. Independent, two-tailed t-tests with Bonferroni correction were calculated between every possible combination of assay time points, comparing the set of five averages (one for each trial). The same letter indicates that those time points were statistically not different and a different letter indicates that those time points were statistically different. Uncertainty bars represent absolute average deviation (AAD). Fifteen *Tetrahymena* were recorded for each trial. Five trials were conducted for each run (n=5)

DISCUSSION

Assuming there was a constant rate of phagocytosis, we originally hypothesized that increasing the duration of *Tetrahymena* exposure to India ink would increase the average number of food vacuoles per *Tetrahymena* in a linear trend, as found in the Carpenter-Boesch experiment (4). We found that the increase in the amount of time exposed to India ink did, in fact, increase the number of food vacuoles per *Tetrahymena* at a rate of 0.5 food vacuoles per minute for the first 20 minutes. This linear increase was also supported by our finding that the first four data points were statistically different (all *p*-values < 0.05, two-tailed t-test with Bonferroni correction). The increasing, linear portion of the graph may be explained by the fact that phagocytosis, the process by which *Tetrahymena* ingest food particles and form vacuoles, is a very specific process. The cilia sweep the food particle into the oral groove, the phagocyte engulfs the food particle and forms a food vacuole, and the lysosomes break down the contents of the food vacuoles using hydrolysis so that the cell can absorb the nutrients. This process does not accelerate as the *Tetrahymena* continue eating, nor does it slow down. The cilia sweep up any food particle close to them until another factor doesn't allow them to. Since only a finite number of food vacuoles can be formed at once, *Tetrahymena* eating is limited by the process of phagocytosis (1).

After 20 minutes of exposure to India ink, the average number of India ink vacuoles remained relatively constant. Here, the rate of increase in food vacuoles was only 0.005 food vacuoles per minute and there was no statistical difference between 20 minutes, 45 minutes, and 60 minutes of exposure to India ink (all *p*-values > 0.05, two-tailed t-tests with Bonferroni correction). One possible explanation for this horizontal linear portion of the graph is that once 20 minutes of exposure to India ink passed, the *Tetrahymena* may have eaten all of the ink that we had given to them. To test this explanation, additional trials could be conducted in which we exposed the *Tetrahymena* to a larger volume of ink. If the number of food vacuoles continued increasing for longer than 20 minutes before becoming constant, then the results would show that the plateau was dependent on the amount of India ink. On the other hand, if no additional food vacuoles formed after adding more ink, this would support another explanation for the plateau in food vacuole formation: the *Tetrahymena* essentially could not consume any more ink, even if additional ink was available, perhaps due to a lack of energy, resources, or space. During our experimentation, after 20 minutes, we observed that the *Tetrahymena* appeared black, as they were filled with India Ink vacuoles. This observation supports the second explanation for the plateau, because it appeared as if no more ink could be consumed.

A source of uncertainty was letting the iodine sit out on the slides. To prepare the slides for the *Tetrahymena* and ink, iodine was placed onto each slide in advance. The amount of time that the iodine was sitting on the slide may have been different for each run. Since iodine is light sensitive and prone to decomposition, the *Tetrahymena* were potentially fixed with different concentrations of iodine. Because of the strong iodine dilution, this uncertainty did not seem to affect most of the trials, as all of the *Tetrahymena* were fixed despite the slightly varied concentrations. However, for one of the 60 minute trials, one *Tetrahymena* was observed moving in the slide after being treated with iodine. If this had been the case for other trials, it would have skewed the averages upwards, because the *Tetrahymena* would have had additional time feeding. A solution for this uncertainty would be to put iodine on the slide right before putting the *Tetrahymena* and ink on the slide. This solution would require multiple people and pipettes.

Several further experiments could be conducted to both improve the precision of this experiment and examine the effects of other variables on *Tetrahymena* feeding. First, the results of this experiment showed that vacuole formation ceased after about 20 minutes of feeding time. To determine the nature of the transition into this plateau (whether there is a sharp change from linear increasing to linear horizontal or a more gradual curved decrease in the feeding rate), more testing could be conducted at 1-minute intervals between 15

minutes and 25 minutes. To examine other factors potentially affecting *Tetrahymena* feeding and vacuole formation, an experiment could be conducted during which the concentration of India ink was varied. Additionally, another type of ink, such as carmine red, could be used instead of India ink, in order to examine whether various foods, with various molecular sizes, structures, and properties might affect vacuole formation and the time at which the number of ink vacuoles becomes constant. Finally, the same experiment could be conducted to compare feeding rates under varying conditions, for instance different temperatures or pHs.

Despite our uncertainty, the background research on the process of phagocytosis, the experimental data, and the statistical testing support the hypothesis that an increasing linear relationship exists between time exposed to 2% India ink and average number of vacuoles formed per cell in *Tetrahymena pyriformis*. After 20 minutes of feeding time, the average number of vacuoles per *Tetrahymena* remained constant at about 10 vacuoles, as shown by the near-zero rate of vacuole formation (0.0048 food vacuoles per minute). Independent, two-tailed t-tests revealed no statistical difference between the 20-minute, 45-minute, and 60-minute runs (all *p*-values > 0.05, two-tailed t-test with Bonferroni correction). Overall, this experiment revealed that after the linear increasing relationship that was hypothesized, the rate of *Tetrahymena* vacuole formation decreases until the average number of ink vacuoles stops at a constant maximum, due to either a lack of remaining ink or lack of energy to create more food vacuoles. Our results could potentially relate to the metabolic rate of organisms and how these organisms budget their energy. Although we exposed the *Tetrahymena* to India ink, a substance that does not provide sugar or nutrients, the creation of food vacuoles would be the first step in the metabolic process when digesting actual nutrient-rich particles (5). In our case, the *Tetrahymena* likely had sugar stored from before the experiment that they used in respiration to generate ATP to create food vacuoles.

Because the India ink does not give the *Tetrahymena* any energy, the process of making food vacuoles only depletes energy overall. Potentially, as a result, they stop ingesting India ink and use their remaining energy for other processes in order to survive. This cessation in phagocytosis could explain the plateau in food vacuole formation on our graph. This explanation could also shed light on the mechanisms organisms use to budget their energy when they have a shortage of food in their environment. Many organisms will face shortages in food caused by environmental and ecological changes (6). It is important to know not only the optimal conditions for survival, but also how these organisms will allocate energy to survive even when faced with these suboptimal conditions.

MATERIALS AND METHODS

Tetrahymena Culture

Two pipette drops of a *Tetrahymena* culture were put into a test tube of *Tetrahymena* medium from Carolina Biological Supply Company and incubated at 25 °C. After five days, Iodine-Potassium Iodide Solution (Carolina Biological Supply Company) was diluted to 50% by combining 11 drops each of iodine and water in a microtube and vortexing. The 50% dilution of iodine (Iodine-Potassium Iodide Solution) was chosen because a lower concentration might have failed to kill all of *Tetrahymena*. To fix the *Tetrahymena*, three drops of the 5-day old culture were combined with one drop of this 50% iodine dilution in another microtube and vortexed. One drop of this solution was pipetted into a hemocytometer, which was then placed under a Swift compound microscope (400x magnification). The cells were visible due to the iodine stain. 52 *Tetrahymena* were counted in the 0.9mm^3 square. This value was converted to cell concentration in units of cells/mL by the following calculations:

Conversion: $1\text{mm}^3 = 1000\mu\text{l} = 1\text{ml}$
4/3 accounts for 3:1 dilution of *Tetrahymena* to iodine

Thus, the *Tetrahymena* culture used for experimentation had an approximate concentration of approxamtely 77,000 cells/mL. For the second round of final testing, the *Tetrahymena* culture's cell concentration was again counted using a hemocytometer. This time, 111 cells were counted, so a 1:1 dilution of *Tetrahymena* culture to *Tetrahymena* medium was created to standardize the concentration used for both days of final testing.

Preparing Solutions

In five different microtubes, one for each trial, 12 pipette drops of the 77,000 cells/mL *Tetrahymena* culture were combined with 8 pipette drops of 2% India ink, as shown in **Figure 2**. The *Tetrahymena* to ink ratio was kept to 3:2 for all of final testing because the Carpenter-Boesch experiment indicated that variation of food concentration might affect the number of vacuoles formed (4). Immediately after the first drop of India ink was added to each microtube of *Tetrahymena*, an iPhone stopwatch was started. Microtubes were then closed, vortexed, and returned to the tray to incubate.

Assays

One drop of 50% iodine was pipetted in the center of each of the five microscope slides, corresponding to the five microtube trials **(Figure 3)**. Five sterile pipettes were used to remove one drop from each of the five microtubes at each of the predetermined time points (5 minutes, 10 minutes, 15 minutes, 20 minutes, 45 minutes, and 60 minutes). The 60-minute time point served as the control group because maximum vacuole formation was expected at 60 minutes. In order to fix the *Tetrahymena* at the correct time, these *Tetrahymena* and ink drops were immediately placed atop the 50% iodine drops on the corresponding microscope slides. Meanwhile, the remaining *Tetrahymena* in the microtubes

continued eating ink as the timer continued. With the microscope set at 400x magnification, the total number of ink vacuoles in each of the first 15 *Tetrahymena* observed were counted per trial, as shown in **Figure 4**.

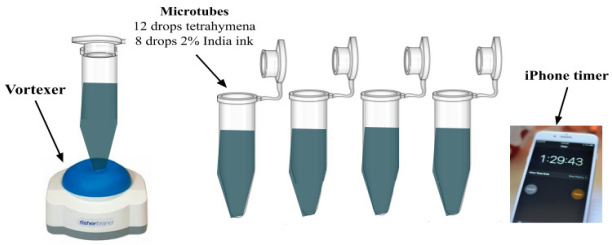

Figure 2: Microtube Set-Up. Five microtubes, one for each trial, were filled with 12 drops of Tetrahymena culture and 8 drops of 2% India ink, then closed and vortexed. The iPhone timer was started after the initial drop of India ink was dropped into the microtube.

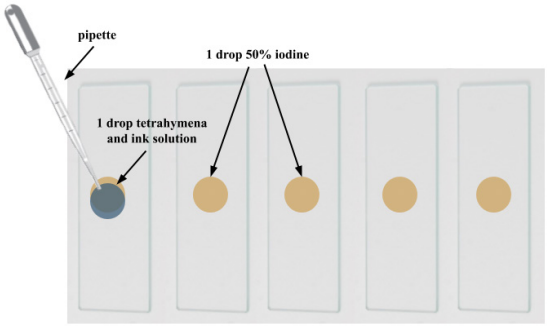

Figure 3: Microscope Slide Set-Up and Iodine Procedure. One drop of 50% iodine dilution was pipetted into the center of five microscope slides, one for each trial. At each of the different time points (5 min, 10 min, 15 min, 20 min, 45 min, 60 min), one drop of the *Tetrahymena* and ink solution was removed from each microtube and dropped atop the iodine on the corresponding slide.

Statistical Testing

Within each trial, the average number of vacuoles in the 15 counted *Tetrahymena* was calculated; then the average of these averages was calculated, and this value was displayed on the graph for each time interval. Independent, two-tailed t-tests with Bonferroni correction were calculated, using excel spreadsheets, between the set of averages for every possible combination of assay time points. Furthermore, the slopes of the two best fit lines were used to represent the rate of food vacuole formation.

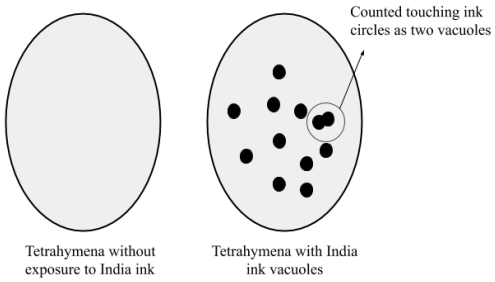

Figure 4: Example of *Tetrahymena* before and after exposure to India ink. Under microscope magnification 400x total number of India ink vacuoles was counted in the first 15 *Tetrahymena* observed.

Received: Feb 26, 2019
Accepted: Sep 6, 2019
Published: October, 2019

REFERENCES

1. Rosales, Carlos, and Eileen Uribe-Querol. "Phagocytosis: A Fundamental Process in Immunity." *Biomed Research International,* June 12, 2017. https://doi.org/10.1155/2017/9042851.
2. Coyne, Robert S. "*Tetrahymena*." *eLS*, 2011, pp. 1-9, doi:10.1002/9780470015902.a0001972.pub3.
3. Skriver, L., and J.R. Nilsson. "The Relationship between Energy-dependent Phagocytosis and the Rate of Oxygen Consumption in *Tetrahymena*." *Microbiology Society,* pp. 359-66.
4. Carpenter-Boesch, Genevieve, et al. "The effect of time and food concentration on vacuole formation in *Tetrahymena* thermophila." *The Expedition*, vol. 5, 2016, pp. 1–11, ojs.library.ubc.ca/index.php/expedition/article/view/188337.
5. Pollock, Christopher John, and Alison Kingston-Smith. "The Vacuole and Carbohydrate Metabolism." *Advances in Botanical Research 25* (April 15, 2008): 195-215. https://doi.org/10.1016/S0065-2296(08)60153-6.
6. CNRS (Délégation Paris Michel-Ange). "Even single-celled organisms feed themselves in 'smart' manner." *ScienceDaily*. 15 February 2010.

Copyright: © 2019 Cherry, Reilly, and Edgar. All JEI articles are distributed under the attribution non-commercial, no derivative license (http://creativecommons.org/licenses/by-nc-nd/3.0/). This means that anyone is free to share, copy and distribute an unaltered article for non-commercial purposes provided the original author and source is credited.

JOURNAL OF
EMERGING INVESTIGATORS

Article

The effects of knowledge, lack of knowledge, and deception on rate of perceived exertion and performance during workouts

Jamir Howard, Jason Scott
The Neighborhood Academy, Pittsburgh, Pennsylvania

SUMMARY

The purpose of this study is to examine how knowledge, lack of knowledge, and deception affect the rate of perceived exertion (RPE) and actual performance of moderately trained teenagers engaged in sprint training. This study has two hypotheses. The first hypothesis is that athletes who do not know their sprint duration will have a lower reported RPE and actual performance, compared to athletes who are aware of their sprint duration. Our second hypothesis is that athletes deceived with a lower sprint duration will report a higher RPE and performance compared to when they have knowledge of their duration. The order of the experimental conditions was knowledge, deception, and then lack of knowledge. Participants started from the midfield line of an indoor soccer field and ran to the end of the field and back to midfield ten times for all conditions. While on their way back, they reported their RPE to an assigned assistant who was timing them. We found that participants ran the slowest and reported the lowest RPE throughout the ten sprints in the lack of knowledge condition. We also found that the knowledge condition had a slower average sprint time than the sprints during deception, but the knowledge condition yielded the fastest and most consistent speeds. Coaches should strongly consider telling their athletes the truth about workout duration since our study along with many others suggests that it is the best way to maximize performance and RPE.

INTRODUCTION

The information provided to an athlete about the duration of a workout may have an effect how their effort and performance. In this study, we investigate how knowledge, lack of knowledge, and deception affect the rate of perceived exertion (RPE) and performance of moderately trained high school athletes engaged in sprint training. This is important because most studies have well-trained adult participants while this study includes moderately-trained teenagers. According to the NCAA, there are over eight million student athletes across the United States that play every year (1). Since RPE has been proven to be a reliable way to measure exhaustion, athletes can be trained more effectively once we determine whether the best method to maximize RPE is using knowledge, lack of knowledge, or deception (2, 3).

The rating of perceived exertion (RPE) is usually used during exercises to measure the perceived intensity of the person working out. The measure of the participants' perceived exertion is recorded by using the Borg scale. The scale ranges from 6-20, with 6 being extremely light perceived exertion and 20 being extremely difficult (2). Studies have demonstrated that RPE is a reliable way to measure the actual physical exertion of people (3). The brain adjusts RPE and one's actual performance, based on the amount of energy that remains from the beginning of the exercise (2). RPE is a reliable and accurate way to measure workout intensity; prior research suggests that regardless of the length of exercise and desired intensity, the subject's RPE and actual workout intensity showed no difference (4).

The proposed relationship between knowledge of endpoint and RPE is that the degree of knowledge that someone has about the length of their exercise affects how hard they believe they are working. Studies have found that knowing the duration of the workout increased ratings of perceived exertion, therefore suggesting that knowledge improves the actual intensity of the participant (5, 6). Another study considered if the brain makes a perceived exertion strategy not only in the expected duration of the workout but in how much someone believes in the workout length they were told. The results of the study supported the idea that knowledge of the exercise's endpoint proved to result in a more aggressive pacing strategy that produced superior performance (7).

Previous studies have also investigated the role of deception of endpoint or duration on rating the participants' perceived exertion. One study found that when deceived, a runner's RPE increased significantly compared to the first control trial of a known distance (8). Studies have also investigated the influence of prior knowledge of the length of an exercise on pacing strategies during game-based activities. Twelve men competed in a game under three different conditions (deception, control, unknown). In the deception and unknown groups, the intensity was found to be higher than in the control group. Players alter their pacing strategies during games based on their anticipated endpoint (9).

While there have been many studies on RPE, no other study using the three conditions (known, unknown, deception) has also measured performance and used sprint training as opposed to running/cycling. Also, instead of using well-

trained adults like in other studies, this study will examine high school children who exercise moderately. We hypothesize that lack of knowledge of sprint duration will have a lower reported RPE and lower actual performance, compared to the control condition. This agrees with previous research, which found that lack of knowledge leads to a more conservative pacing strategy and lower RPE (5, 6, 7). We also predict that deception of sprint duration will have a higher RPE compared to control, in agreement with prior sources (8, 9, 10). Lastly, we hypothesize that deception of sprint duration will increase the overall performance because the participants will believe that the amount of work they are told to do is not that much, and they will work harder, despite the possible lack of motivation when it's revealed that they must exercise longer.

RESULTS

This study's purpose was to examine how the knowledge, lack of knowledge, and deception of exercise duration affect the rate of perceived exertion (RPE) of moderately trained high school athletes engaged in sprint training. Eleven students participated in ten sprints for each trial day over the course of four weeks. After every other sprint, the participant's RPE was reported along with their sprint time. The order of the conditions was knowledge, deception, and then lack of knowledge. In the deception condition, athletes were told to run five sprints, but at the end of the five sprint were told to run five additional. In all conditions, the reported RPE of the participants saw a gradual increase throughout the workout, but the lack of knowledge condition had the lowest reported numbers overall (**Figure 1**). The participant's actual performance was generally slower in the lack of knowledge condition compared to the knowledge and deception conditions (**Figure 2**). The average reported RPE in the deception condition was fastest initially but slowed down drastically after participants realized they had to run more. The average reported RPE in the knowledge group was the fastest of all conditions but still decreased as the number of sprints increased, due to the duration of the exercise.

Next, differences in RPE and performance across the three conditions for each of the five sprints were measured for each sprint (**Table 1**). There were three significant

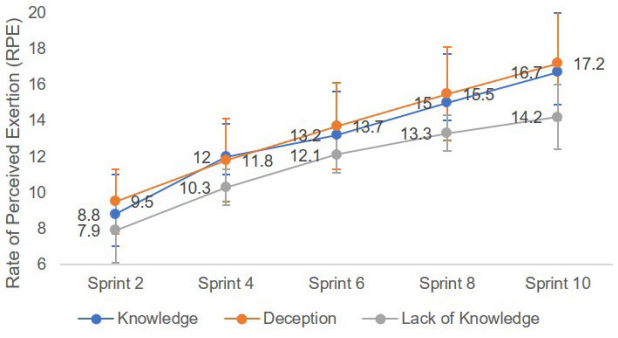

Figure 1: Sprint number vs. rate of perceived exertion. The average RPE for each sprint and each condition is displayed above. The error bars represent standard deviations.

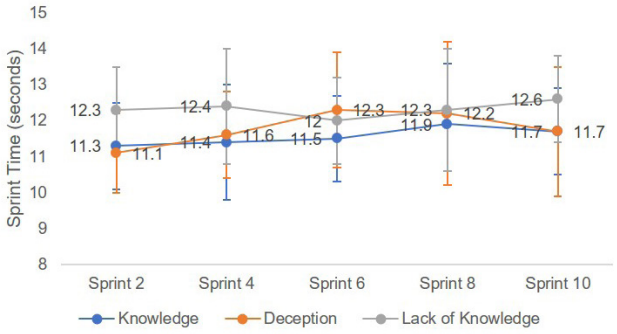

Figure 2: Sprint number vs. performance. The average sprint time for each condition is displayed above. Participants were told of the deception regarding workout length at the end of sprint 5.

differences. During sprint 4, the lack of knowledge condition (12.4 ± 1.0) was slower than the knowledge condition (11.4 ± 1.6, $p < 0.05$; **Figure 2**). In sprints eight and ten, there were differences in RPE (**Figure 1**). In sprints 8 and 10, runners in the lack of knowledge condition reported a lower RPE (13.3 ± 3.0), compared to the knowledge (15.0 ± 2.7) and deception (15.5 ± 2.5, $p < 0.05$) conditions. Overall, our results show that the lack of knowledge group did not think they were working hard but the data show that their performance was actually not significantly different from the other two conditions (**Table 1**).

In order to identify if the moment of deception (sprint five), affected the athletes' performance, we also investigated differences in performance and RPE between sprint four and sprint six. We found that there was a significant difference in the participant's actual performance in the deception group ($p = 0.019$) unlike in the knowledge and lack of knowledge groups. In the deception group, the average time from sprint 4 to sprint 6 went from 11.6 ± 1.2 seconds to 12.3 ± 1.5 seconds.

In all three conditions, there was a significant increase in RPE. In the knowledge condition, RPE increased by 1.2 points ($p = 0.007$), 1.9 points in the deception condition ($p = 0.03$) and 1.8 points in the lack of knowledge ($p = 0.0003$). The deception condition had the largest average increase. There were no overall differences in performance between the three conditions across all ten sprints. ($p = 0.10$). However, there was a clear trend between the conditions with the average increasing from the fastest condition (knowledge, 11.6 ± 1.2), to deception (11.8 ± 1.1), to the slowest condition (lack of knowledge, 12.3 ± 0.9).

DISCUSSION

We hypothesized that a lack of knowledge of sprint duration will result in a lower RPE and actual performance, compared to the control condition. The results of the study showed that the participants ran the slowest and reported the lowest RPE throughout the ten sprints in the lack of knowledge condition (**Figures 1 & 2**). Therefore, the first hypothesis was partially supported, since lack of knowledge had the slowest overall sprint time and reported RPE, although only some of

	Performance				
	Sprint 2	Sprint 4	Sprint 6	Sprint 8	Sprint 10
Knowledge	11.3 (1.2)	11.4 (1.6)	11.5 (1.2)	11.9 (1.7)	11.7 (1.2)
Deception	11.1 (1.1)	11.6 (1.2)	12.3 (1.5)	12.2 (2)	11.7 (1.3)
Lack of Knowledge	12.3 (1.8)	12.4 (1)	12 (1)	12.3 (1)	12.6 (1.3)
p-value	0.09	0.02	0.25	0.8	0.09
	Rate of perceived exertion (RPE)				
	RPE 2	RPE 4	RPE 6	RPE 8	RPE 10
Knowledge	8.8 (2.2)	12 (1.8)	13.2 (2.4)	15 (2.7)	16.7 (3.3)
Deception	9.5 (1.9)	11.8 (2.3)	13.7 (2.4)	15.5 (2.5)	17.2 (3.2)
Lack of Knowledge	7.9 (1.8)	10.3 (2.5)	12.1 (3)	13.3 (3)	14.2 (3.3)
p-value	0.18	0.07	0.09	0.007	0.00023

Table 1: Averages of RPE and performance through all sprints and across all conditions. The mean performance (in seconds) and mean RPE (6-20 on the Borg scale) for each sprint and condition are listed above with standard deviations in parentheses.

the sprint speeds had significant differences (**Table 1**).

We also predicted that deception of sprint duration will increase RPE and performance, compared to the control. The control group (knowledge condition), had a faster average sprint time compared to deception due to the significant drop in performance when it was revealed that they had been lied to (**Table 2**). Their speed at the beginning of the deception trial averaged with the decrease in speed after the lie, revealed their overall time to be not significantly different to the control group. At the moment of deception, there was a significant increase in RPE, but it was not larger than the increase in RPE in the control condition (**Table 2**). However, overall, the RPE was higher during the four of the five sprint measurements, but not significantly (**Figure 1**). Therefore, the second hypothesis was not supported because although there was a trend which showed that the overall reported RPE for deception was higher than the knowledge condition, the difference was not significant for the actual overall performance. In addition, the deception conditions performance was worse compared to the knowledge condition, which was not supportive of our second hypothesis.

	Performance	
	Sprint 4	Sprint 6
Knowledge	11.4 (1.6)	11.5 (1.2)
Deception	11.6 (1.2)*	12.3 (1.5)*
Lack of Knowledge	12.4 (1)	12 (1)
	RPE	
	Sprint 4	Sprint 6
Knowledge	12 (1.8)*	13.2 (2.4)*
Deception	11.8 (2.3)*	13.7 (2.4)*
Lack of Knowledge	10.3 (2.5)*	12.1 (3)*

Table 2: Difference of RPE and performance between sprints 4 & 6 The difference between sprints 4 and 6 for mean performance (seconds) and mean RPE at the moment of deception (sprint 5) are listed above. Significant differences between sprint 4 and sprint 6 are marked with an asterisk. Standard deviations are in parentheses.

Our results are consistent with a study by Billaut, who examined the effect of prior knowledge of the number of sprints during a repeated sprint exercise (10). Billaut hypothesized that anticipation of having to do fewer sprints would lead to higher skeletal muscle recruitment and that lack of knowledge on a number of sprints to be performed would result in more conservative pacing strategy. It was found that there was more muscle recruitment, higher power, and more work done in the deception trial than in trials control and unknown due to the fact that they believed they were doing fewer sprints during the first five sprints. The deception trial in the second half of the sprints was lower than the others in terms of muscle EMG, work, and power, but the average for the entire workout was higher. In our experiment, we found that overall performance was higher in the knowledge condition but like Billaut's study, lack of knowledge was still last. For RPE, all three trial groups had a positive linear pattern throughout the sprints but there was no difference within those groups. Billaut's groups consisted of in-shape members of a university's track team. Our results revealed the same trend between all trial groups while our groups consisted of average high school students. It is shown that through both studies, not telling people how much exercise they will be doing, is a sure way for them to not work as hard compared to lying to them or telling them the truth. Results on using deception are inconclusive. If used, it might help improve performance, but a proven way to get people to work their hardest is to tell the truth about exercise duration.

One possible reason many of the results of the study were not significant may be due to the number of participants as well as the length of the exercise. If the exercise was longer, the effect of deception would be greater since their attitude towards having to do more exercise than initially planned would be more negative. If there were more participants in

the study, there would be more data which would affect the averages enough for the results to possibly be significant. Another limitation was the participants' knowledge that we would only be recording every other sprint, so they may not have fully sprinted on the sprints that we would not record. They ran full speed on the sprints we recorded so the results would be better, which was not the purpose of the experiment.

To improve this study, it would be beneficial to have a fully planned schedule for the entire experiment for each participant. During our research, the times at which participants took part in the study were not consistent, although they did have enough days in between for rest. Also, it would improve data collection if we ensured that all participants had appropriate clothing on for running. Due to the school's uniform policy, runners sometimes complained that their attire could have slightly held them back. Another possible limitation was that the order of the three different conditions was not random, which might have caused an undesired effect. However, we did so to be consistent with other studies' methods (5,10). Future researchers should consider counterbalancing the order of the conditions for different participants, to see if the order of the conditions plays a role in the results. In particular, varying the lack of knowledge condition to see if it actually produces the slowest speed due to the lack of knowledge of sprint duration and not because it is the last condition.

Overall, based on our findings as well as those from other researchers, we recommend that high school coaches should tell their players the truth about workout length if they want them to work their hardest. It was found that not telling people how much exercise they will be doing has the most negative effects on both RPE and sprint performance, of the three conditions we tested. Lying to the athletes is an option that may work at times, as it produced similar or improved results in certain studies (8). There will likely be a drop in performance after the deception and if lied to too many times, the players may not believe the coach's instructions. We conclude that telling the truth by providing details of the duration and endpoint was found to be the best choice for coaches wishing to maximize sprint performance.

MATERIALS AND METHODS

A total of 11 students in a high school athletic activity participated in the study. All participants in this study were males between the ages of 13 and 17. Athletes were well conditioned, with conditioning practice five days a week for an hour each time for nine weeks prior to the study. In order to help collect data, assistants were recruited from the student body who did not participate in the exercise. Assistants were not aware of the study's hypotheses. The research assistants used a data sheet with three columns to record the sprint number, sprint time, and the RPE. The assistants were instructed to record data for the participants' sprint time for every other sprint only, by using a stopwatch on their phone.

The participants were asked to provide their availability to participate in the study either during the conditioning part of their practice or gym class, with at most four participants at a time. They started from midfield line of an indoor soccer field and ran to the end and back to midfield ten times for all conditions. While on their way back, they reported their RPE to their assigned assistant who was timing them. A 15-second break was given between each sprint. The order of the conditions was knowledge, deception, and then lack of knowledge. Conditions were in this order because knowledge was the controlled condition. It is likely that the participants will believe they will not do the same exercise two times in a row, so the deceiving them would be most appropriate condition to do next. This order is consistent with a similar study (9). In the deception condition, they were told that they would be only running five sprints, but after the fifth, they were told to run five more. Lack of knowledge was the last condition. Between each condition, participants waited at least three days before taking part in the next condition while also taking into consideration their availability. After each trial, participants were asked not to share information about the length of the exercise they did.

In order to analyze the collected data, differences between conditions for each sprint number were analyzed with a one-way ANOVA with correlated samples with a Tukey HSD post-hoc analysis to locate individual differences. Differences at the moment of deception were investigated for each condition used dependent t-tests, and overall differences in RPE and performance across the three conditions were also analyzed using a one-way ANOVA with correlated samples with a Tukey HSD post-hoc analysis to locate individual differences.

ACKNOWLEDGEMENTS

We would like to acknowledge Demetri Bose, Jalen Yates, Jelani Seals, Shakir Daniel, John McClelland and Ty'Jer Clayton for their assistance in gathering data by timing some of the runners.

Received: April 9, 2019
Accepted: May 30, 2019
Published: October 2019

REFERENCES

1. Probability of Competing Beyond High School. *Ncaa.org*, NCAA, ncaa.org/about/ resources/research/probability-competing-beyond-high-school. Accessed 7 Mar. 2019.
2. Eston, Roger. "Use of Ratings of Perceived Exertion in Sports." *International Journal of Sports Physiology and Performance*, vol. 7, 2012, pp. 175-182.
3. Billat, Veronique, and Murielle Garcin. "Perceived Exertion Scales Attest to Both Intensity and Exercise Duration." *Perceptual and Motor Skills*, vol. 93, 2002, pp. 661-671.
4. Kang, Jie, and Gregory B. Biren, Alysia Mastrangelo and Jay R Hoffman. "Regulating Intensity Using Perceived Exertion: Effect of Exercise Duration." *European Journal of Applied Physiology*, vol. 105, 2009, pp. 445-451.
5. Miller, Danneka. "Effect of Knowledge About Exercise

Duration in Ratings of Perceived Exertion and Mood." *SENTIENCE: Undergraduate Journal of Psychology*, vol. 6, 2012, pp. 9-13.
6. Coquart, Jeremy, and Murielle Garcin. "Knowledge of the Endpoint: Effect on Perceptual Values." *International Journal of Sports Medicine*, vol. 29, no. 12, 2008, pp. 976-979.
7. Swart, J., et al. "Exercising with Reserve: Exercise Regulation by Perceived Exertion in Relation to Duration of Exercise and Knowledge of Endpoint." *British Journal of Sports Medicine*, vol. 43, 2009, pp. 775-781.
8. Baden, D. A, et al. "Effect of Anticipation During Unknown or Unexpected Exercise Duration in Rating of Perceived Exertion, Affect, and Physiological Function." *British Journal of Sports Medicine*, vol. 39, 2005, pp. 742-746.
9. Gabbett, Tim, et al. "Influence of Prior Knowledge of Exercise Duration on Pacing Strategies During Game-Based Activities." *International Journal of Sports Physiology and Performance*, vol. 10, no. 3 pp. 298-304.
10. Billaut, Francois, et al. ¨Influence of Knowledge of Sprint Number on Pacing during Repeated-Sprint Exercise." *Medicine & Science in Sports & Exercise*, vol. 43, no. 4, 2011, pp. 665-672.

Copyright: © 2019 Howard and Scott. All JEI articles are distributed under the attribution non-commercial, no derivative license (http://creativecommons.org/licenses/by-nc-nd/3.0/). This means that anyone is free to share, copy and distribute an unaltered article for non-commercial purposes provided the original author and source is credited.

JOURNAL OF
EMERGING INVESTIGATORS

Article

Heavy metal contamination of hand-pressed well water in HuNan, China

Yuxi Long[1], Xiangbao Long[2], and Jichang Xiao[3]
[1]McCallie School, Chattanooga, Tennessee
[2]Shenzhen Smoore Technology Limited, Shenzhen, China
[3]Shanghai Institute of Organic Chemistry, Chinese Academy of Sciences, Shanghai, China

SUMMARY

Unprocessed water from hand-pressed wells is still commonly used as a source of drinking water in Chenzhou, the "Nonferrous Metal Village" of China. Because of the industry of mining and smelting, groundwater is vulnerable to having undue amounts of heavy metals and causing serious health problems. To study the heavy metal contamination levels and potential health effects in this area, 160 household water pump samples were collected in this research. The samples were analyzed through Inductively Coupled Plasma Optical Emission Spectroscopy (ICP-OES) and the concentrations of 20 metal elements, which are either monitored in drinking water or the main metal elements in local mineral resources, including aluminum (Al), boron (B), beryllium (Be), calcium (Ca), cadmium (Cd), cobalt (Co), chromium (Cr), copper (Cu), iron (Fe), potassium (K), lithium (Li), magnesium (Mg), manganese (Mn), sodium (Na), nickel (Ni), lead (Pb), silicon (Si), zinc (Zn), zirconium (Zr) and silver (Ag), were measured. Results showed that although none of the samples had dangerous levels of heavy metals, the concentrations of Al, Fe, and Mn in many locations substantially exceeded those suggested in the Chinese Drinking Water Standard and the maximum contaminant levels of Environmental Protection Agency (EPA). The percentage of samples with the concentration of Al, Fe, and Mn higher than Chinese standards are 20.6%, 12.5%, and 14.4%, respectively. The samples with the highest concentrations exceeded the standard by 54 times, 11 times, and 13 times, respectively. Although these elements do not cause immediate poisoning, long-term ingestion might lead to damages to the brain and other health issues. Therefore, we suggest that water treatment systems should be built for these households to ensure the quality of their water.

INTRODUCTION

According to the research report from Chinese Center for Disease Control and Prevention, 74.87% of rural population use underground water such as hand-pressed wells water, and 25.13% use surface water such as open wells water and spring water (1). Despite blazing developments of China and the increasing prevalence of tap water in recent years, it is still common for remote villages to use a hand-pressed well as drinking water resource in each household. A hand-pressed pump is a tool for drawing groundwater (2). There is a piston on top and a valve at the bottom, both of which are one-way valves, preventing air from going downward. Upward movement of the piston draws water upward, and downward movement creates a vacuum under the valve. After the water is released, air replenishes the chamber, resetting the pump. Thus, with vertical movements of the hand, water is drawn up (**Figure 1**). This mechanism is versatile and widely used, but it does not provide an easy way to protect its users from drinking polluted water, such as by purifying groundwater through a filter.

Due to the dissolution of underground materials and mining, groundwater is vulnerable to being polluted (1, 3). Pumped water without purification may contain high levels of metals, including toxic heavy metals, which is defined as metals and metalloids with densities of more than 5 g/cm^3, such as lead (Pb), arsenic (As), cadmium (Cd), mercury (Hg), and hexavalent chromium (Cr(VI)), which would do profound damage to the human body (1). Lead is not an essential element for the human body, and excessive intake can damage the nervous, skeletal, circulatory, enzymatic, endocrine, and immune systems (4). Children, pregnant women, and elderly people are particularly sensitive to lead exposure,

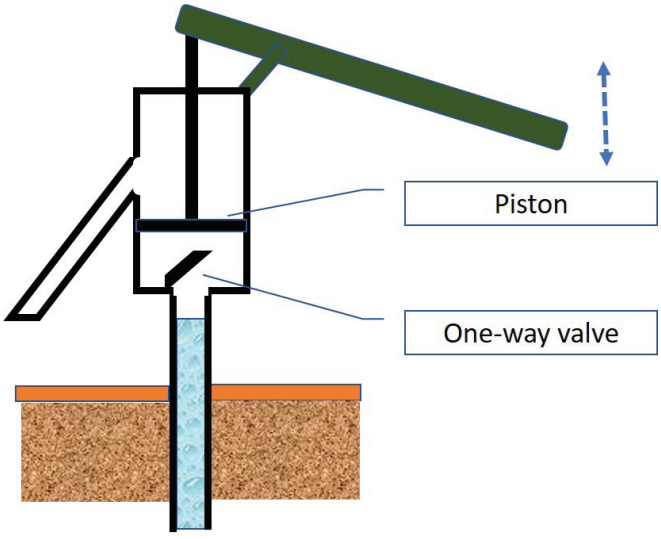

Figure 1: Schematic drawing of a hand-pressed pump. It is a popularly used tool for drawing underground water in Southern China. The piston and the one-way valve prevent air from going downward. Upward movement of the piston draws water upward, and downward movement creates a vacuum under the valve. With vertical movements of the hand, water is drawn up.

and lead also has significant negative effects on intelligence quotients and physical development in children (4). A study from Shen et al. (5) and governmental information (6) show that irreversible damage to their intelligence development occurs when children's blood lead levels are above 10 μg/dL. Minerals, such as iron (Fe), aluminum (Al), silicon (Si), calcium (Ca), magnesium (Mg), and zinc (Zn), are essential elements of the human body, but excess intake can be harmful (7-11). For example, a study by Abeywickarama *et al*. showed that drinking water from natural springs with high mineral content, particularly calcium, carried the risk of kidney stone formation (7). Another mineral, Zn is an important element for the human body, but it can also have harmful effects if in excess. It is an essential component of various enzymes and enzyme activators and supports growth, tissue regeneration, and the immune system (4). Nevertheless, excessive Zn intake can cause stomach cramps, nausea, and vomiting; high-dose, long-term Zn exposure can affect cholesterol balance, diminish immune system function, and even cause infertility (4). The level of Zn in a healthy adult is approximately 1 μg/mL in serum. Harmful effects generally begin at Zn levels 10-15 times higher than the amount needed for good health (8). Al is toxic to some extent, prolonged intake damages the brain, leading to dementia (9) and it could also cause anemia, or osteoporosis, and damage the development of infants and children (10). Besides, a high amount of Fe intake could result in immediate vomiting and worsening conditions in 20 hours with fever, pneumonia, shock, coma and convulsion, and death (11).

There have been quite a few reports and news stories on heavy metal pollution around Chenzhou, China and areas around it. You Town has been exposed, producing rice containing high levels of cadmium (12). With huge reserves and a wide variety of mineral resources, Chenzhou City in South Hunan, China, is called the "Nonferrous Metal Village," and it is the most important area of the multi-mineral belt in Hunan Province (**Figure 2**) (1). As the major non-ferrous metals industry base in China, 112 different types of mineral deposits had been found in Chenzhou as of 2017. The reserve amounts of 46 of the deposits have been determined. Chenzhou holds the highest amount of tungsten deposit and the second highest amount of bismuth deposit in mass globally. Additionally, it has the highest amount of molybdenum deposit, the third highest amount of tin deposit, and the fourth highest amount of zinc deposit in China. YongXing Town of Chenzhou is named "China's Capital of Silver." In total, there

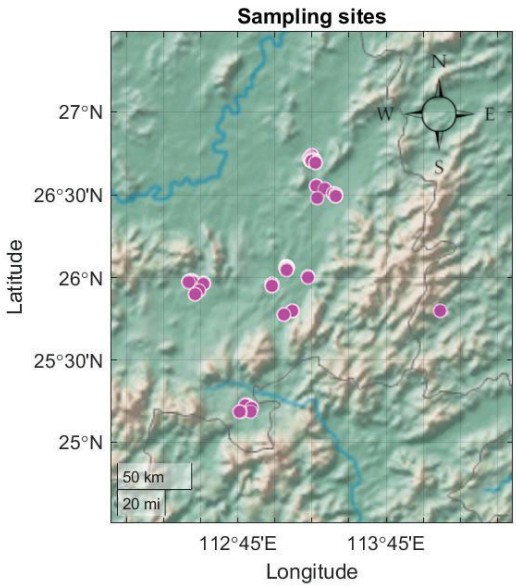

Figure 2: Map of the sampling area, Chenzhou. Chenzhou lies in the south of Hunan Province, Southern China, and has a total area of 19,387 km2. The dots represent the sampling sites of hand-pressed well water covering the counties of Chenzhou such as Anren, Guiyang, Yizhang and Zixing.

are 1112 mining enterprises in Chenzhou (13). However, no survey has yet been conducted in the whole Chenzhou area with so many mineral activities, and a large population is potentially exposed to relatively high contaminant levels.

We hypothesized heavy metal levels in the hand-pressed well water of this area would exceed the related drinking water safety limits. In this study, we collected water samples from hand-pressed wells in the countryside of Hunan Province, then measured the contaminant levels using Inductively Coupled Plasma Optical Emission Spectroscopy (ICP-OES) (14). Results for each metal were evaluated using EPA standards and the Chinese Drinking Water Standard (15, 16), and we determined that Al, Fe, and Mn in the water were at unsafe levels in some places and recommended that measures such as installation of water purification system and implementation of education program to be takes for this region.

RESULTS

In total, 160 hand-pressed well water samples were collected and determined by ICP-OES. ICP-OES is a powerful instrument. It can perform up to 60 elements of simultaneous

	Al	B	Be	Ca	Cd	Co	Cr	Cu	Fe	K	Li	Mg	Mn	Na	Ni	Pb	Si	Zn	Zr	Ag	Total hardness
Wavelength(nm)	396.152	182.591	313	396.8	214.438	228.616	267.716	324.754	259.941	766.491	670.78	279.553	257.611	258.592	231.604	220.353	251.612	213.856	339	328	
DL(mg/L)	0.009	0.002	0.0006	0.002	0.0005	0.0008	0.002	0.002	0.002	0.07	0.002	0.002	0.0006	0.03	0.002	0.006	0.02	0.0005	0.001	0.002	
Concentration(mg/L)	BDL-10.8	BDL-0.986	BDL	121.9	BDL-0.003	BDL-0.036	BDL-0.001	BDL-0.06	BDL-3.30	BDL-42.7	BDL-0.852	BDL-56.4	BDL-1.3	BDL-15.5	BDL-0.007	BDL	BDL-6.77	BDL-1.02	BDL	BDL	BLD-540
Sample no.(> Chinese drinking water standard)	33	3	0	0	0		0	0	20				23		0	0		1		0	6
% (> Chinese drinking water standard)	20.6%	1.9%	0.0%		0.0%		0.0%	0.0%	12.5%				14.4%		0.0%	0.0%		0.6%	0.0%	0.0%	3.8%
Chinese drinking water standards(mg/L)	0.2	0.5	0.002		0.005		0.05(Cr VI)	1	0.3				0.1		0.02	0.01		1		0.05	450
EPA MCL(mg/L)	0.05-0.2		0.004		0.005		0.1TCr	1	0.3				0.05			0.015		5		0.1	

BDL: Below detection limit.
MCL: Maximum contaminant level. The level of a contaminant in drinking water below which there is no known or expected risk to health.

Table 1: Summary of heavy metals concentration in hand-pressed well water from South Hunan of China, and the DL and wavelength of ICP-OES.

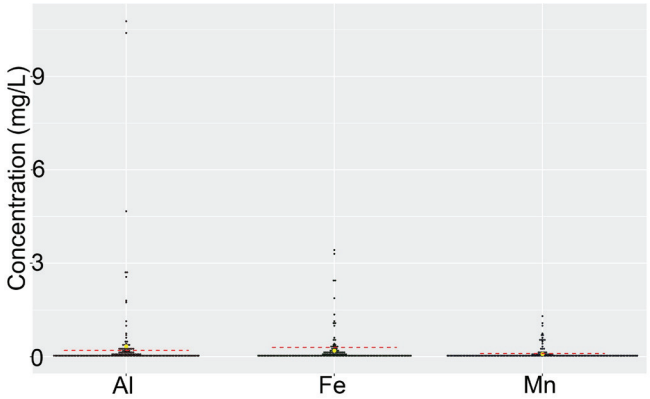

Figure 3: Distribution of Al, Fe, and Mn concentration (mg/L) in all hand-pressed well water samples in Chenzhou. For each element, the red dotted line represents the Chinese drinking water limit and the yellow dot represents the mean values of all 160 samples. The percentage of sample numbers above the Chinese drinking water limits for Al, Fe, and Mn were 20.6%, 12.5%, and 14.4%, respectively.

elemental analysis, with wider linear working range, typically 0.1 to 1000 µg/mL (17). In ICP-OES, the sample, usually in form of a solution, is changed into an aerosol by a nebulizer and is further carried into the hot plasma for atomization. Characteristic emission spectra for each element are produced and dispersed by diffraction grating and detected by CCD. Quantitative analysis is conducted by analyzing the spectra intensity, as it depends on the amount of each element within the sample.

The ICP-OES the results have been summarized (**Table 1**). The total hardness is one important item in water monitoring. It is defined as the sum of Ca, Mg, Fe, and Mn contents and related to industry application and taste of the water. It can be measured directly in the form of carbonate or be calculated by the sum of the metal ions and expressed by the concentration of $CaCO_3$ in water. Based on the atomic weight of Ca, Mg, Fe, and Mn, as well as molecular weight of $CaCO_3$, the following hardness equation can be inferred (18):

$$\text{Total hardness value} = \left(\frac{Ca}{12} + \frac{Mg}{12} + \frac{Fe}{18.6} + \frac{Mn}{27.5}\right) \times 50$$

The determined heavy metal concentrations in hand-pressed well water have been compared with the drinking water standards in China and the USA (15, 16). The common toxic heavy metal elements such as Pb, Cd, Ni, Cr, and Be were not found or were below Chinese and EPA drinking water standards. On the other hand, some other metals were found to be substantially above the drinking water standards, especially Al, Fe, and Mn (**Figure 3**). We found that the Al concentration in 20.6% of samples were above the drinking water limit. The highest concentration was 53 times above the standard, which was from Liufengzhen, Guiyang County, Chenzhou (**Figure 4**). 12.5% of samples had Fe content higher than the standards, and the highest concentrations were 11 times above the standard value. The highest concentration of Fe was found in both Liufengzhen of Guiyang County and Yongle of Anren County (**Figure 5**). Furthermore, the results showed that 14.4% of samples contained Mn contents higher than the standards, and the highest concentration was 13 times of the standard values. The Mn concentration from the drinking water of Santongchong of Anren County, Zhushangcun of Anren County, Liufengzhen of Guiyang County, and Dongjiangdong of Yizhang County were very high (**Figure 6**). In summary, the common toxic heavy metals such as Pb, Cd, Ni, Cr and Be were not found or were below Chinese and EPA drinking water standards, while other less toxic ones such as Al, Fe, and Mn were at unsafe levels in some sites.

DISCUSSION

Health effect of Al, Fe, and Mn, and their source

The metal levels in the hand-pressed well water in

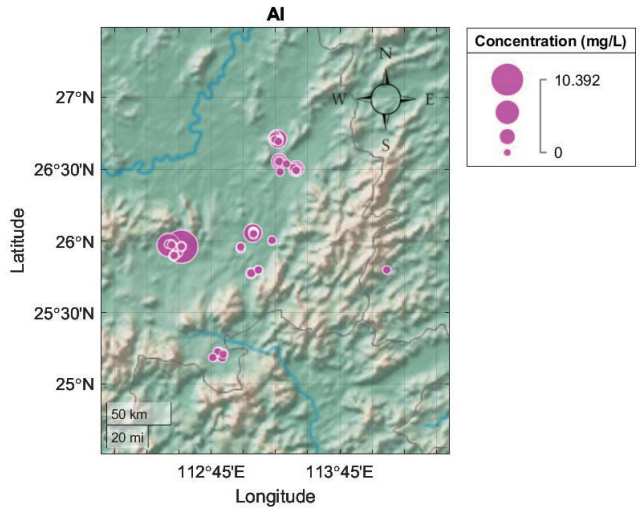

Figure 4: Al concentration (mg/L) in hand-pressed well water in Chenzhou. Dot sizes represent Al concentration. The highest concentration was found in Liufengzhen, Guiyang County and was 54 times greater than the standard.

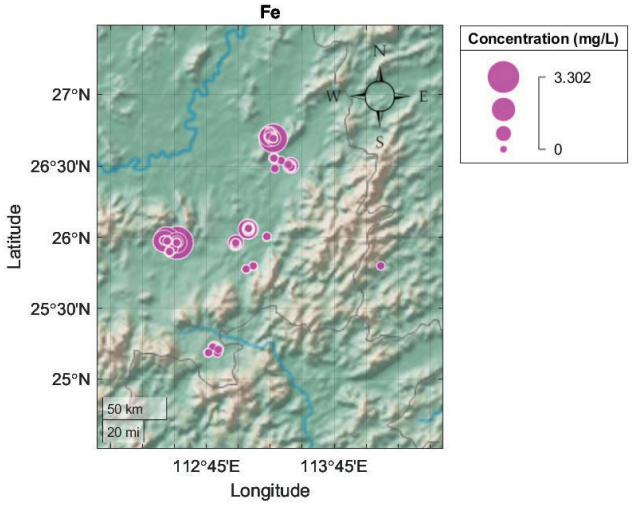

Figure 5: Fe concentration (mg/L) in hand-pressed well water in Chenzhou. Dot sizes represent Fe concentration. The highest concentrations were 11 times above the standard value, which were found in both Liufengzhen of Guiyang County and Yongle of Anren County.

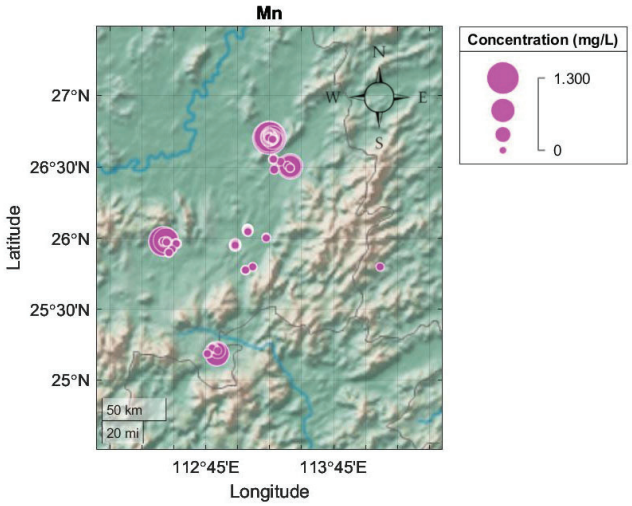

Figure 6: Mn concentration (mg/L) in hand-pressed well water in Chenzhou. Dot sizes represent Mn concentration. The highest concentrations were 13 times greater than the standard values, which were from Santongchong of Anren County, Zhushangcun of Anren County, Liufengzhen of Guiyang County, and Dongjiangdong of Yizhang County.

Chenzhou can potentially be influenced by local industrial activities of mining and smelting. In the study the status on the heavy metal levels in those households who still use hand-pressed well water as a drinking water resource was investigated. Results showed no increase in toxic heavy metals, while high levels of Fe, Mn, and Al in several areas across Chenzhou were discovered. Al, Fe, and Mn are listed as contaminants in National Secondary Drinking Water Regulations of EPA which are non-enforced guidelines. Nevertheless, they are somewhat toxic: aluminum is toxic to some extent, although it does not cause immediate poisoning. Only 10-15% of aluminum ingested gets excreted, while the rest piles up within the body, binding with various proteins and enzymes and affects many biological processes, and prolonged intake damages the brain, leading to dementia (9). It could also cause anemia, or osteoporosis, and damage the development of infants and children (10). Households which use hand-pressed well water in Liufengzhen of Guiyang County are at very high risk of Al exposure, which could cause the above health effects. Oral exposure to high amounts of manganese, on the other hand, can result in adverse neurological effects, and neurodevelopmental effects. Changes in behavior, memory, and learning ability have been observed in children exposed to extremely high levels of manganese (19). High levels of Mn in the drinking water of Santongchong of Anren County, Zhushangcun of Anren County, Liufengzhen of Guiyang County, and Dongjiangdong of Yizhang County could potentially cause such health problems to the people. Additionally, research has shown that intake of a high amount of iron could result in immediate vomiting and worsening conditions within 20 hours with fever, pneumonia, shock, coma, and convulsion followed by death (11). Our finding that both Liufengzhen of Guiyang County and Yongle of Anren County contain high amounts of Fe in hand-pressed well water shows there could be such a health risk for local residents. Among all the findings, Liufengzhen of Guiyang County has the highest levels of Al, Fe, and Mn in the hand-pressed well water. In this region we would suggest the installation of a filter system to the hand-pressed pump.

How these high levels of Fe and Al could emerge could have different reasons. Groundwater chemistry involves interaction of groundwater with aquifer minerals. Geochemical composition of groundwater is affected by several natural factors, including weathering, dissolution, and precipitation of minerals, mixing of different types of water, evaporation, decay of organic materials, selective uptake of ions by vegetation, and resident time of water. The above processes govern the content of major, minor, and trace elements in groundwater (7, 20). Among all the major elements in the earth, Al and Fe have the highest concentrations in the Earth's crust, at 8% and 5%, respectively; they could enter the groundwater through various processes (9). Furthermore, acid rains, due to industrialization and smelting activities, could potentially have pH of 5.0 or lower, greatly increasing the solubility of Al and Fe (9).

Take home message for the reader

Considering how great some of the samples exceeded the standard and how sparsely the household hand-pressed wells spread, we strongly suggest that household water treatment systems should be used to process pump water. There are many devices employing the principles of filtration, absorption, reverse osmosis, and ionic exchange on the market that could purify groundwater (21).

However, education levels of many villages are quite low, and their residents lack the necessary knowledge about water process and water processing, and the effects of metal pollution will only show in the long term. Therefore, it is necessary to inform and remind people to regularly check the quality of processed water and replace the filters to ensure proper functioning of the devices following related guidelines from the water purification system suppliers or local authorities. To implement that, an educational program is proposed for those areas with high amounts of Al, Fe, and Mn in the hand-pressed well water. Brochures containing information on the levels of heavy metals in hand-pressed well water, health risks, and safety measures such as water treatment devices and their maintenance could be delivered to the residents through local village committees. Moreover, lectures on the safety of drinking water could be taught to the students in local elementary or secondary schools. With the increased awareness of this issue and necessary measures taken, the potentially harmful health effects associated with high levels of Al, Fe, and Mn in the hand-pressed well water of this area could be eliminated.

For Liufengzhen of Guiyang County where the highest levels of Al, Fe, and Mn in hand-pressed well water were found, future actions including further investigations on the

root cause and implementation of an educational program are necessary. Besides, considering the high amount of non-ferrous ores in Chenzhou and the high amount of mining activities in this area, it is necessary to further investigate the local water quality, focusing on the areas close to the ores or mining activities to check if there any direct influences.

METHODS

Sampling

Chenzhou City lies between 24°53′ and 26°50′ N latitude and between 112°13′ and 114°14′ E longitude, Hunan Province, Southern China. The total area of the city is 19,387 km^2. The climate is subtropical, and the average rainfall is about 1500 mm yearly. The water quality survey points were randomly selected. The sampling sites cover the counties of Chenzhou City including Anren, Guiyang, Yizhang, and Zixing. (**Figure 2**).

Before sampling, a preliminary investigation was conducted to find out the areas in which hand-pressed well water was still used, and sampling was planned accordingly. Water samples were collected with the assistance of a local person working as a driver and guide from May 27th to May 31st, 2018, after summer holiday started in McCallie School. PET sampling bottles were rinsed with sample water three times before sampling. 100 mL of water samples were collected, and samples were acidified in situ with concentrated nitric acid to pH < 2. Finally, a total of 160 hand-pressed well water samples were collected.

Analysis and quality control

Sample analysis was conducted at the lab of the Shanghai Institute of Organic Chemistry (SIOC), Chinese Academy of Sciences after the collection of samples. Heavy metal concentrations in water were measured at an ICP-OES (SPECTRO ARCOS FHS12, Germany), with operation parameters: RF power: 1430 W, plasma gas (Ar) flow rate: 12 L/min, auxiliary gas (Ar) flow rate: 0.9 L/min, nebulizer gas (Ar) flow rate: 0.78 L/min.

The 20 elements of multi-element standard solution, including Al, B, Be, Ca, Cd, Co, Cr, Cu, Fe, K, Li, Mg, Mn, Na, Ni, Pb, Si, Zn, Zr, and Ag, was prepared from 100 or 1000 mg/L certified stock solutions (Agilent Technologies) and diluted gravimetrically with 2% HNO_3 to 5 different concentrations with 0 ppm (blank), 0.1 ppm, 0.2 ppm, 0.5 ppm, 1.0 ppm. Pure water with a resistivity of 18.2 MΩ/cm, produced by a Milli-Q water purification system (Millipore, USA) was used for standards preparation.

Water samples were measured, and quality control measures were taken according to the standard (9). Duplicate blanks using 2% nitric acid in each batch of measurement were employed. Duplicate measurements of samples were conducted in every 10 samples. Quality control samples were measured at the end of each batch measurement. The detection limit (DL) of each element was the concentration corresponding to a signal of three times of the standard deviation of 11 times the measurement of the blank solution. The DL and wavelength of each element are listed in **Table 1**.

Received: April 19, 2019
Accepted: September 26, 2019
Published: October 20, 2019

REFERENCES

1. Huang, Xiao, *et al*. "Different Choices of Drinking Water Source and Different Health Risks in a Rural Population Living Near a Lead/Zinc Mine in Chenzhou City, Southern China." *Int. J. Environ. Res. Public Health*, vol.12, 2015, pp. 14364-14381.
2. Guo, Lianxu, "An automatic way to obtain water using hand-pressed well.", *Agricultural Engineering Technology*, vol. 01, 1994, pp.24.
3. Rodriguez-Lado, Luis, *et al*. "Groundwater arsenic contamination throughout China." *Science*, vol. 341, 2013, pp. 866–868.
4. Zhang, Xiuwu, *et al*. "Impacts of lead/zinc mining and smelting on the environment and human health in China." *Environ. Monit. Assess*. vol. 184, 2012, pp. 2261–2273.
5. Shen, Xiaoming, *et al*. "Review of Children's lead poisoning in China." *The Journal of Clinical Pediatrics*. vol. 3, 1996, pp. 200-202.
6. "Toxicological Profile for Lead", U.S. Department of Health and Human Services, Agency for Toxic Substances and Disease Registry, 2019. www.atsdr.cdc.gov.
7. Abeywickarama, Buddhika, *et al*. "Geoenvironmental factors related to high incidence of human urinary calculi (kidney stones) in Central Highlands of Sri Lanka." *Environmental Geochemistry and Health*, vol. 38, 2016, pp. 1203-1214.
8. "Toxicological Profile for Zinc", U.S. Department of Health and Human Services, Agency for Toxic Substances and Disease Registry, 2005. www.atsdr.cdc.gov.
9. Yang, Zhong-lian *et al*. "Progress in the Research of Concentration, Speciation, Hazard and Control of Residual Al in Drinking Water." *Fine Chemicals*, vol. 30, 2013, pp. 412-419 (in Chinese).
10. Guy, B. "Aluminum speciation in relation to aluminum bioavailability." Metabolism and Toxicity, *Coord Chem Rev.*, vol. 228, 2002, pp. 319-341.
11. Donaldson William E.: in *Introduction to Biochemical Toxicology* ed. By Hodgson E *et al*., Blackwell Scienctific Publications, 1980, pp330.
12. Wang, Meie, *et al*. "Risk assessment of Cd polluted paddy soils in the industrial and township areas in Hunan, Southern China." *Chemosphere*, vol. 144, 2016, pp. 346-351.
13. "The overall planning of mineral resources in Chenzhou (2001-2010)", Chenzhou Municipal People's Government, 2002. www.czs.gov.cn.
14. Mendham, J. *et al*. *Vogels's Textbook of Quantative Chemical Analysis*. 6th edi., Pearson, 2000, pp. 622-629.

15. United States Environmental Protection Agency (2009), National Primary Drinking Water Regulations, EPA 816-F-09-004, www.epa.gov/ground-water-and-drinking-water/national-primary-drinking-water-regulations.
16. GB 5749-2006 Standards for drinking water quality (in Chinese).
17. GB/T 5750-2006 Standard examination methods for drinking water (in Chinese).
18. GB/T 5750.4-2006 Standard examination methods for drinking water-Organoleptic and physical parameters (in Chinese).
19. "Toxicological Profile for Manganese", U.S. Department of Health and Human Services, Agency for Toxic Substances and Disease Registry, 2012. www.atsdr.cdc.gov.
20. Subramani, T. *et al*. "Groundwater geochemistry and identification of hydrogeochemical processes in a hard rock region, Southern India." *Environmental Monitoring and Assessment*, vol. 162(1–4), 2010, pp.123–137.
21. Wang, Song, "Progress of research and development on drinking water purification technique." *Chinese Industry & Economy*, vol. 6, 2015, pp 78-81 (in Chinese).

Copyright: © 2017 Karuppiah and Ramiah. All JEI articles are distributed under the attribution non-commercial, no derivative license (http://creativecommons.org/licenses/by-nc-nd/3.0/). This means that anyone is free to share, copy and distribute an unaltered article for non-commercial purposes provided the original author and source is credited.

JOURNAL OF
EMERGING INVESTIGATORS

Article

Nintendo Da Vinci: A Novel Control System to Improve Performance in Robotic-Assisted Surgery

Ibrahim S. Al-Akash[1] and Samhar I. Al-Akash[2]
[1]Veterans Memorial High School, Corpus Christi, Texas
[2]Driscoll Children's Hospital, Corpus Christi, Texas

SUMMARY

Complications of robotic-assisted surgery are on the rise, partly due to surgeons not receiving proper training. Using the current Da Vinci (DV) surgical system, surgeons require anywhere between 150 and 3,000 surgeries to achieve adequate proficiency. To improve performance, we have developed a new system using Nintendo Joycon (NJ) controls. We hypothesized the NJ controls would improve surgical performance, so we compared the NJ and DV systems with two user groups (doctor and gamer). The doctor and the gamer performed a defined task using NJ and the DV control systems, in a simulated skills assessment in 2-dimensional (2D) and 3D modes. The task completion time and error rate were used to calculate a Fundamentals of Robotic Surgery Skills Assessment (FRS) score. The FRS was then used to calculate the learning rate using the learning rate formula. The task completion time, error rate, FRS scores, and the learning rate were significantly better with NJ. The error rate risk ratios indicated that the DV control system carried a higher risk of error compared to the NJ control system. The NJ control system was associated with a better task completion time by 83% for the doctor and 88% for the gamer, a lower error rate by 73% for the doctor and 82% for the gamer, and better FRS score by 72% for the doctor and 46% for the gamer, and better LR by 84% for the doctor and 86% for the gamer. This study shows that implementing a NJ control system is associated with improved surgical performance and LR compared to DV.

INTRODUCTION

It is a national mission to reduce surgical morbidity, reduce healthcare costs, and accelerate learning for training and practicing surgeons (1-3). Robotic-assisted surgery is being implemented to complete this mission. The Federal Drug Administration approved the Da Vinci Surgical System in 2000. Only Da Vinci Surgical Systems are used for robotic surgery and are in 3,800 hospitals worldwide (4). The system itself costs upwards of $2 million in acquisition and maintenance (5). Therefore, many surgeons do not have the necessary training on it. Over the past few years, complications associated with robotic-assisted surgery have skyrocketed (5). This is likely due to surgeons not completing the recommended training, which requires surgeons to perform at least 150-3,000 surgeries to be proficient in robotic-assisted surgery. Many surgeons only do between 50-120 procedures, which is ineffective and may potentially endanger patients (6). In fact, the frequency of complications associated with robotic surgery is grossly underreported, so it isn't possible to find exactly how many injuries and deaths result from robotic surgery (7). Patients often need to travel to distant cities to find a surgeon qualified to do robotic-assisted surgery (8).

To address this issue and reduce the risk of complications, we developed a new surgical system to replace the current Da Vinci control system with an easy-to-use Nintendo Joycon control system. Our study is the first to do this. We selected Nintendo Joycons for this study because the Nintendo Switch Joycon has more advanced technology, enabling more precise movements of the Da Vinci Surgical System, and the controls feel natural, making it easy to use (9). The Da Vinci controller has ergonomic issues which the Joycon can fix such as comfort and an efficient design. Many doctor trainees are familiar with the Nintendo Switch Joycons. In fact, 80% of students in medical school play videogames (10). We hypothesized that an easier control system would reduce the amount of training surgeons need to be proficient by accelerating the learning curve and reducing operating (task completion) time, and errors. We used 3D models of the Da Vinci controllers and official Nintendo Joycons for our experimentation. A gamer was used because of their proficiency in using the Joycons. Our results found the Nintendo Joycon control system significantly improved performance by improving FRS scores, reducing error, reducing task completion time, and accelerated the learning rate.

RESULTS

A doctor and a gamer each performed seven fundamentals of robotic surgery skills assessment (FRS) (see methods section) pegboard tasks for each test (n = 7 Nintendo Joycon 2D, n = 7 Nintendo Joycon 3D, n = 7 Da Vinci 2D, n = 7 Da Vinci 3D). The pegboard task is a test that trains a surgeon the fundamental skills needed in robotic surgery by using the task completion time and error from moving rings between poles to calculate an FRS score. The Nintendo Joycon control system and the Da Vinci control system were used in the simulated Fundamentals of Robotic Surgery Skills Assessment (FRS) in

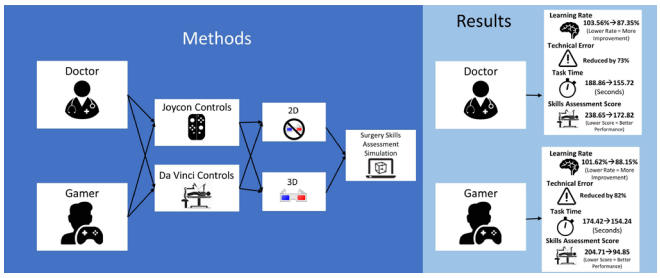

Figure 1. Visual summary of the study. The left side shows a flow chart of the procedure and the right side shows the results collected.

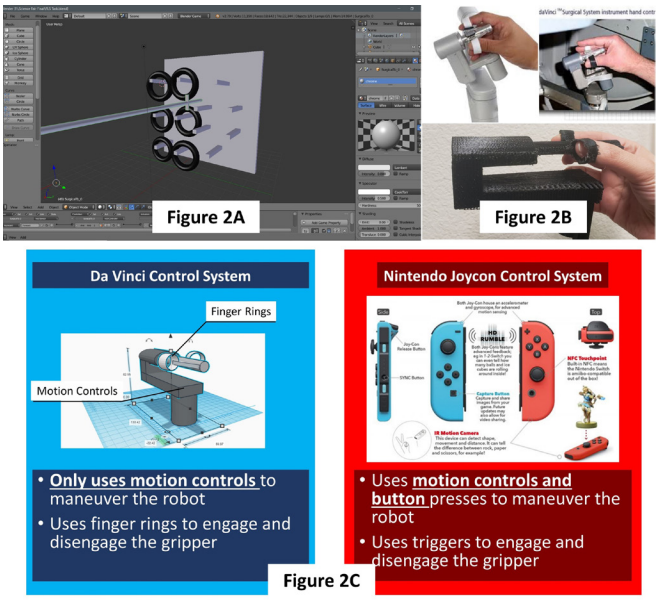

Figure 2. Fundamentals of Robotic Surgery skills assessment (FRS) pegboard task. A) The pegboard task requires moving rings from the left pole to the right pole. B) Top image shows the official Da Vinci controller used in modern robotic-assisted surgery and the bottom image is the Da Vinci controller created by the student researcher. C) Comparison of Da Vinci controller and Joycon controller systems. Left image created by author in Tinkercad. Right image from images.nintendolife.com.

2D and 3D by both users (**Figures 1 and 2**). A doctor and a gamer were recruited to show that no matter whether the user has prior experience with the Joycons, there will still be a significant improvement in surgical performance with the Joycon system compared to the Da Vinci system. Sessions 1 and 2 tested whether the Nintendo Joycon control system improved simulated surgical performance for the doctor in 2D (session 1 is 2D Nintendo Joycon, and session 2 is 2D Da Vinci). We found a statistically significant decrease in mean task time (-33.16 seconds, p = 0.016), mean error (-19.07%, p = 0.015), mean FRS score (-74.06, p = 0.012), and mean learning rate (-28.64%, p = 0.0094) when using the Nintendo Joycons (**Table 1 and Figure 3**). The proportion of tasks with errors favored the Nintendo Joycon control system and was statistically significant (relative risk ratio=3.0, p = 0.0398) (**Table 3**). Sessions 3 and 4 (3D Nintendo Joycon and 3D Da Vinci) tested whether the Nintendo Joycon control system improved simulated surgical performance for the doctor in 3D. We measured a statistically significant decrease in mean task time (-33.11 seconds, p = 0.016), mean error (-16.73 percent, p = 0.0021), mean FRS score (-66.17, p = 0.0013), and mean learning rate (-3.79 percent, p = 0.047) when using the Nintendo Joycons (**Table 1 and Figure 3**). The proportion of tasks with errors favored the Nintendo Joycon control system and was statistically significant (relative risk ratio = 4.5, p = 0.0451) (**Table 3**). These results indicate the doctor learned the task faster and did so with less error when using the Nintendo Joycons. Sessions 1 and 2 (2D Nintendo Joycon and 2D Da Vinci) tested whether the Nintendo Joycon control system improved simulated surgical performance for the gamer. We measured a statistically significant decrease in mean task time (-36.29 seconds, p = 0.0002), mean error (-35.72%, p = 0.0009), mean FRS score (-89.14, p = 0.0003),

2D	Da Vinci (n = 7)		Joycon (n = 7)			
Outcomes	Mean	SD	Mean	SD	Difference	P Value
Task Time (s)	206.14	37.86	172.98	31.67	33.16	0.016
Error (%)	28.57	0.76	9.52	0.78	19.07	0.015
FRS Score	265.81	67.97	191.75	56.17	74.06	0.012
Learning Rate (%)	111.09	25.56	82.45	9.82	28.64	0.0094
3D	**Da Vinci (n = 7)**		**Joycon (n = 7)**			
Outcomes	Mean	SD	Mean	SD	Difference	P Value
Task Time (s)	171.58	21.47	138.47	13.55	33.11	0.016
Error (%)	21.43	0.49	4.70	0.49	16.73	0.0021
FRS Score	211.50	29.07	145.33	22.49	66.17	0.0013
Learning Rate (%)	96.02	6.93	92.23	5.48	3.79	0.047

Table 1. Outcomes for doctor. Top, 2D simulation. Bottom, 3D simulation. FRS, Fundamentals of Robotic Surgery. SD, standard deviation. A p-value less than 0.05 was considered significant.

2D	Da Vinci (n = 7)		Joycon (n = 7)			
Outcomes	Mean	SD	Mean	SD	Difference	P Value
Task Time (s)	137.70	23.23	101.41	16.82	36.29	0.0002
Error (%)	42.86	1.13	7.14	0.53	35.72	0.0009
FRS Score	198.53	34.89	109.39	25.98	89.14	0.0003
Learning Rate	98.61	9.78	86.65	7.21	11.96	0.004
3D	**Da Vinci (n = 7)**		**Joycon (n = 7)**			
Outcomes	Mean	SD	Mean	SD	Difference	P Value
Task Time (s)	170.80	25.09	76.52	6.42	94.28	0.000006
Error (%)	23.81	0.98	4.76	0.49	19.05	0.02
FRS Score	210.87	44.55	80.33	11.99	130.54	0.000002
Learning Rate	104.63	8.71	89.66	5.54	14.97	0.008

Table 2. Outcomes for gamer. Top, 2D simulation. Bottom, 3D simulation. FRS, Fundamentals of Robotic Surgery. SD, standard deviation. A p-value less than 0.05 was considered significant.

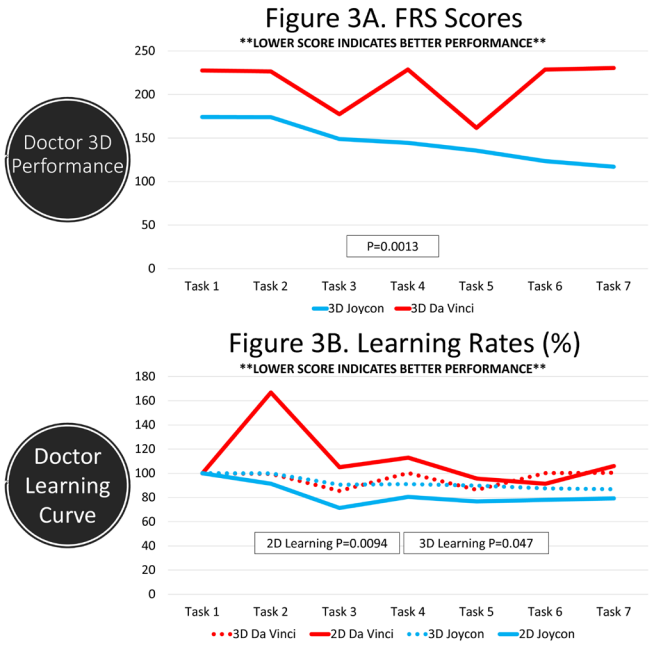

Figure 3. FRS scores and learning curve for doctor in 2D simulation and 3D simulation. A) The doctor's FRS (Fundamentals of Robotic Surgery Skills Assessment) scores for the Joycons and the Da Vinci in the 2D simulation and the 3D simulation. A lower FRS score indicates better performance. B) The doctor's learning curve for the Joycons and the Da Vinci controls in 2D and 3D simulations. A lower learning rate indicates better performance.

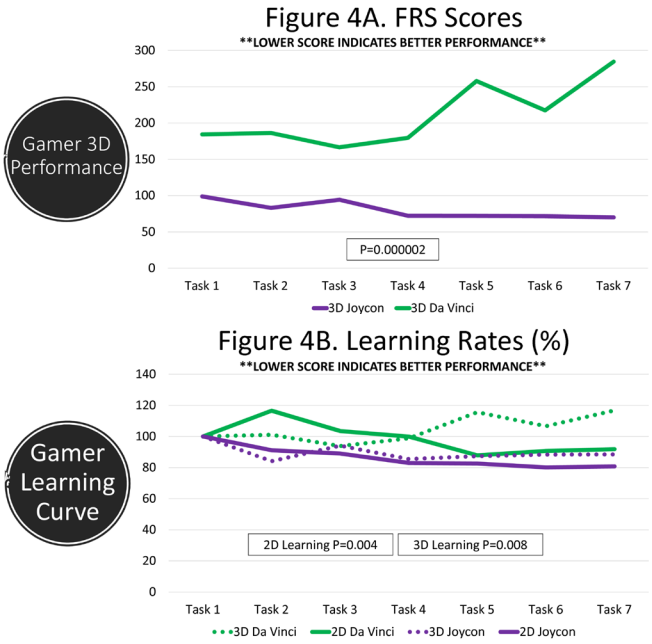

Figure 4. FRS scores and learning curve for gamer in 2D simulation and 3D simulation. A) The gamer's FRS (Fundamentals of Robotic Surgery Skills Assessment) scores for the Joycons and the Da Vinci in the 2D simulation and the 3D simulation. A lower FRS score indicates better performance. B) The gamer's learning curve for the Joycons and the Da Vinci controls in 2D and 3D simulations. A lower learning rate indicates better performance.

and mean learning rate (-11.96%, p = 0.004) when using the Nintendo Joycons (**Table 2 and Figure 4**). The proportion of tasks with errors favored the Nintendo Joycon control system and was statistically significant (relative risk ratio = 6.0, p = 0.0022) (**Table 4**). Sessions 3 and 4 (3D Joycon and 3D Da Vinci) tested whether the Nintendo Joycon control system improved simulated surgical performance for the gamer. We measured a statistically significant decrease in mean task time (-94.28 seconds, p = 0.000006), mean error (-19.05%, p = 0.02), mean FRS score (-130.54, p = 0.000002), and mean learning rate (-14.97%, p = 0.008) when using the Nintendo Joycons (**Table 2 and Figure 4**). The proportion of tasks with errors favored the Nintendo Joycon control system and was statistically significant (relative risk ratio = 5.0, p = 0.0304) (**Table 4**). These results indicate the gamer learned the task faster and did so with less error when using the Nintendo Joycons. Our data indicates that implementing a Nintendo Joycon control system could significantly improve surgical performance by accelerating the learning rate and by reducing error.

DISCUSSION

We hypothesized that implementing a Nintendo Joycon control system would improve surgical performance on Da Vinci virtual reality tests. We demonstrated that the Joycon control system improves performance and reduces error (**Tables 1 and 2**). The Nintendo Joycon's better functionality and intuitive controls may explain the improved performance

2D	Da Vinci (n=7)		Joycon (n = 7)				
Outcomes	Mean	SD	Mean	SD	RR	95% CI	P Value
Error (%)	28.57	0.76	9.52	0.78	3	(1.0523 to 8.5530)	0.0398
3D	**Da Vinci (n=7)**		**Joycon (n = 7)**				
Outcomes	Mean	SD	Mean	SD	RR	95% CI	P Value
Error (%)	21.43	0.49	4.70	0.49	4.5	(1.0333 to 19.5969)	0.0451

Table 3. Risk ratios for doctor. Top, 2D simulation. Bottom, 3D simulation. SD, standard deviation. RR, relative risk. CI, confidence interval. In the simulations, RR = X means that the gamer was X times as likely to have error when using the Da Vinci system compared to the Joycon system. A p-value less than 0.05 was considered significant.

2D	Da Vinci (n = 7)		Joycon (n = 7)				
Outcomes	Mean	SD	Mean	SD	RR	95% CI	P Value
Error (%)	42.86	1.13	7.14	0.53	6	(1.9093 to 18.8546)	0.0022
3D	**Da Vinci (n = 7)**		**Joycon (n = 7)**				
Outcomes	Mean	SD	Mean	SD	RR	95% CI	P Value
Error (%)	23.81	0.98	4.76	0.49	5	(1.1650 to 21.4592)	0.0304

Table 4. Risk ratios for gamer. Top, 2D simulation. Bottom, 3D simulation. SD, standard deviation. RR, relative risk. CI, confidence interval. In the simulations, RR = X means that the gamer was X times as likely to have error when using the Da Vinci system compared to the Joycon system. A p-value less than 0.05 was considered significant.

compared to the Da Vinci. For example, the Da Vinci only uses the gyroscope and accelerometer to control the robot, while the Joycon uses analog sticks and buttons in addition to the gyroscope and accelerometer. This refines the movement and enables more precise maneuvers than the Da Vinci. The Joycons combine analog and digital controls, which also enhance precision of the maneuvers (11). A review of several studies of digital and analog technology found that digital technology advancements were associated with improved flexibility, programmability, system reliability, sensitivity to parameter variation, and easier system integration (11). While the Da Vinci may be more sophisticated, that may not be its most important quality. Developers of Nintendo games rely on the intuitive controls and ease-of-use rather than sophisticated controls to appeal to the majority of people and to ensure its widespread use. This is a fundamental observation because, to date, no studies have been made concerning implementing a new control system such as the Nintendo Joycon control system in robotic-assisted surgery. Furthermore, these results show that if virtual reality results are consistent with real results, then when Joycon control systems are implemented, operation times should decrease, complications should decrease, and the learning curve should accelerate. Decreased operation times would widen accessibility to patients since the surgeons may have more time for additional operations. Decreased complications would reduce healthcare costs. Accelerated learning would also reduce healthcare costs since less money would be spent on surgical training, surgeons would have more time to work. Also, it would increase accessibility to patients since more surgeons would be qualified to perform robotic-assisted surgery. The Joycon control system could potentially save a lot of money because it is much cheaper than the Da Vinci control system. Also, since an 84% acceleration in learning was observed, the amount of procedures surgeons need for proficiency could be significantly reduced from between 150-3,000 procedures down to between 20-420 procedures using the Joycon control system.

There were some key limitations in this study that should be mentioned. First, we did not use official Da Vinci controls manufactured by Intuitive Surgical due to the limited accessibility and the high cost of the controls, which is upwards of two hundred thousand dollars. To circumvent this issue, a 3D model of the Da Vinci controls was created, and the accelerometer and gyroscope of the Nintendo Joycon were integrated into the model (**Figure 3**). The same gyroscope and accelerometer were used in the Da Vinci controller as the Joycons to keep the sensitivity of the motion-sensing technology controlled and accurately test the impact of the Joycon controller design.

Second, the findings were unambiguous in a virtual reality setting, yet the true test of the Joycon control system will need to be in the operating room. This was not possible given the circumstances because the Da Vinci surgical system robot costs about on average two million dollars. The fundamental research in the robotic virtual reality setting, however, highlights the potential benefit of employing a Joycon control system for improving patient outcomes and reducing costs. These findings may be easily translatable into the OR due to the parity between the simulated FRS skills assessment and the real FRS skills assessment.

Potential future experiments include testing more complex surgical tasks such as ligating loops, suture strength, round incision, and camera targeting, in addition to the pegboard task. These tasks are widely accepted by the Society of American Gastrointestinal and Endoscopic Surgeons and the American College of Surgeons, and are used to train surgeon fundamentals in robotic surgery that can be translated to the operating room. The ligating loop task and the suture strength task both train the surgeon how to suture the incision and how to estimate how much pressure and force the robot is exerting on the patient. The round incision task trains the surgeon how to be precise and how to maneuver the robot in complex environments. The camera targeting task trains the surgeon how to maximize the efficiency of the camera by figuring out the optimal placement and the direction the camera is facing.

The fact that the authors serve as subject participants in this study potentially introduces a bias in observation, data recording, and interpretation. However, we felt this was not a major concern because we designed this as a pilot study with the intention for validation in future studies. For validation, more subjects will be recruited, excluding the authors as study subjects, to address the small sample size and eliminate that potential bias. The next steps of this study include improvement in the Joycon design by incorporating the strengths of the Da Vinci system, such as the higher end gyroscope to further improve the range of motion.

In conclusion, implementing a Nintendo Joycon control system improved robotic surgery task performance and reduced errors for the doctor and the gamer in a virtual reality setting. Further investigation is required to see if these results translate to the operating room. Our data provides a foundation for future predictive validation studies assessing the role of implementing a Nintendo Joycon control system for improved patient outcomes, reduced operative cost, and paves the way for investigation of this novel control system in all areas of robotic surgery.

METHODS

Subject selection

A pediatric nephrologist with minimal surgical experience in biopsies from Driscoll Children's Hospital and a 15-year-old gamer (gamer defined as someone who spends more than 5 hours playing video games per week) from Veterans Memorial High School were recruited for this study. Neither the doctor nor the gamer had experience with the Da Vinci system, but the gamer was familiar with the Nintendo Joycons.

Robotic surgery systems

The simulation was made in Blender3D using models provided by Intuitive Surgical. The Nintendo Joycon control

system was integrated into the simulation and the use of JoyToKey software to translate the controller button presses into key presses for Blender3D to read. The Joycon control system is a hardware add-on which uses the Da Vinci software. The Da Vinci control system was 3D printed and integrated into the simulation by incorporating the Joycon's accelerometer and gyroscope in the Da Vinci control 3D model. This was purposely done since the same gyroscope and accelerometer were used and the precision and accuracy were controlled. For both systems, the motion controls were converted into key presses using the JoyToKey software, as well.

Task design

Both users received 5 minutes of practice prior to performing the Fundamentals of Robotic Surgery Skills Assessment (**Figure 2A**). Seven tasks were performed by each user using the Nintendo Joycon control system in 2D and 3D and using the Da Vinci control system in 2D and 3D, for a total of twenty-eight tasks for each user. The task consisted of a pegboard with twelve poles: six on the left side arranged in a rectangle formation and six on the right arranged in a diamond formation (Figure 2A). The users had to move the rings from the left side to the right side. This task was designed to test fundamental skills needed in the operating theatre including hand-eye coordination, bimanual dexterity, speed, and precision. Task time started when the user touched the first ring with the surgical instrument and ended when the last ring was released by the instrument. Each dropped ring counted as 16% error. The skills acquired from the peg transfer task directly translate into better bimanual handling of needle and other small objects during surgery (12). The pegboard task is endorsed by the American College of Surgeons and approved by both, the Food and Drug Administration and the Advanced Medical Technology Association. Each task had 3 levels of difficulty: low, intermediate, and high based on the distance and angle the rings in the simulation module had to be moved during the task.

Performance metrics

The primary outcomes analyzed were task time, error frequency, learning rate, and FRS score for each user using each control system in 2D and 3D modes. The results of the gamer and the doctor were analyzed separately to show if the individual's simulated surgical performance improves when using the Nintendo Joycon control system compared to the Da Vinci control system. The tasks were completed in four sessions: session 1 tested both users using the Nintendo Joycon control system in 2D, session 2 tested both users using the Joycon control system in 2D, session 3 tested both users using the Da Vinci control system in 2D, and session 4 tested both users using the Da Vinci control system in 3D. Each session was separated by a time period of one week to mitigate the potential for compounded learning from previous sessions.

Based on existing surgical curricula validation studies, the following performance metrics were tracked in the simulated skills assessment:

1. Mean task time (seconds) = (sum of task times) / (number of tasks)
2. Technical errors (percentage) = ((number of rings dropped) / (total rings moved)) × 100%
3. FRS score (lower is better) = (task time in seconds) + (% error × task time in seconds)
4. Learning rate (percentage) = 10^{(ln[(FRS Score of *n*th Task)/(FRS Score of first Task))×log(2)]/[ln(*n*th Task)]}

Statistical methods

The primary comparison was a test for the mean difference between the results when using the Joycon control system and the Da Vinci control system. The users were not compared to each other because this study was focused on improving a given user's individual performance. Student's t-test was used to test for a significant difference between study groups, and a p-value < 0.05 was considered statistically significant. Mean and p-value calculations were made in Microsoft Excel. To calculate the significance of error, the relative risk was calculated using an online risk calculator. The name of the website is MedCalc Statistical Software.

REFERENCES

1. "Robotic Surgery Linked to 144 Deaths in the US." *BBC News*, BBC, 22 July 2015, www.bbc.com/news/technology-33609495.
2. Gumus, Eyup, *et al*. "The Learning Curve of Robot-Assisted Radical Prostatectomy." *Journal of Endourology*, vol. 25, no. 10, 2011, pp. 1633–1637., doi:10.1089/end.2011.0071.
3. Lendvay, Thomas S., *et al*. "Virtual Reality Robotic Surgery Warm-Up Improves Task Performance in a Dry Laboratory Environment: A Prospective Randomized Controlled Study." *Journal of the American College of Surgeons*, vol. 216, no. 6, 2013, pp. 1181–1192., doi:10.1016/j.jamcollsurg.2013.02.012.
4. "The Most Advanced Surgical System of the World in IMED Valencia Hospital." Da Vinci, 11 July 2016, davinci.imedhospitales.com/en/robotic-system-da-vinci/.
5. Scott, Cameron. "Is Da Vinci Robotic Surgery a Revolution or a Ripoff?" *Healthline*, Healthline Media, 10 Aug. 2016, www.healthline.com/health-news/is-da-vinci-robotic-surgery-revolution-or-ripoff-021215#1.
6. Sridhar, Ashwin N., *et al*. "Training in Robotic Surgery—an Overview." *Current Urology Reports*, vol. 18, no. 8, 2017, doi:10.1007/s11934-017-0710-y.
7. Makary, Martin A., *et al*."Johns Hopkins: Robotic Surgery Complications Grossly Underreported." *FierceBiotech*, 4 Sept. 2013, www.fiercebiotech.com/medical-devices/johns-hopkins-robotic-surgery-complications-grossly-underreported.
8. "Medical Tourism: Lisbon Becomes Automatic Choice for Robotic Surgery." *Medical Tourism Magazine* | Blog, www.medicaltourismmag.com/news/2015/02/medical-tourism-

lisbon-becomes-automatic-choice-robotic-surgery/.
9. Kuchera, Ben. "Nintendo's Joy-Cons Brilliantly Solve a Modern Day Console Nuisance." *Polygon*, Polygon, 8 June 2018, www.polygon.com/2018/6/8/17442750/nintendo-switch-joy-cons-best-thing. Kirkendoll. "Medical Students Open to Learning with Video Games." *The University Record Online*, University of Michigan, 16 Aug. 2010, ur.umich.edu/0910/Aug16_10/1431-medical-students-open.
10. Talbot, J.e., and B.g. Lipták. "Controllers—Electronic Analog and Digital." *Process Control*, 1995, pp. 177–192., doi:10.1016/b978-0-7506-2255-4.50033-7.
11. Arikatla, Venkata S., *et al*. "Towards Virtual FLS: Development of a Peg Transfer Simulator." *The International Journal of Medical Robotics and Computer Assisted Surgery*, vol. 10, no. 3, 2013, pp. 344–355., doi:10.1002/rcs.1534.
12. Bach, Christian, *et al*. "Training in Robotics: The Learning Curve and Contemporary Concepts in Training." *Arab Journal of Urology*, vol. 12, no. 1, 2014, pp. 58–61., doi:10.1016/j.aju.2013.10.005.
13. Brinkman, Willem M., *et al*. "Da Vinci Skills Simulator for Assessing Learning Curve and Criterion-Based Training of Robotic Basic Skills." *Urology*, vol. 81, no. 3, 2013, pp. 562–566., doi:10.1016/j.urology.2012.10.020.

Received: April 05, 2019
Accepted: October 10, 2019
Published: October --, 2019

Copyright: © 2019 I. Al-Akash and S. Al-Akash. All JEI articles are distributed under the attribution non-commercial, no derivative license (http://creativecommons.org/licenses/by-nc-nd/3.0/). This means that anyone is free to share, copy and distribute an unaltered article for non-commercial purposes provided the original author and source is credited.

Sponsorship

Editor's Circle $10,000+

ALLOY THERAPEUTICS

Patron $5,000+

NEW ENGLAND BioLabs® Inc.
enabling technologies in the life sciences

PORTFOLIOS WITH PURPOSE®

Institutional Supporters

HARVARD UNIVERSITY

HARVARD MEDICAL SCHOOL

Tufts UNIVERSITY

Charitable Contributions

We need your help to provide mentorship to young scientists everywhere.

JEI is supported by an entirely volunteer staff, and over 90% of our funds go towards providing educational experiences for students. Our costs include manuscript management fees, web hosting, creation of STEM education resources for teachers, and local outreach programs at our affiliate universities. We provide these services to students and teachers entirely free of any cost, and rely on generous benefactors to support our programs.

A donation of $30 will sponsor one student's scientific mentorship, peer review and publication, a six month scientific experience that in one student's words, 're-energized my curiosity towards science', and 'gave me confidence that I could take an idea I had and turn it into something that I could put out into the world'. **If you would like to donate to JEI, please visit https://emerginginvestigators.org/support, or contact us at questions@emerginginvestigators.org.** Thank you for supporting the next generation of scientists!

'Journal of Emerging Investigators, Inc. is a Section 501(c)(3) public charity organization (EIN: 45-2206379). Your donation to JEI is tax-deductible. '

emerginginvestigators.org